PolySat Helmholtz Cage

by

Nicolas Le Renard

Alex Nichols

Jordan Skaro

Louie Thiros

Madeline Tran

College of Engineering

California Polytechnic State University

San Luis Obispo

2017

Statement of Disclaimer

Since this project is a result of a class assignment, it has been graded and accepted as fulfillment of the course requirements. Acceptance does not imply technical accuracy or reliability. Any use of information in this report is done at the risk of the user. These risks may include catastrophic failure of the device or infringement of patent or copyright laws. California Polytechnic State University at San Luis Obispo and its staff cannot be held liable for any use or misuse of the project.

Table of Contents

List of Figures

List of Tables

Executive Summary

The MagCal5 Helmholtz cage project is an interdisciplinary approach to provide the PolySat/CubeSat research lab with a magnetic testing environment for the calibration of magnetic components and verification of various control laws. The Cal Poly CubeSat organization is the home of the CubeSat Specification, and acts as a testing and integration facility for CubeSats built by universities across the world. The PolySat organization is a CubeSat developer that works with numerous industry partners to design, manufacture, and operate CubeSats to further scientific advancement. The addition of a magnetic test stand to the lab will allow CubeSat to extend to the range of testing it can provide to other universities and will allow PolySat to perform more extensive attitude determination and control system testing on their CubeSats before they are put into orbit.

This project piggybacks a master's thesis completed by Justin Foley in 2012, who developed a small-scale functional cage as a proof of concept. This cage was capable of holding a 1U CubeSat, and was used on PolySat's CP-8 and CP-10 spacecraft to calibrate magnetometers. Recent damage to that cage, paired with expanding scopes of PolySat's missions, creates the need for a larger, more robust cage. The Helmholtz cage developed for this project is large enough to hold and test a 12U CubeSat, yet collapsible such that storing it between uses is feasible. The cage was constructed using more durable materials than the original cage to ensure its functionality for years to come.

The solution reached by the MagCal5 team is broken into structural, electrical, and software subsystems. Structurally, a collapsible 4ft cubic cage will be capable of testing an assembled 12U CubeSat. The structure is broken into the Helmholtz cage itself, the clean room box which houses the CubeSat during testing, and the pedestal, that centers the clean room box in the cage and aligns the coordinate systems. A control box has been designed containing three off-the-shelf H-bridge motor drivers to control the magnitude and the direction of the magnetic fields in each of the three axes independently. These H-bridges are controlled using an ST microcontroller, and receive commands from a dedicated raspberry pi work station. Users are able to upload CSV files to the cage through the Raspberry Pi to define test profiles, which can then be sent to the cage.

The entirety of the cage was manufactured utilizing the Mustang '60 Shop on campus. The assembly of the cage took place in the high bay of the Bonderson Project Center. A cart was made to act as a work station, as well as provide storage for the cage, clean room box, and pedestal while the cage is not in use. The control box houses the raspberry pi, the control boards, and three power supplies within a computer case. Braided pairs lead from the control box to the cage to reduce extra magnetic fields from being generated.

Mechanical testing of the pedestal showed that it could hold over 200 pounds, at least a factor of safety of 3 for a 12U CubeSat (~60lb), with negligible risk of tipping. The cleanroom box is completely sealed and latched such that a cleanroom environment can be maintained out of the CubeSat cleanroom. Electrical testing showed that the Helmholtz could produce a magnetic field as verified with a cell phone magnetometer. Testing was halted due to an isolation issue in the off-the-shelf motor controllers, that caused ground loops, resulting in unexpected yet repeatable current flow and eventual burning of wire insulation. New motor controllers are being investigated to correct this issue.

1.0 Introduction

1.1 Sponsor Background and Needs

The PolySat Magnetic Calibration Team, MagCal 5, is designing a Helmholtz cage for the calibration and verification of magnetic components on CubeSats, namely magnetometers. CubeSats are small satellites developed by a conglomeration of students and professionals as a relatively cheap way to perform experiments on orbit that do not necessarily require a full sized spacecraft. PolySat is an on campus research lab that develops CubeSats, like ExoCube pictured in Figure 1. As CubeSats become more popular and technology advances, the kinds of experiments these satellites can complete become much more complex and can require a higher degree of attitude (orientation) knowledge and control capability. Reading and reacting to Earth's magnetic field is one way in which this knowledge and pointing requirements can be obtained.

Figure 1. IPEX (CP8) & ExoCube (CP10): Examples of 1U & 3U CubeSats

A Helmholtz cage is a 3-axis magnetic field generator. The purpose of a Helmholtz cage is to cancel out Earth's local magnetic field in San Luis Obispo and superimpose orbital magnetic fields. With such an environment, PolySat members will be able to calibrate the many magnetometers present on each CubeSat in one step, and run simulations to test the response of magnetic actuators (magnetorquers) in response to a changing field. Further, they will be able to better measure the effects of the satellites electronics on the readings of magnetometers, allowing internal noise to be filtered out. All of these results will allow PolySat to develop more intricate satellites and better understand the environmental conditions their CubeSats experience in orbit.

This project was overseen by engineering advisor Dr. James Widmann, and was primarily produced for Dr. Jordi Puig-Suari and future PolySat members pursuing undergraduate and graduate degrees in various engineering and technical science fields. The purpose of this document is to showcase our critical design and receive a customer check off before moving onto the manufacturing phase.

1.2 Formal Problem Definition

The objective of this project is to create a magnetic calibration device, i.e. a Helmholtz Cage, that can be used to calibrate the magnetic sensors on CubeSats. It should be able to counteract the Earth's local magnetic fields and create a magnetic environment equivalent to what the satellite will experience in space orbit. This will allow PolySat to calibrate and verify magnetometers and Attitude Determination Control System (ADCS) control laws for its future missions. The device will leverage the multidisciplinary skills of the group and ultimately be more mechanically, electrically, and software resilient than PolySat's prior Helmholtz cage, built as an individual's thesis. The device should also be easy to transport between different buildings and rooms on Cal Poly's campus, and provide a clean environment for flight hardware. In addition to testing PolySat's CubeSats, this cage could allow Cal Poly become a CubeSat magnetic testing hub for universities around the country in the same way that it's vibrations and thermal vacuum testbeds are.

The Helmholtz Cage will interface with a nearby workstation that will be operated by a PolySat engineer. STK is a commonly used modeling software that serves as the bridge between the user and the cage. However, as simplicity is an objective, both STK and MATLAB were cut from the development process upon realizing that a self-contained GUI in a language of our choice would not only be more feasible to develop, but more user-friendly. The device will feature a custom control board that is capable of setting the magnetic field that it produces to user specified levels, as shown in Appendix C.2. Higher level decisions and user interactions will take place on a larger workstation capable of making large magnetic field calculations and capable of providing a more robust user experience. The communication between the workstation should be done in such a way that either component can be easily replaced or upgraded.

In order to make the Helmholtz cage easy to use, the software should include its own, intuitive, user interface, and a self-contained software stack to interface with the cage. At the top of the software stack is a user interface that allows users to specify their mission, set start and stop times for their simulation, scrub through their mission with a slider, calibrate the device with a guide, and start and stop their simulation. Underneath the interface layer, the software will to calculate an orbit from mission parameters, and then use a model of earth's magnetic field to plan a simulation. A communications layer will be used to control the cage and execute simulation. From a UX standpoint, the device needs to be usable to aerospace engineers with limited software experience. It should be easy to train newer members on using the device correctly.

A QFD analysis was completed to determine our engineering requirements based on our customer inputs and competitors' benchmarks. This analysis can be found in Appendix B.2. We started with a list of the customer requirements, listed on left side, and weighted them to the customers' requests. From there we created technical requirements and noted strong, medium, and weak correlations between the rows and columns. Then we assigned nominal values for each correlation, and found a weighted value for each technical requirement, seen along the bottom of the QFD chart. The most important requirement from this analysis was having the cage capable of supporting a 60lb satellite, and creating a uniform magnetic field large enough for a 12U CubeSat, approximately 24cmx24cmx38cm. We will focus most our design around these requirements, and the remaining requirements as prioritized by these values. Our technical specifications are listed below, with target values and tolerances.

1.3 Design Specifications

Working through the problem definition above, we worked out a complete list of customer requirements as well as interpreted engineering requirements from them. The complete list can be found in Appendix B.1, with a summary of the main requirements in Table 1. We further deduced risks involved with not meeting each specification. As we have moved through our design to this point we have repeatedly checked that these specifications have been met. In Section 5 we will discuss how we will verify these specifications in our final design.

Table 1. Technical Specifications

Spec #	Parameter Description	Requirement or Target (units)	Tolerance	Risk
1	Generated Field Strength Range	100 μT	Min	Inaccurate Simulations
2	Magnetic Vector Accuracy	+/- .5uT	N/A	Inaccurate Calibrations
3	Size	36cm Uniform Field	+/-1cm	Inaccurate Calibrations
4	Budget	$3800	Max	Not finishing Project
5	Power	500 W	Max	Unsafe Work Conditions
6	Satellite Weight	60lb	Min	Satellite Destruction

1.4 Acronyms and Abbreviations

#U	CubeSat satellite unit of (#) size, 10cmX10cmx10cm cube
A	Ampere
ADCS	Attitude Determination and Control System
AWG	American Wire Gauge
Cal Poly	California Polytechnic State University, San Luis Obispo
CDR	Critical Design Review
CNC	Computer Numerical Control
COM	Computer-On-Module
COTS	Commercial Off-The-Shelf
CSV	Comma-Separated Values
FTDI	Future Technology Devices International
GUI	Graphical User Interface
IPS	In-Plane Switching
MagCal 5	Magnetic Calibration 5 Task Force
MATLAB	Matrix Laboratory
MPN	Manufacturer Part Number
PCB	Printed Circuit Board
PDR	Preliminary Design Review
PVC	Polyvinyl Chloride
PWM	Pulse Width Modulation
RS	Recommended Standard
STK	System Tool Kit: Analytical Graphics, Inc.
T	Tesla
TCP / IP	Transmission Control Protocol / Internet Protocol
UART	Universal Asynchronous Receiver / Transmitter
USB	Universal Serial Bus
V	Volt

2.0 Background

Helmholtz cages are an industry standardized method of calibrating the magnetic behavior of satellites. PolySat had a Helmholtz cage designed by Justin Foley for his master's thesis [3]. The project was completed in 2012, maintained a volume large enough for a 1U CubeSat, and has since broken. Figure 2 depicts the current state of PolySat's Helmholtz Cage, which was primarily held together with wooden dowels and hot glue. The PolySat Magnetic Calibration 5 team will make an improved version of Foley's model. Improvements include automated magnetic field calibration, the ability to house at least a 12U CubeSat, and an easy to use GUI which accepts orbital inputs.

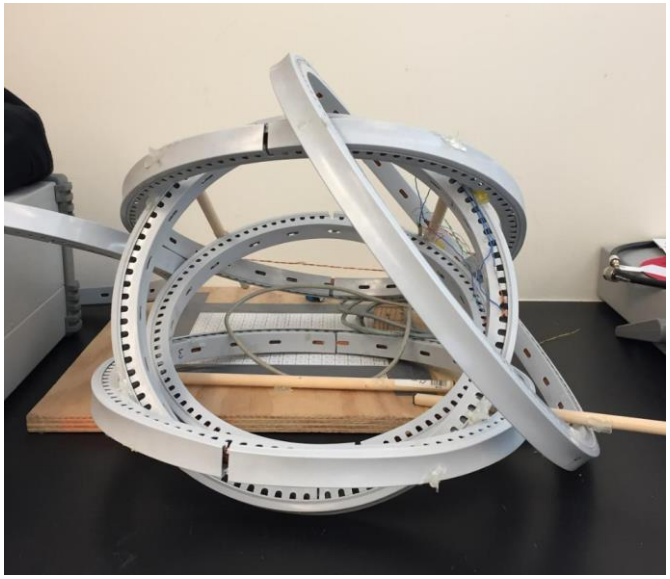

Figure 2. PolySat's current obsolete Helmholtz cage

A Helmholtz cage is capable of producing a magnetic dipole vector in any direction through the use of three orthogonal sets of coils. When current is run through these coils, a magnetic field is induced inside the coil, normal to the plane of the coil, as given by:

$$B = \left(\frac{4}{5}\right)^{3/2} \frac{\mu_o n l}{R}$$

Equation 1. Magnetic field of coil with current

for a spherical cage, where n is the number of turns per coil, I is the current, and R is the radius[3]. By carefully controlling the current through the three sets of coils in relation to each other, a magnetic dipole can be achieved with any desired direction. Helmholtz cages have been designed using many different shaped coils (e.g. circular, square, octagonal) and different numbers of coils in each axis (e.g. 2, 4). These design decisions impact the strength and uniformity of the magnetic field generated, as well as the manufacturability of the cage. We traded these various options to produce the most efficient (i.e. cost, power, size) Helmholtz cage specialized to PolySat's usage.

2.1 Existing Models

2.1.1 Air Force Institute of Technology

The Air Force Institute of Technology has created a similar Helmholtz Cage [4], with the user interfacing achieved via a MATLAB script which opens an STK 'scenario,' subsequently accounting for the ambient magnetic field gathered by the truth magnetometer, individually calculating each coil's requisite current to obtain the scenario's desired geomagnetic field, utilizing *gpib* (STK library) to calibrate the coils, and finally verification of the end result to the expected result. The algorithm, coded into the Arduino platform on the tested CubeSat model, allows for raw data to be stored to the workstation for future analysis. While MagCal 5 is currently aiming for a spherical cage for optimization purposes, the team will likely seek to emulate the software integration technique of the Air Force Institute of Technology's model. Due to its production as a work of the United States government, the practices outlined are not subject to copyright protection.

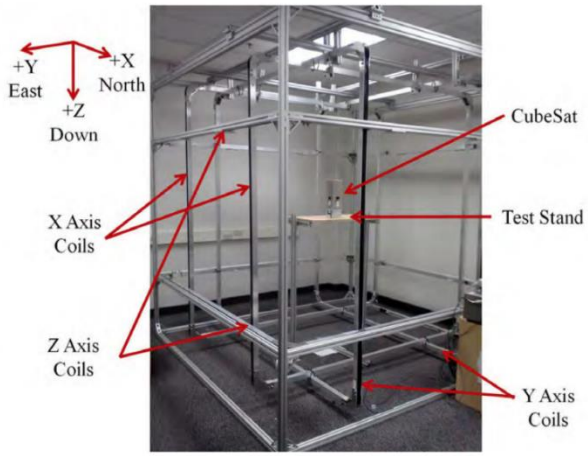

Figure 3. Air Force Institute of Technology's Helmholtz cage

2.1.2 Delft University of Technology [1]

The following are specifications of the Helmholtz cage developed by Delft University of Technology, pictured in Figure 1:

→ Support structure of 2 m^3 in size, composed of aluminum
→ Three sets of two 2 m^2 coils: each with 80 windings and 2.2 mm diameter
→ Maximum current through coils of 10 amps at 30 volts
→ Six power supplies for individual coil control via RS-232 connection
→ Computer console to control and measure coil performance
→ Swivel to hang satellite (or any desired test item)
→ High resolution webcam for recording movement within the cage
→ 3-axis magnetometer
→ Located in cleanroom

Figure 4. Delft University Helmholtz Cage

2.1.3 LightSail

The LightSail program[5], in which momentum is carried by photons such that a reflective sail moves by starlight through space without worry in regards to fuel, is a mission involving 3U CubeSat spacecraft. While the logistics of the satellite itself aren't necessarily pertinent, part of the cycle of deploying it to space (overseen by Cal Poly) involves Helmholtz cage calibrations, which weren't done locally as a result of an inadequate incumbent model. Current artificial magnetic field ADCS testing is typically conducted at sites such as the University of California, Los Angeles (who hosts a hexagonal Helmholtz cage) or Utah State University. An objective of this project, detailed later, will be to make Cal Poly a go-to location for Helmholtz cage testing.

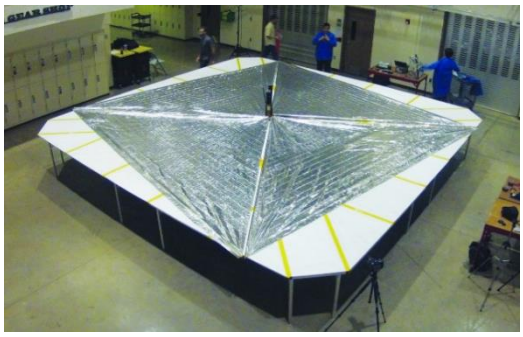

Figure 5. LightSail set up in Cal Poly's Bonderson Project Center

2.1.4 Macintyre Electronics Design Associates, Inc.[7]

Macintyre Electronics Design Associates (MEDA) sells Helmholtz cages for commercial use to cancel the environmental ambient magnetic field and to provide precise stable magnetic fields in a control volume. The commercial price is unknown. Their Helmholtz cage has the following specifications and features:

→ Three square concentric orthogonal Helmholtz coils available in 1,2 and 4 meters.
→ Automatic cancellation of ambient field.
→ 1 nT control volume null.
→ ±200,000 nT control field range.
→ 0.05% basic accuracy.
→ Maximum range of ±270,000 nT.
→ Control range of ±199,999 nT.
→ Resolution: 1 nT.
→ Accuracy: ±0.05% of setting.
→ Field Uniformity: less than 0.1% within a 13.9 inch diameter sphere about coil center.
→ Axis Orthogonality: ±0.1 degree maximum.
→ Overall Coil Size: 80 in x 80 in x 82 in.
→ Control Unit Size: 22.06 in W x 34.12 in H x 26.4 in D.
→ Operating Temperature: 0° C to 50° C.
→ Cost: Unknown.

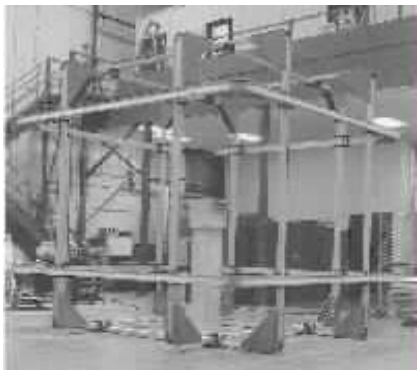

Figure 6. Helmholtz cage produced by Macintyre Electronic Design Associates

2.1.5 Massachusetts Institute of Technology Space Systems Laboratory [6]

The Merritt 4-Coil Helmholtz cage at MIT's Space Systems Laboratory employs a 4 coil per axis system to maximize the volume in which a uniform field is created within the Helmholtz cage, seen in Figure 2. This allows for the calibration and testing of larger objects, i.e. satellites, without the need of a large apparatus. The 60" rectangular cage has a 16-inch sphere, large enough for a 27U CubeSat in which the magnetic field is uniform to within .1% of the desired field strength. One additional goal of this cage was to provide a microgravity environment in which a CubeSat could rotate via its magnetic actuators. The first attempt involved a spherical air bearing. While nearly frictionless, the air bearing is inherently unstable with a large, tall mass like a 3U CubeSat, basically an inverted pendulum. Any movement in the horizontal plane allows gravity to overcome any force created by magnetics. Further, air bearings are very expensive, and are very heavy. They resorted to the 'piñata' rig, first used by Cal Poly's ExoCube team, in which the CubeSat is suspended in the cage by a string to perform uniaxial tests.

Figure 7. Merritt 4 Coil Helmholtz Cage at MIT Space Systems Laboratory

2.2 Existing Patents

There are currently only a few existing patents that concern the calibration of specific magnetic sensor devices through the use of Helmholtz coils, and many are geared towards magnetic compensation processes. If the team is able to invent a new process of calibration, it would be beneficial to try to patent the process. One existing patent is US7436120B2, which covers a means to compensate a magnetic field using a feedback signal [1]. The claims covered by this patent indicate that it describes a device used to compensate magnetic fields and the feedback calculations used to sustain the compensation. The Helmholtz Cage that is to be designed will be used for calibrating sensors, and likely can do little with this information that this patent provides.

Another related patent deals with the calibration of three-axis magnetometers, as the Helmholtz cage will be doing. Patent US7259550B2 covers the design of a device used by CERN to calibrate their magnetic "sensor cards"[10]. The device features moving coils and other rotating parts to calibrate specific card-shaped devices in a homogenous magnetic field. While this patent contains information that could be useful for developing methods of field generation, it does not meet the likely constraint of immovable coils, stationary sensors, and compact size. However, there is relevant information in the document pertaining to the generation of homogenous magnetic fields for the purpose of calibration.

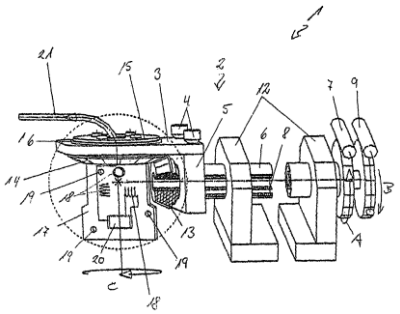

Figure 8. The magnetic calibration device patented by CERN

Yet another related patent was granted to PNI Corp, an electronic sensor company for a method to automatically calibrate a three axis compass [1]. An electronic compass is a specialized magnetometer. The processes described in the patent relate to the use of two compasses to generate a characterization of their magnetic environment and provide an accurate heading. The Helmholtz cage being designed will only be used to calibrate a single magnetometer, meaning that most of the data in the patent document will be of little use. However, it is still possible to see how distortion correction would be performed, which might be useful when creating the software that calculates the magnetic field of the earth at a specified point in space along with the data necessary for compensating the magnetic field currently in place at the device itself.

3.0 Design Development

3.1 Concept Generation

3.1.1 Structural Ideation

The first question asked during the ideation phase was what the general form of the coils would be. There was very little ideation to do with this topic, as the shape needs to be symmetric for the magnetic field to be uniform. We created a list of possible shapes: circular, square, octahedral, all of which can be made into a 2 coil of 4 coil per axis configuration.

From rough calculations in our background phase, we know that the rough size of the cage, regardless of shape, is approximately 2.5 to 3.5 feet across to achieve the desired volume of field uniformity. This means that we need a collapsible design to achieve the requirement of fitting through the PolySat / CubeSat cleanroom door. Our ideation phase for cage collapsibility boiled down to three separate designs, a telescoping bar and block design, a single motion folding cage, and a removable z axis folding design.

The telescoping block method was based on a block designed to route the coils of three axes very closely together, minimizing the difference in size of coils, simplifying the control algorithms. These blocks were then connected using a telescoping rod. This allowed the design to fold down to half of its size, well within the realm of fitting through a door. The wires of the coils themselves would be placed in wire tracks or bundled in zip ties and stored away from the cage in the collapsed state.

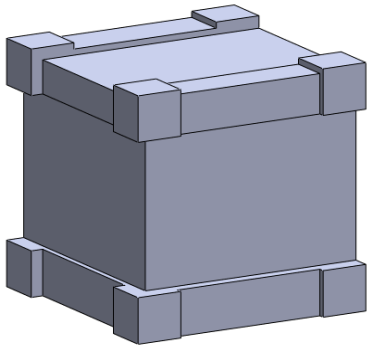

Figure 9. Corner block for telescoping Helmholtz cage

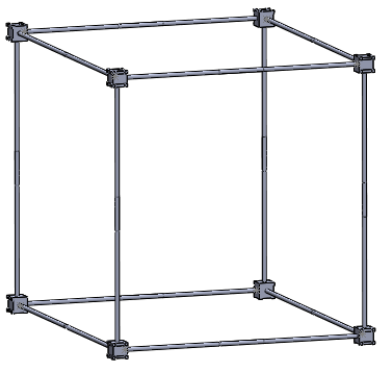

Figure 10. Telescoping block Helmholtz cage

The two folding designs are based on the same X and Y coil design. We allowed rotation at the 4 intersections between the coils, allowing the cage to distort into a diamond shape. The result it a cage that is narrower and longer than the usable state, but capable of fitting through the door. With the X and Y coils worked out, we needed to determine how the Z axis should compensate for the distortion. Our first thought was to hinge the four corners of the Z coils. This creates a rhombus shape in the Z direction.

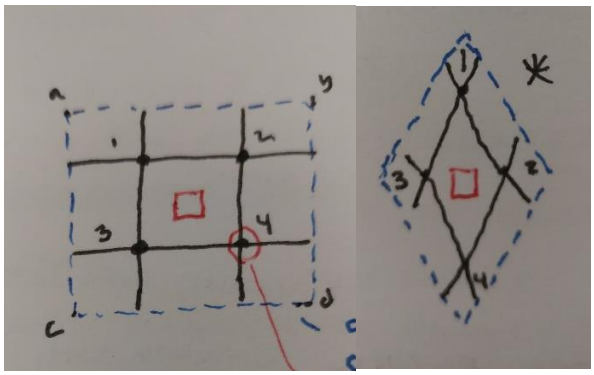

Figure 11. Collapsing cage conceptual sketch with folding Z-axis

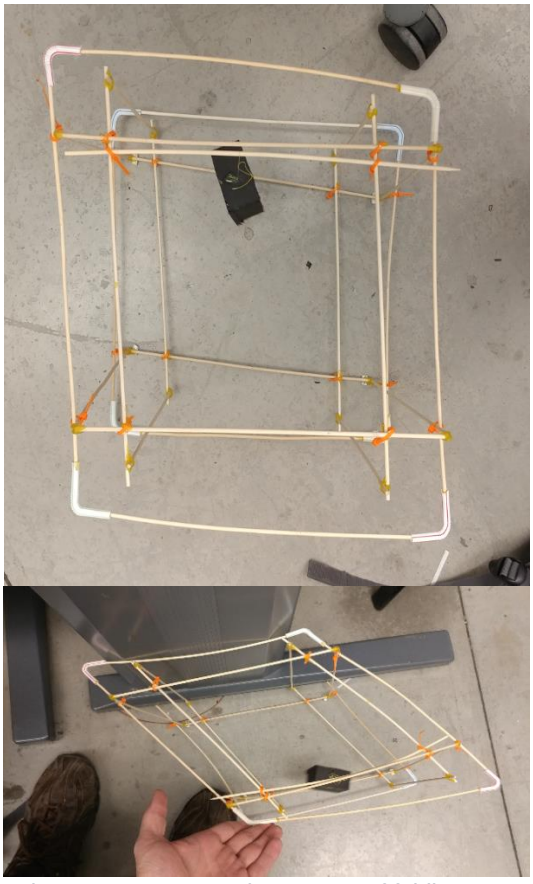

Figure 12. Conceptual prototype of folding cage

The second main solution to the Z axis coil in our foldable design was make the Z axis easy to remove, and storable on one of the other two coils. This gets the Z axis out of the way from the X and Y folding modes, as well as keeping the Z axis rigid, which is beneficial against fatigue failure. Stemming from this design was the need for a way to mount the Z axis to the others in a quickly to remove manner. We went through the designs of several spring-loaded stops and well as folding shelves.

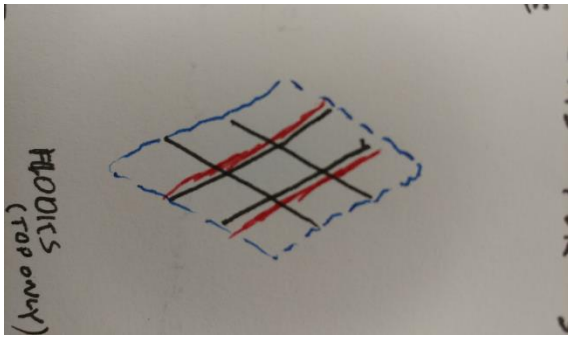

Figure 13. Rigid Z coils (red) store on the side of one of the other axis during transportation

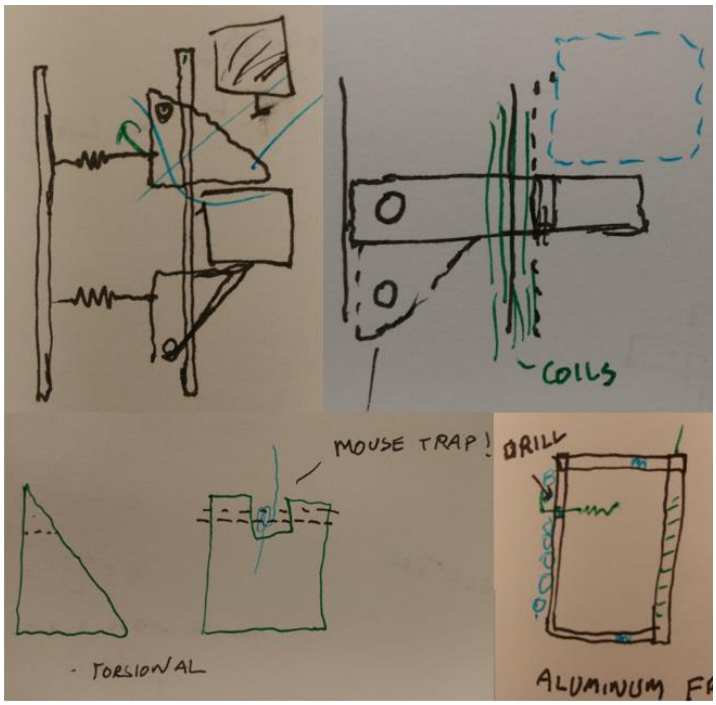

Figure 14. Methods for supporting the coils in a removable fashion

To allow our cage to effectively verify the ADCS, it must have a rotational mechanism. While this portion of the Helmholtz cage was cut out of the scope, the ideation process may be helpful down the line should this capability become necessary. Many concepts for rotational mechanisms were developed that allowed up to three degrees of rotation. The first one thought of was the 'piñata' method which is a mechanism previously used by the PolySat ExoCube team. Other concepts were variations of gimbals, air bearings and combinations of the two all with the desire of achieving two or three degrees of freedom.

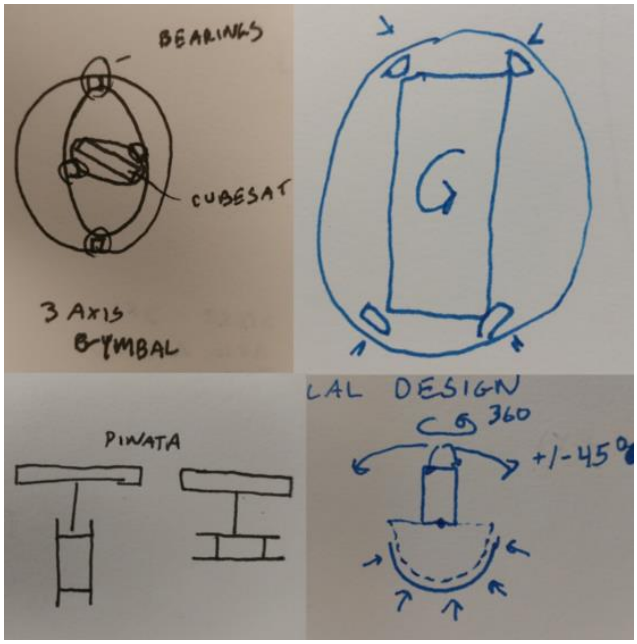

Figure 15. Various rotational degree of freedom schemes

The 'piñata' method would be composed of a string hanging the CubeSat from the top of the cage. This would allow the CubeSat to rotate freely in the z-axis about wherever you attach the string to the CubeSat. This method is simple since the only limiting factor would be finding a string made of a strong enough material to withstand the weight of the CubeSat which could be up to 60 lbs., and adding a bar from which to support it. The drawback would be that verifying ADCS couldn't all be done in one step, there would have to be three separate steps of rehanging the satellite to have it rotate about its own X, Y and X axes.

The gimbal was going to be a fixture for the CubeSat made up of metal support structures and low-friction ball bearings to eliminate the resistance to motion in up to three axes of rotation. This sort of device would be very hard to manufacture as it requires large, rigid cylinders to hold on to the satellite during testing. An air bearing was considered to be used as a way of allowing multiple degrees of freedom of the satellite while verifying the ADCS. Studies on air bearings have reported a coefficient of friction lower than that of a ball bearing by a factor of 10. All that is needed for an air bearing is an air compressor and a fixture that withstand the pressure from the air compressor while providing an air film thick enough to allow no contact to the object being supported. An air bearing could be in the form of two flat plates with one levitating on top of the other or a spherical air bearing could be used which a ball is floating inside a bowl shaped support that has the compressed air flowing through it. For both a gimbal and an air bearing, it's ideal to get the COM of the object being levitated aligned with the axis or axes of rotation of the gimbal or air bearing. This allows the inertia to be as small as possible which is important since the satellite should be in a micro-gravity state.

Achieving a cleanroom environment within our Helmholtz cage opened the door for very little ideation, as it must follow the standards for a class 100,000 cleanroom. With what freedom we did have, we considered hanging the walls along the outside of the cage, or within the inner square formed between the intersections of the X and Y coils. For the top and bottom we looked at designs consisting of interchangeable plates for deployed and stowed states, as well as an elastic cover that could move with the cage as it transitioned from one state to another. A result from our PDR presentation with our sponsor brought the idea of a clean room box to the table. This would be a much smaller, easier to clean environment that allows the spacecraft to be kept clean outside of the clean room while not having it installed in the cage.

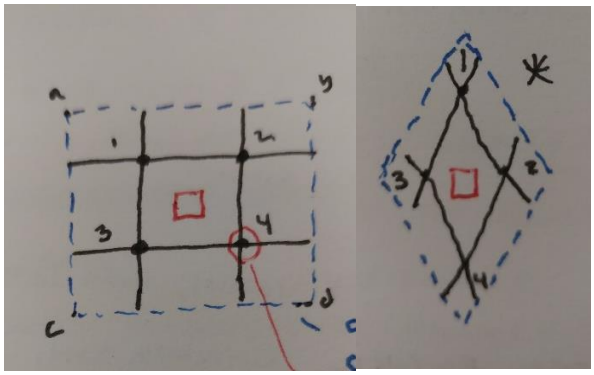

Figure 16. Top view of cage with cleanroom curtains (blue). Curtains may be hung between points 1, 2, 3, and 4

3.1.2 Electrical Ideation

A printed circuit board would need to be designed to interface with the software GUI and the physical cage. The PCB will be populated with connectors to the computer, the power supplies, and the coils of the cage. A microcontroller will interface the user inputs and communicate the current necessary to generate the desired magnetic field per coil to the hardware. The microcontroller will control a current controller to regulate the current to each coil for each axis. A feedback system will also be designed to minimize the effects of external noise. Designing a power supply was also considered.

A wire gauge of 13 AWG was picked for the magnetic copper wire. The maximum current for the coils was set at 5A per coil for safety considerations. 13 AWG wire has a current limit of 20 A. Calculations were done assuming a 50% factor of safety, which is a current limit of 10A. The 50% factor of safety will prevent using the magnet wire to its limit such that the wire can be used for a longer period of time before having to be changed.
The following equation was used to determine the number of turns per coil, N, with a magnetic field, B, range of 100 µT to 150 µT: $B = \frac{4\mu_o NI}{\pi a(1+\gamma^2)\sqrt{2+\gamma^2}}$, where a is the half the coil length, μ_o is the permeability in a vacuum, and γ is the relationship between the coil length and the distance between the coils. With the coil lengths set to be 34", 36", and 38", the associated number of turns and wire lengths are shown in Table 2. Extra turns will be added to round off the calculated number of turns into whole turns. Extra turns can also be added to account for calculation error.

Table 2. Number of Turns and Total Wire Length per Coil

Coil Length [in.]	Number of turns for low magnetic field (100 µT)	Wire Length [ft.]	Number of turns for high magnetic field (150 µT)	Wire Length [ft.]
34	5.2	61	7.9	91
36	5.6	68	8.5	102
38	5.9	76	8.8	113

After the preliminary design review with our sponsor and some PolySat members, it was suggested to include heat sinks to help dissipate heat on the PCB from the high current. Other wire gauges were also suggested to be considered to bring down cost and weight from the coil bundles.

Initially, the complexity of the electrical systems required a powerful microprocessor, and the 32 bit arm family of the ST processors was selected. This line of processors featured enough peripherals and clock speed to manage the closed loop control of three coils controlled with a moderately complex power management control system, and possibly calculate basic behaviors of an orbital simulation. As the scope of the simulations shrank, the responsibilities of the microcontroller receded until only basic communication controls were needed. At this point, it was deemed sufficient to use a device from the ATMEGA family, which would be cheaper and easier to program and would use less physically intrusive programming methods. As the control method shifted to PWM, the microcontroller responsibilities increased, but not to the point that using an ST would provide any concrete advantages.

3.1.3 Software Ideation

From the software development standpoint, prior to the conception of the custom GUI development, integration of STK and MATLAB were considered but quickly discarded before the preliminary design review as a result of talks with users of the application who claimed it was too difficult to use and needlessly complex for our purposes. Consequentially, the idea of a custom GUI was conceived, for which three languages were considered for implementation. The three, Python, Java, and C, were selected not only for the team's familiarity with said languages, but also for their relevant structure in relation to the system architecture the GUI will be required to implement to interact with the Helmholtz cage. The choice of operating system came down to Windows 10 for, once again, general familiarity regarding its usage, and Linux for the ease of development offered to programmers. MacOS was left out of the concept generation process as the operating system itself is not available to the public for implementation into custom built workstations or small-scale computers. Initial concept design for the GUI's layout was of complex essence, given that we planned for the software to be able to take any form of orbital element data set and convert it to the relevant magnetic field information. At which point, we were left with a choice of using a world map representation of the desired magnetic field to be simulated with quantifiable data shown in Euler's angles, or a 3D graph view of the field at any given moment.

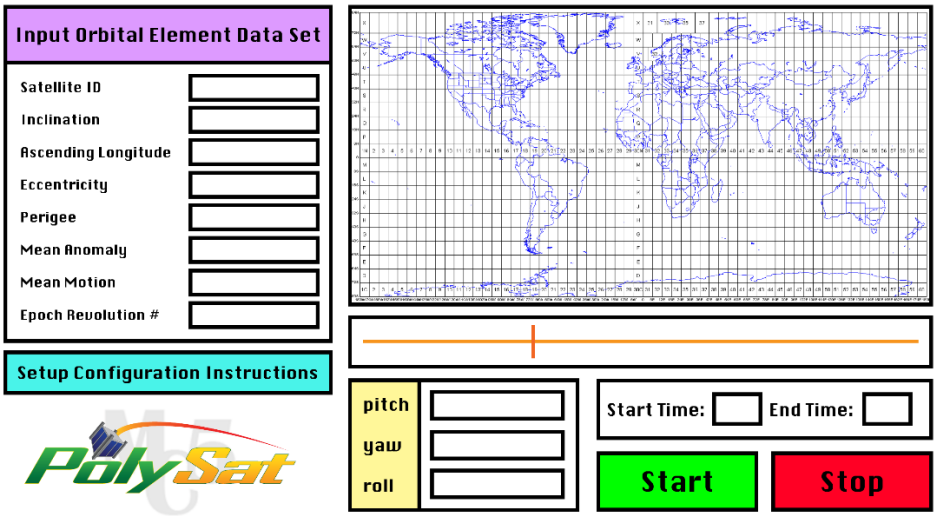

Figure 17. Original idea for GUI with world map and TLE input

Following multiple meetings with the customers and potential users, the scope of the software was reduced in complexity to accommodate more custom simulation workflows. The result was software that would simulate magnetic fields from a provided list, and alert the user to any problems that might occur during simulation.

3.2 Concept Selection

3.2.1 Structural Decisions

Once we had a long list of ideas we began the selection process through the use of Pugh matrices. This allowed us to compare ideas to one another looking at individual qualities, and see where designs are better and worse. These visual displays led group discussions on each subcategory, allowing us to make informed decisions. This selection will go over several key decisions, but a full set of Pugh matrices can be found in Appendix B.3.

The general shape of the cage was selected to be square. This decision will result in a cage that is easier to manufacture than a circular cage at the size we need. Further it should result in a volume of uniform magnetic field more representative of the CubeSats we are testing (Spherical cages make spherical volumes of uniform field, cube cages make a cube of uniform magnetic field). From a collapsibility standpoint, we opted to use the distortion method with a removable Z-axis as it allows us to keep all the coils rigid, protecting against fatigue of the magnetic wire. This will ensure the cage remains operational for a long time without replacing one of the most expensive and

time consuming parts (copper wire). A clean room box has been selected as our method for keep the spacecraft clean as in will provide a better seal than curtains on the cage, be easier to clean when we want to use it, as well as allow us to transport the spacecraft separate from the cage. The latter was an important factor for consideration as the collapsed cage was very unstable and would likely be a risk to a potentially multimillion dollar spacecraft.

The best method for achieving the rotational degrees of freedom is a spherical air bearing. We have a concept for a 360° spherical air bearing, but we cannot hold the required tolerances using our available tooling. The next best guess was an off the shelf air bearing, however this is out of our budget for this project. As a result, we chose to stick with the piñata method where the satellite is hung from a string and spun in one axis at a time. That said, we are designing the cage to be large enough to where a COTS spherical air bearing will fit should one become available.

3.2.2 Electrical Decisions

After determining some of the main minimum requirements and taking safety considerations into account, we decided to go with a COTS power supply versus designing a power supply. We decided that with currents of up to 10 A and voltages close to 40 V, it would be more reliable to utilize a power supply that has been fully tested and commercially approved. Designing, testing, and verifying the functionality of a customized power supply would also take extra time that could be used to progress the design of the controller board. So we decided to look for a single power supply rated at 40 V at 12 A. We considered purchasing multiple power supplies at lower ratings but we wanted to minimize the number of external wire connections to the PCB. However, cost for a single power supply at higher ratings was exponentially higher than purchasing three power supplies, so in the end, we decided to purchase three power supplies and wire them in series for a total of 40 V at 12 A.

All parts on the PCB will be COTS components. The coils will connect to the PCB through Molex connectors. The Raspberry Pi will connect to the PCB through a USB-B connector. The data from the user will be communicated to the coils through an FTDI and then through the chosen microcontroller. We originally decided to utilize the ATMEGA328P-MMHR microcontroller, which is the same microcontroller on board the Arduino Uno. Most of us have used the Arduino Uno microcontroller and it had the basic functionality necessary to accomplish what we needed it to do. There are two 8-bit timers and one 16-bit timer, each of which would need to be allotted to an individual coil. This would vary the resolution of one of the coils. To avoid this, we looked at other microcontrollers in the same family and found the ATMEGA328PB-MNR, which has three 16-bit timers, meeting our needs. A current sensing integrated circuit would be needed in series with each coil, thus the current limit would need to be at minimum 3.6 A. The current controlling integrated circuit would have the same requirements.

3.2.3 Software Decisions

The software oriented part of the team, knowing the GUI would need to be updated in real time at relatively fast intervals, could hence eliminate C from the choice of language for its inherently static nature. Research was conducted into Java's Maven library, whose object-oriented reusable classes boded well for a GUI's development. However, consultation with an industry software engineer led to the sentiment that Maven is needlessly difficult to develop with. Via process of elimination, Python was deemed to be the optimal choice. Not solely chosen for lack of other options, Python's QT (PyQt) framework hosts a module called PySide2, which offers a plethora of GUI development widgets, XML handling, network communication, and firmware integration options, more than serviceable to the team's requisitions.

The operating system would prove to be an integral junction in the budgeting process, as Windows 10 would require a dedicated laptop or desktop, while Linux would only require a simple single-board computer such as a Raspberry Pi (likely a difference of $1000). However, Linux, for its friendly inclination towards developing programmers, is generally unfamiliar to aerospace engineers (people who would be using the cage). For this reason, this concern was brought to potential users of the cage. In said meeting, it was established that so long as clear instructions were laid out for the software's utilization, Linux would be a suitable option, thus saving the team from accounting for a Windows-based computer into the budget. After discussions with the customer, it was established that the program should not do any aerospace-related calculations, but only display the magnetic field to be simulated. This was not a matter of functionality, but rather meant as a learning experience for those using the cage, such that they may understand what the magnetic field should look like prior to the simulation.

3.3 Preliminary Analysis & Testing

There is very little testing we could do prior to manufacturing and assembling our cage, aside from the simple prototypes built in class and shown in the previous sections. As the software team goes as we move out of high level design there is some testing that can be done on the old cage with a little bit of hot-glue maintenance. Preliminary magnetic field calculations and thermal analysis was done to get ball park coil windings and temperatures; however these analyses have been greatly improved upon for our critical design, and will be showcased in detail in the next section.

4.0 Description of the Final Design

4.1 Cage Design

The design presented in this section improves upon our preliminary design presented in section 3.2 with feedback from our conceptual design review as well as significant detailed design work to rework and optimize our design. On a conceptual level, the main structural change includes breaking an all in one package into three distinct parts, the cage, the clean room box, and the pedestal, as shown in Figure 18. The cage will serve its original function of housing the copper wire required to create the magnetic fields. The clean room box will allow the satellite to maintain a clean environment outside of the cleanroom for testing without confiding it to only be transported in the cage. The pedestal will serve as the interface between the cage and the clean room box, both aligning the satellite with the center of the cage and supporting the weight of the spacecraft. Each section will be outlined in the following sections, with detailed drawings in Appendix C.1.

The standard use case for our cage will be as follows:

- User takes the clean room box into the clean room and secures the spacecraft inside
- The spacecraft is transported to the test site, where the pedestal and collapsed cage are waiting (1-2 people)
- The clean room box is placed on the pedestal (1-2 people)
- The cage is expanded from its collapsed state (2-3 people)
- The cage is lifted over the pedestal/cleanroom box and is aligned with the base of the pedestal (2 people)

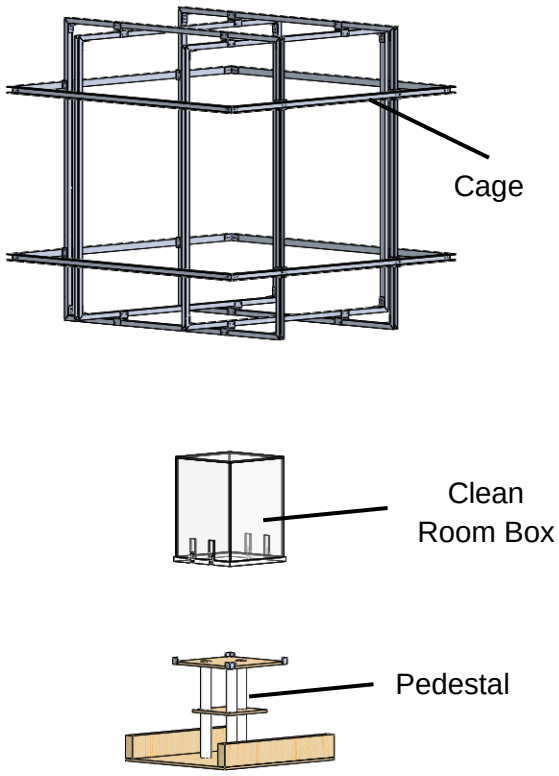

Figure 18. Overview of our final structural design

4.1.1 Cage (Part # 100000-102006)

The main purpose for the cage is to provide a structure for the copper wires that create the magnetic field. The cage its self will have outer dimensions of 48” by 48” by 46”, with coil tracks of length 46.75” by 44.75” by 42”. We have increased the size from our conceptual review by about a foot to better utilize material (U-channel comes in 8ft sections) as well as increase the uniformity of the magnetic field at negligible cost increase. The coils will be

labeled with the following convention through the report: the X direction is composed of the smallest coils, the Y direction is the medium coils, and the Z direction is the largest coils. The coils will be constructed from aluminum U-channel to provide a protected area for the copper wire, reducing the chance of fatigue failure. The coils will be fastened using rivets, as the coils should never need to be completely disassembled.

The X and Y axis coils will be mounted to one another using a translation bracket assembly, as shown in Figure 19. These brackets allow both rotational and translational degrees of freedom when collapsing the cage. It is made up of 2 U-channel stock slightly larger than the coil such that it nests around it with a 1/8" gap. We will fill this gap with Delrin pads to act as a linear bushing, as shown in the exploded view in Figure 20. Initially we looked at Teflon as a bushing material, however opted away from that for its poor wear resistance. Ultra-High Molecular Weight Poly Ethylene (UHMWPE) has also been recommended for this purpose as a lower friction, higher wear resistance material, and we will look closer into that before purchasing Delrin.

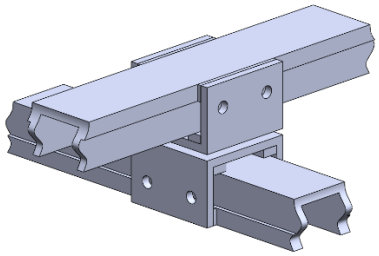

Figure 19. Translation bracket assembly

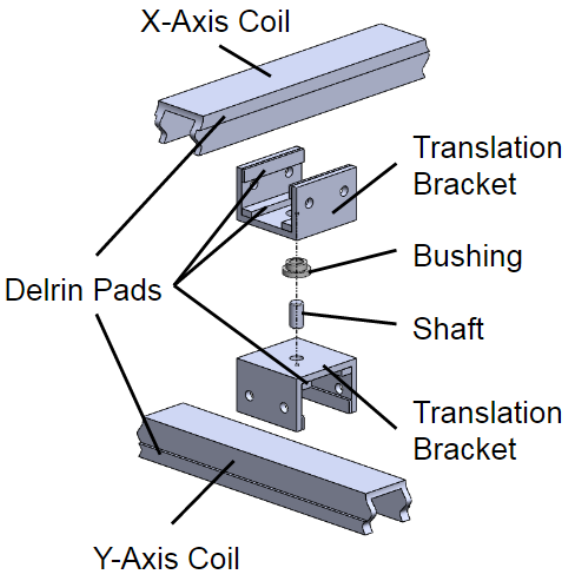

Figure 20. Exploded translation bracket

In addition to the linear bushings, a standard flanged shaft bushing has been selected to achieve rotational the rotational degree of freedom in as small of a package as possible. The bushing will be pressed into one of the translation brackets, and the shaft into the other. Again, a Delrin bushing was selected. As this is a magnetic testing apparatus, iron components were avoided at all costs, including ball bearings. Plastic bushings will not affect the magnetic field. 1/8" cotter pins, Figure 21, will be used to lock the cage into the set position, ensuring proper distances between coils for testing.

Figure 21. A cotter pin

The Z axis will be secured to the Y axis using a similar bracket, minus the rotational aspect, as seen in Figure 22. The bracket will rivet to the Z coil, and again cotter pins will be used to properly locate the coils. The same Delrin linear bushing scheme will be used for this application as well for alignment purposes.

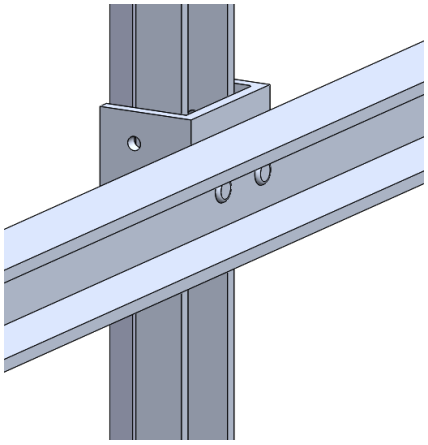

Figure 22. Z Axis attachment point

Collapsing and setting the cage will be a two or three-person job to ensure neither the users nor cage is damaged during the process. The steps are chronicled below, with color coded images:

Table 3. Collapsing Technique

Step	Image
0. Assembled Cage	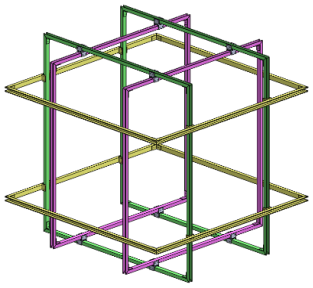

Step	Image
1. Remove the cotter pins holding the Z-Axis (yellow) coils on, one coil at a time. Lift coils off.	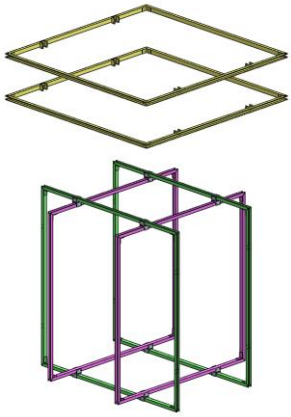
2. Remove the cotter pins aligning the X and Y axes, both top and bottom of the cage.	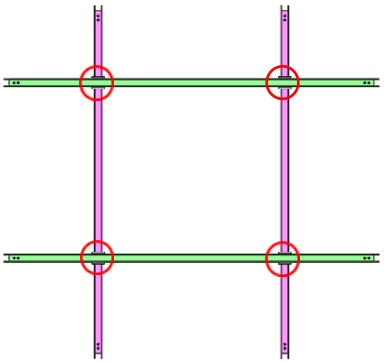
3. Collapse the X and Y axes until the Y axis is touching	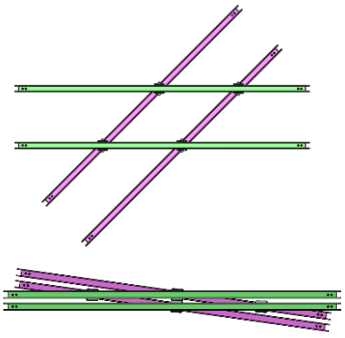
4. Place the Z-Axis coils around the collapsed X,Y axes	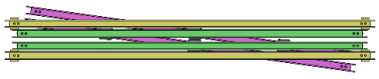
5. Completely collapsed	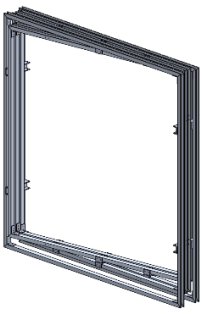

4.1.2 Clean Room Box (Part # 103000-103005)

The clean room box, shown in Figure 23, allows the satellites to be tested outside of Cal Poly's clean room. Thus, the clean room box must be able to maintain a clean environment. The box will be made from 4 walls that're 11.34" by 16" by .220", a top that is 11.56" by 11.56" by .220", and a base that is 12" by 12" by .708". The base is .708" thick to take into the extra load on it from the satellite. The top portion of the box will be made from the 4 walls and the top using epoxy. Small pieces of acrylic will be used to bring draw latches planar to the walls of the base. To create a seal, we've implemented 4 draw latches that attach to the walls and the base to close the gap between the top and base. A slot will be machined out for the O-ring which will be compressed when the draw latches are closed. The compressed O-ring will be what prevents more particulates from getting into the clean room box. Holes will be drilled and tapped into the base to allow for satellite supports to be fastened. Multiple configurations will be allowed for 1, 2, 3, 6 and 12U CubeSats to be supported.

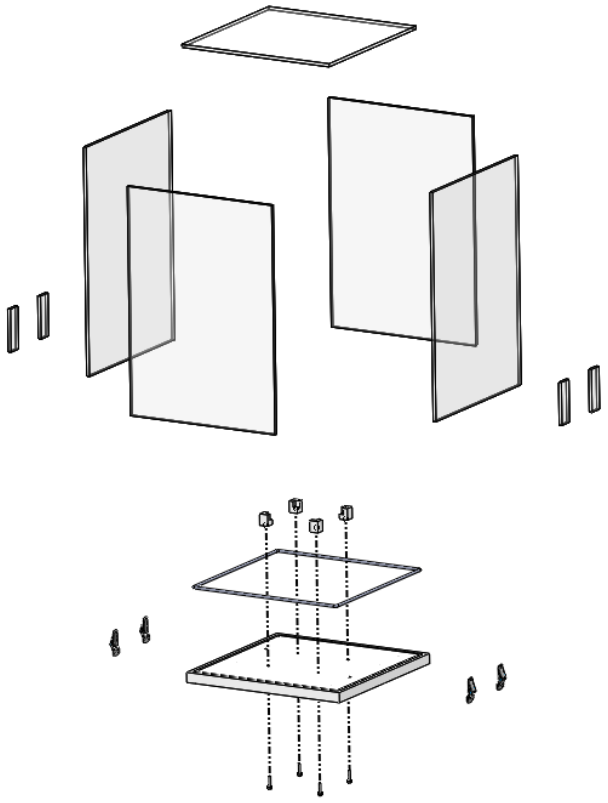

Figure 23. Clean room box assembly

4.1.3 Pedestal (Part # 104000-104005)

The pedestal, shown in Figure 24, will be made to support the satellite while centering the satellite inside the cage to make sure it's inside the uniform field. The pedestal will be made from a base, centering boards, a top board, PVC pipe and angle brackets. The PVC pipe is 6.25" OD and 5.9" ID. The pine plywood base and top will be 23.37" by 21.25" and 12" by 12", respectively. The base and top will have a hole drilled in the center of 6" to allow a .125" interference fit to secure the PVC to the base and the top fixture to the PVC. Epoxy will be used if additional securing is needed. 2x4's will be screwed to the base that will allow for a max clearance of .12" between the pedestal and the cage. Aluminum angles will be screwed onto the corners of the top fixture and serve to center the clean room box on the pedestal.

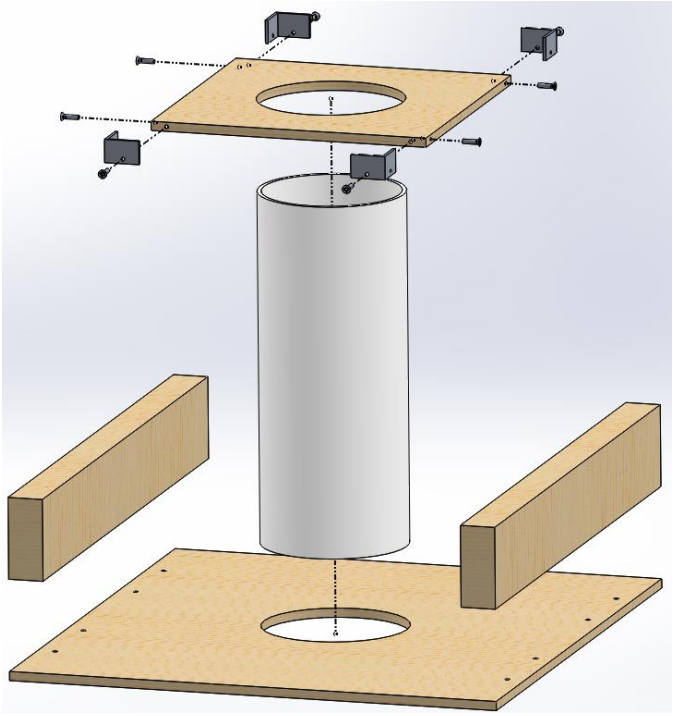

Figure 24. Exploded pedestal assembly

4.2 Rotational Degrees of Freedom

No rotational degrees of freedom will be in our design since it was not prioritized by our sponsor. Instead, we will be focusing on making our cage design compatible with a spherical air bearing that Cal Poly's aerospace department has. The base of the spherical air bearing is approximately 12" by 12" so fitting it inside will be simple. We will have to adjust the height of the cage to allow for the satellite to be in the uniform magnetic field when placed on the spherical air bearing.

4.3 Electrical Controller

4.3.1 Overview

The PCB will obtain all details regarding current regulation from the Raspberry Pi, which is powered off a 5VDC supply. The coils will be powered through three power supplies in series. We opted to purchase three power supplies and apply them in series to each other instead of one higher-rated power supply for budgeting purposes. The current to the coils will be regulated on the PCB. Each axis consists of two coils. Both coils in each axis will be wired in series and all three axes will be wired in parallel. The coils will be wired in series on the PCB and not externally to prevent discontinuities or accidental opens in the current flow. The Raspberry Pi will connect to the PCB and communicate via a USB link. A high-level block diagram for the electrical subsystem overview is shown in Figure 25. The complete schematic for the PCB can be found in Appendix C.2.

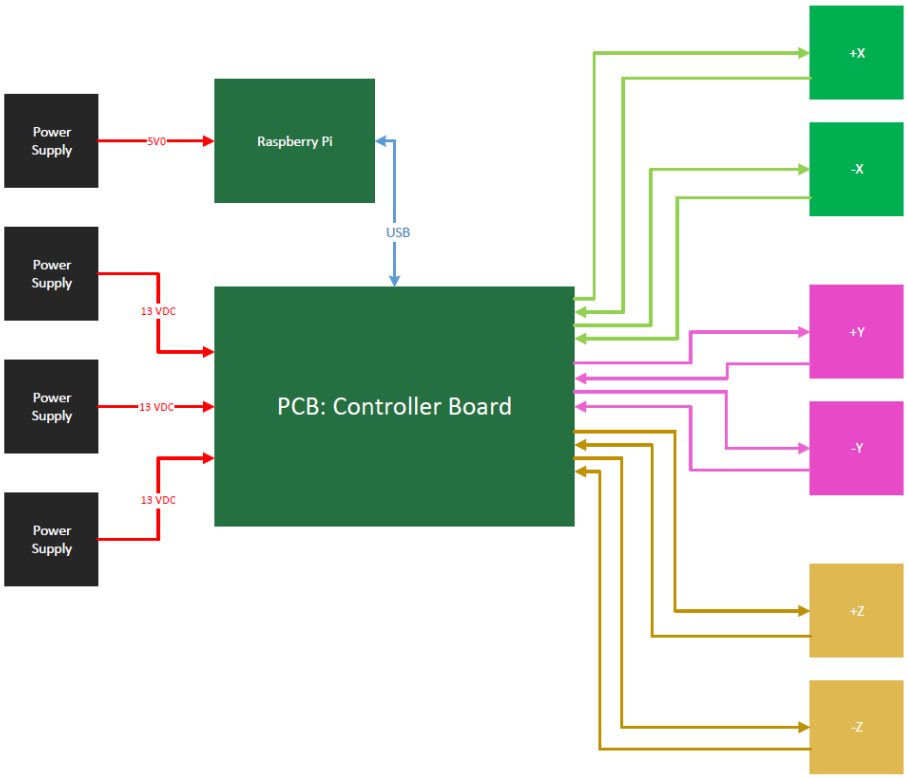

Figure 25. Electrical subsystem high-level block diagram

4.3.2 Coil Analysis

The wire gauge was revisited and we found that using 20 AWG wire would reduce cost, weight, and reduce the maximum current through the coils. 20 AWG wire has a maximum current of 7.5 A at a 50% factor of safety of 3.75 A. This allows us to operate the coils at a lower current than our original design, which is preferred due to limited availability of integrated circuits at higher rated current limits. The 18 AWG wire is slightly more expensive, operates at a lower voltage, and has a lower power consumption than the 20 AWG wire. However, a bundle of 18 AWG wire requires 5 A for operation. An active and currently sold current controller component that operates at 5 A could not be found. The 20 AWG wire is less expensive than the 18 AWG and has a lower operating voltage and power consumption than the 22 AWG wire. This analysis can be found in Appendix F, Magnetics Attachment. With the coil lengths adjusted to 46.75" by 44.75" by 42", each coil would require, 18.6 V, 17.2 V, and 15.9 V, respectively. This would result in 37.2 V, 34.4 V, and 31.8 V per axis with each coil per axis in series.

The following equation was used to determine the number of turns per coil, N, with a magnetic field, B, range of 100 µT to 150 µT: $B = \frac{4\mu_o NI}{\pi a(1+\gamma^2)\sqrt{2+\gamma^2}}$, where a is the half the coil length, μ_o is the permeability in a vacuum, and γ is the relationship between the coil length and the distance between the coils. At lengths of 46.75" by 44.75" by 42", the associated number of turns and wire length is shown in Table 4. Extra turns will be added to round off the calculated number of turns into whole turns. Extra turns can also be added to account for calculation error.

Table 4. Number of Turns and Total Wire Length per Coil, Final Design

Coil Length [in.]	Number of turns for low magnetic field (100 µT)	Wire Length [ft.]	Number of turns for high magnetic field (150 µT)	Wire Length [ft.]
42	17.5	245	26.2	367
44.75	18.6	278	27.9	417
46.75	19.4	302	29.2	455

4.3.3 Power Considerations

With each axis wired in parallel, the minimum required supply voltage is 37.2 V. To save on cost, we planned to purchase three power supplies rated at 13.8 V at 12 A and wire them in series for a total power supply rating of 41.4 V at 12 A instead of purchasing one power supply rated at 40 V at 12 A. Each power supply will connect to the PCB through a power jack, MPN PJ-025. Heat sinks will be populated on board the PCB to dissipate the heat generated by the high current. A voltage regulator will regulate the 40 V down to 5 V to power the integrated circuits on the PCB. The high-level block diagram for the PCB is shown in Figure 26.

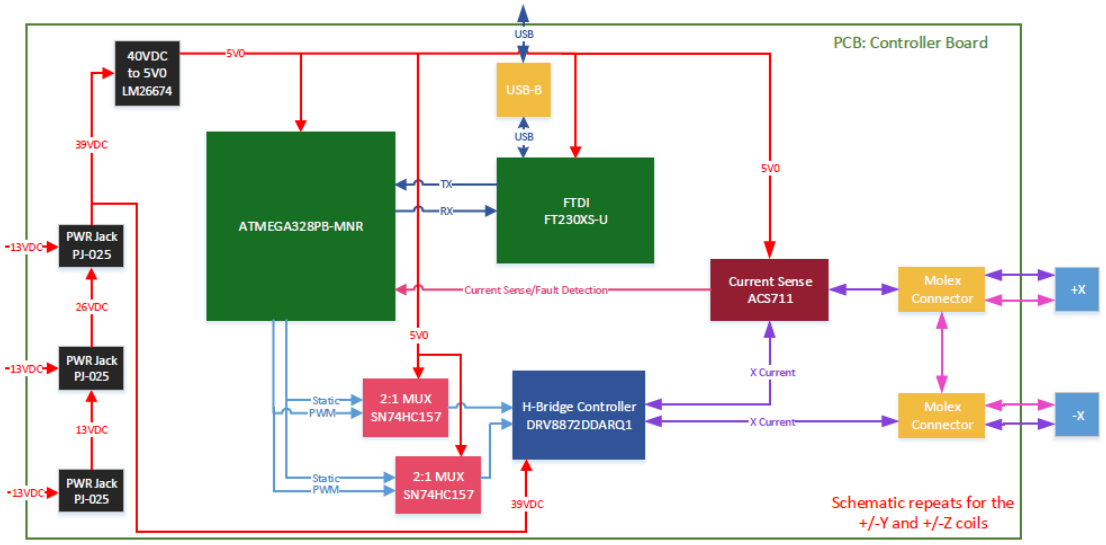

Figure 26. Controller board high-level block diagram – simplified

4.3.4 Current Control

The Raspberry Pi will communicate the user parameters to the PCB via a USB link. A USB-B will be populated on the PCB for this purpose. This connection will be wired to an FTDI, FT230XS-U, to instruct the microcontroller, ATMEGA328PB-MNR, to adjust the current by altering the frequency and duty cycle of PWM signals. The chosen ATMEGA328PB-MNR is of the same microcontroller family as the microcontroller on board the Arduino Uno. The microcontroller used on the controller board has two more 16-bit timers than the microcontroller on the Arduino Uno, for a total of three 16-bit timers. This will allow us to operate all three axes of coils at the same resolution.

To regulate the current, an H-bridge controller was chosen to have a maximum input of 45V and have a current limit of 3.6 A. The chosen H-bridge MPN is DRV8872DDARQ1. This H-bridge is designed to control DC motors. The H-bridge has controllable outputs to control the magnitude of the current as well as the direction. Varying the inputs will configure the H-bridge to operate with forward current or reverse current. The H-bridge has two inputs. Depending on whether IN1 or IN2 receives a PWM'ed signal or a static 0 or 1 will determine whether the output current is in forward or reverse. The PWM signal input will also configure the H-bridge on what magnitude to regulate the current. The SN54HC157 is a 2:1 multiplexer, which will allow us to vary the PWM and static signals from the ATMEGA to the H-bridge to control the direction of the current.

A current sensing integrated circuit, MPN ACS711, will be wired in series with the coil to detect any open circuits. This will catch set-up errors or faults in the coil. If any opens are detected, then there will be no current flow. This will be caught by the current sensor so that the operator can be alerted of the concern for analysis.

The coils are connected to the PCB with four pin Molex connectors, for a total of six Molex connectors. Two of the four pins on each connector will be used and the other two will be no-connects (NC), as shown in Figure 26. This will act as a failsafe for user error when the operator is connecting the coils to the PCB. If the operator connects the coil to the wrong connector on the PCB, then there will be opens in the loop and current will not flow through the coil. This will be detected by the current sensor and alert the operator via the GUI of a set-up error. On one connector, one pin will be an in-out and the other pin will connect to the other coil in the axis for a series connection. Figure 26 shows the connections for one of the axes. The complete Controller Board high-level block diagram can be found in Appendix C.2.

The H bridge circuitry will be controlled with the ATMEGA328PB microcontroller. The microcontroller will use three 16-bit timers to generate one PWM signal per axis. In addition, each H bridge will be prefixed by two 2:1 multiplexers. The components are connected such that each axis' H bridge can be connected to a single pin providing a PWM signal, and another pin to control polarity. The frequency of the PWM signals will not exceed 200 KHz, as specified by the selected H bridges, but the final frequency will be determined during characterization, and can be changed in firmware, or controlled by software if necessary. The duty cycle of the each PWM signal will control the intensity of their respective magnetic fields. The microcontroller will interface with the attached computer over a serial link passed through USB and converted to TTL level UART by the FTDI chip on the board.

The microcontroller will also be responsible for some safety and usability features. Each axis is equipped with a current sensor that will be used to determine if an open has occurred in the coils. In such a case, the simulation will cease and the software will be notified of the event. In addition, the microcontroller will expect a message from the computer at regular intervals. If a specified amount of time has passed between messages, the device will assume that it has lost connectivity and shut down.

The microcontroller firmware will be programmed with an AVRISP MKII or similar device over an exposed programming header on the board. The programming pins will potentially conflict with other functions, therefore those programming the device must set or remove specific jumpers before programming. This may be eliminated by writing a bootloader that will use the USB connection over FTDI to load new firmware.

4.4.1 Prototype Software GUI/Controller

The GUI is designed to be simple to use by engineers who will be provided with adequate instructions on how to operate the cage's calibrations and simulations. A drop-down menu of instructions is made available and recommended to be followed as the simulation procedure will not continue with invalid input or order of operations. It features a calibration widget to verify the coils' accuracy and is mandated to be run before any other options can be executed. After calibration verification, the user can choose between simulating in manual or sweep (automatic) mode. Sweep mode is instigated by loading a CSV file in a predesignated four column format, with rows of time, x, y, and z data. Manual mode can be triggered by inputting desired time and vector parameters to function as a makeshift time scrubber feature. Both modes are then substantiated by a simulation-loading validation module to ensure data is not of anomalous nature. This is done as a preventative measure since some simulations may be a lengthy real-time process, thus saving the user from potentially wasted time. Ultimately, the program will then output a 3D model view of the magnetic field at the specified time, which the user can then verify to be correct or not, thus completing the simulation.

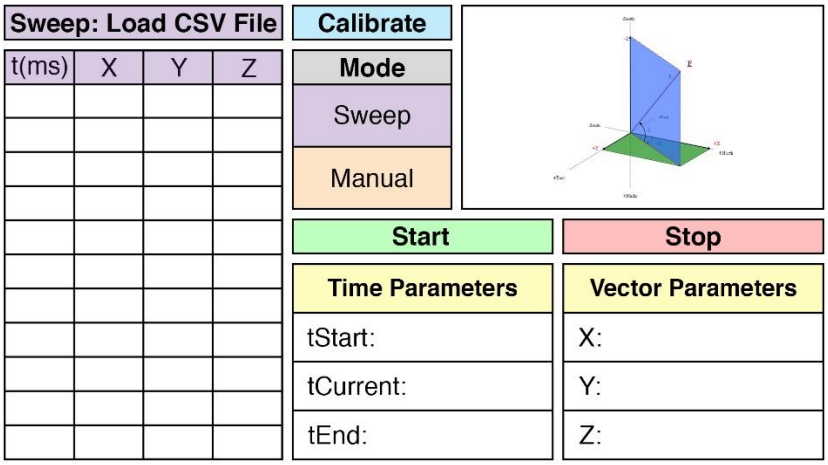

Figure 27. Final GUI mockup

Data flow (Appendix C.3) is an integral segment of the Helmholtz system functionality. At the top of the stack will be the GUI and COM module, embodied within the Raspberry Pi 3 and output to an IPS monitor for visual feedback. Information about the magnetic field to be simulated will be packaged as bytes within the Raspberry Pi, visually handled by the GUI, and transmitted to the custom produced control board. The FTDI semiconductor will receive the packet of bytes and subsequently instruct the AT Mega 328Pb 8-bit AVR microcontroller to manipulate the current within the Helmholtz cage's coils to produce the desired magnetic field to simulate.

4.5 Cost Breakdown

The budget (full breakdown in Appendix C.4, rough breakdown in Table 5.) has been divvied into structural, electrical, and software fields. A substantially smaller percentage has been allocated to the Raspberry Pi 3 and its respective accessories (~9%) due to the removal of the necessity of a fully Windows driven laptop or workstation. The electrical components have been allocated 50% of the budget due to the high level of interaction the custom PCB will be required to maintain with the other aspects of the project, being the Raspberry Pi and the Helmholtz cage's coils. Finally, the remainder of the budget (~41%) is allocated towards the structure itself, being the coils to power the magnetic field via current flow, the pedestal to support the CubeSat, and the cleanroom to protect the CubeSat upon the pedestal.

Table 5. Rough cost breakdown

Subsystem	Price
Mechanical	
Cage	$675.00
Clean room box	$127.00
Pedestal	$45.00
PCB Housing	$35.00
General and Shipping	$668.00
Electrical	
Magnet Wire	$300.00
Power Supplies	$400.00
PCB Fabrication and Assembly	$840.00
Electrical Components	$360.00
Computer	
Raspbery Pi	$100.00
Computer Components	$250.00
Sum	$3,800.00

Table 6. Rough cost breakdown

Mechanical Subsystem Components	Cost Approximation
Aluminum	$556
Plastics	$304
Storage Cart	$100
Miscellaneous (screws, standoffs, etc.)	$468
Electrical Subsystem Components	**Cost Approximation**
Printed Circuit Board (5)	$53
Electrical Components	$64
Electronic Hardware Storage Box	$27
Magnet Wire (2560 ft.)	$465
H-Bridge Controllers (3)	$45
Current Sensors (5)	$18
Power Supplies (3)	$60
Miscellaneous	$26
Software Subsystem Components	**Cost Approximation**
ST Microcontroller Nucleo Dev Board STM32F303ZE	$32
Raspberry Pi 3 Motherboard	$42
Miscellaneous Computer Components	$235
Total Cost	**$2465**

4.6 Analysis

To check our design, thermal and structural analyses were performed, followed by an optimization on the copper magnet wire. Thermal analysis was conducted to check if the wires reach dangerous heat levels. Structural analysis of the pedestal was conducted to check the safety of the satellite when being supported by the pedestal. Optimization of the wire was conducted to minimize price while reaching desired system specifications.

For the thermal analysis, the wire bundle was modeled as a single wire with insulation around it. Free convection and heat generation from electrical power were only considered. The results show that after approximately 200 seconds, the wire bundles reach 52 °C (125 °F). Then, the wire bundles will take about 300 seconds to completely cool down, and after about 1 minute the wires reach 33 °C (91.5 °), which would require ~15 seconds of contact to burn human skin. This analysis is a very conservative estimate. First, it assumes that the entire, maximum field is generated by one coil, it will almost always be a combination of the three coils. Secondly, we assume that the only heat loss occurs through free convection from the bundle itself. Realistically, the bundle will dump heat into the aluminum frame, which will basically act as fins and further reduce this temperature estimate. Given the mild results of this analysis and the generous assumptions made, no further analysis was performed. A simple thermal resistance model was used to validate this numerical calculation with nearly the exact solution.

For the structural analysis, Euler buckling analysis was performed to assess the load capacity of our pedestal. Before performing the analysis, we had to check if the PVC pipe had a slenderness ratio greater than 10 which is needed for Euler buckling analysis. The slenderness ratio for the PVC pipe was less than 10 so we checked the yield strength of our design. The yield strength of PVC was found to be 7,500 psi and a compressive stress was determined to be 30 psi. Thus, our design has a safety factor of 250 against yield.

From the optimization, we used the generic square Helmholtz cage equation and wire specifications to develop models for the number of turns required (related to cost), coil voltage, coil weight, and coil power for an array of magnet wire gauges between 14 and 24 AWG. These values were then plotted so we could make an informed decision on the optimal wire. We chose 20-gauge wire for its low cost, having a voltage under 40V for safety concerns, and okay power consumption. 18-gauge was a strong contender as its slightly cheaper, less power, and lower voltage, however its required current exceeded any easily attainable H-Bridge we could find.

4.7 Safety Considerations

The full breakdown of the safety checklist can be seen in Appendix H. The nature of the project, due to its involvement with sometimes high voltages to create artificial magnetic fields, inherently requires precautions regarding electrical hazards.

The other main safety consideration is the creation of pinch points in the collapsing and expanding of the cage. These points are unavoidable in a collapsible design, but we ensured that they are well marked. Further, we recommend that the cage is assembled in a quiet environment so that the multiple users can communicate with each other effectively should an issue arise. The cage will get warm during use, but will not be hot enough to burn you as proven through testing in section 6.5.

4.8 Maintenance

Minimal maintenance of the device will be required due to its relatively infrequent use. There's a chance that the linear and rotational Delrin bushing would require replacement but that is unlikely. The cage itself will likely have to be calibrated before each use, as transportation would have involved collapsing and subsequent expanding of the coils, which may desync the magnetic field calibration data. There will be minimal stress to the magnetic wire in the coils. This is due to the coils being set in the aluminum channels. The user will not have to move the bundles of magnetic wire for operations nor for storage. The PCB and on-board components will be enclosed in a box and there should be little to no contact between the user and the PCB. The only contact would be to plug in the Raspberry Pi USB, the power supply power jacks, and the Molex connectors to the coils. The most attention should be applied to the Molex connectors to the coils since they will be plugged into the PCB and unplugged, possibly multiple times in the case of user error, for each use. The software will be developed in such a fashion that it will be portable for porting to new platforms should some component in the data flow process die, thus it will be maintainable via generic abstraction.

5.0 Manufacturing

5.1 Design Changes

One change that we made is the location of the UHMW PE pads within the translation bracket. Rather than placing 1/16” sheets on both the bracket and the coils themselves, we used a single piece of 1/8” instead. Most of these pieces were placed on the brackets themselves, to make gluing easier. Table 7 shows which pads are required on each bracket. Four of each configuration were required.

Table 7. Configurations for translation brackets

Bracket Location	Bore Size	Bottom Pads	Side Pads
X – Top	Large	No	No
X – Bottom	Large	Yes	No
Y – Top	Small	No	Yes
Y – Bottom	Small	Yes	Yes
Z	Two Holes	No	No

Strips of closed-cell foam were added to the bottom of the cleanroom box's lid to help provide a seal in addition to the O-ring. This was done because the clamps could’ve provide the force to create a seal via compression of the O-ring without the epoxy between the base and the clamp failing in shear.

Spacers for the translation brackets were made from leftover UHMW PE to prevent the translation brackets from falling while collapsing the cage.

An aluminum plate was manufactured to fasten to the Pedestal base to lower the center of gravity and to enable an interference fit to easily be used to join the PVC to the base. Another aluminum plate was manufactured to put onto of the PVC that would allow the cleanroom box to be mounted to the pedestal using bolts. As A result, the interface on the base plywood change, as well as the length of the PVC pipe.

On the cage, we used plates to support the corners of the coils rather than the L brackets that are proposed in this report, compared in the figure below. We thought this would be an easier way to assemble the coils, but this complicated the UHMW PE bushing locations as defined above. If we had continued with our original plan this could have been avoided, and hence we did not change our recommended design.

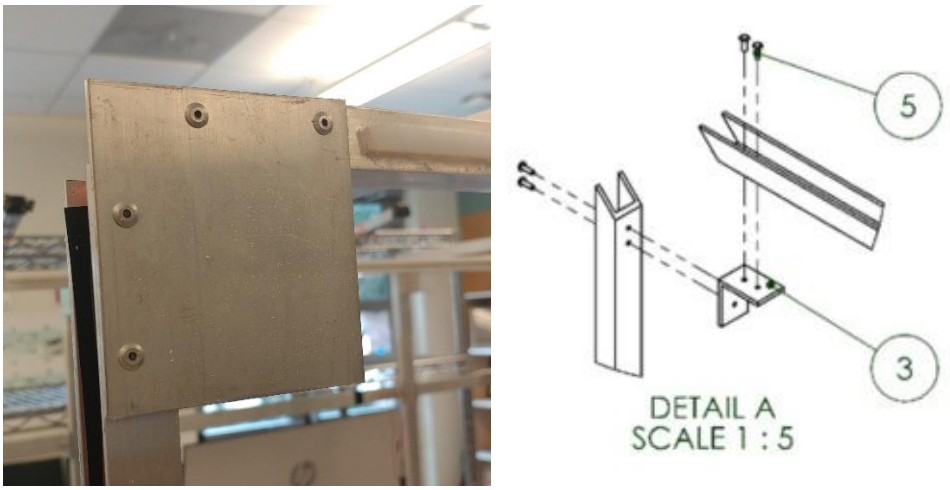

Figure 28. Manufactured design vs. Proposed Design

5.1.1 Electronics Changes

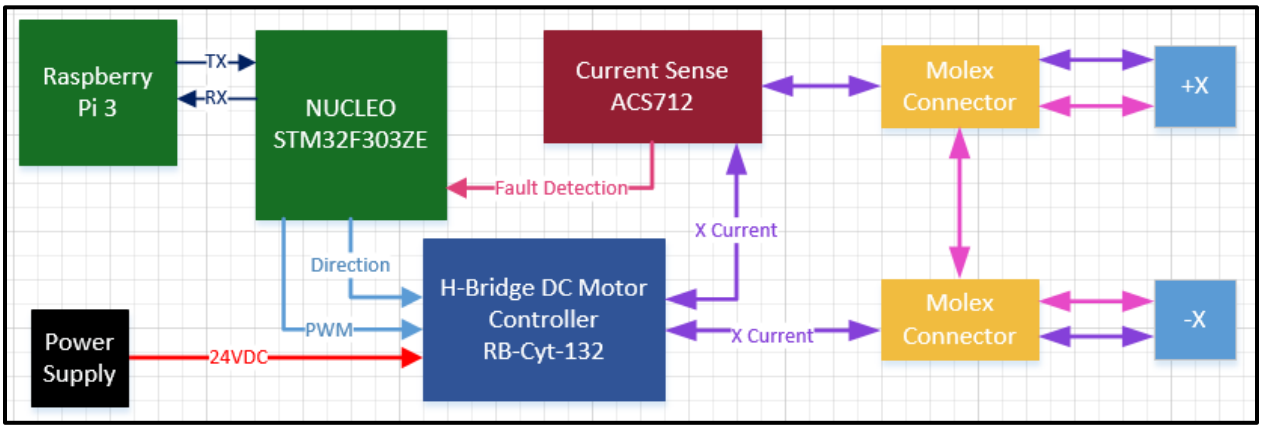

Figure 29. Updated controller board high-level block diagram – simplified

The electrical system did not change conceptually. The design still consists of a microcontroller driving the direction and magnitude of the current through the H-Bridges. That current is then directly delivered to each axis to generate a magnetic field. The main difference is that instead of designing a single PCB with all of these components, we decided to purchase development boards for each main system: the ST Microcontroller, H-Bridge Motor Controller, and Current Sense development boards. The high-level block diagram depicts how each subsystem communicates in Figure 29. This made it possible to start testing sooner instead of waiting for a PCB to be fabricated and shipped. In addition, purchasing and using development boards decreased design time. The PCB would have taken a significant amount of time to design. There is also a higher chance of the development board being functional for its intended purpose since each board has reviews from other users and has heritage. Designing a PCB risked losing unexpected time to troubleshooting and getting another revision of the PCB fabricated.

Figure 30. Electronics box

Figure 30 shows the placement of the development boards in the electronics box. From left to right: ST Microcontroller, Cytron H-Bridge DC motor controllers (one for each axis), current sense boards, fail safe and connector board. The ST Micro connects to the left side of each H-Bridge DC motor controller, each board requiring a direction control signal, a PWM control signal, and a ground. The right side of the H-Bridge DC motor controller connects to the power supplies and the fail safe and connector board. Due to time constraints, the current sense boards did not get included in the program. Each axis is powered by a 24V 13A power supply; each power supply powers an H-Bridge DC motor controller. The H-Bridge motor controller has a voltage input range of 5-30V and can drive 13A continuously, with a peak of 30A for a maximum of 10 seconds. The H-Bridge DC motor controller outputs the PWM controlled current to the fail safe and connector board via screw terminals. The current is

delivered straight to the coils via four-pin Molex connectors. In series with each axis are fuses, which serve as a failsafe in the event that the current is driven too high. Each coil occupies two pins of the four-pin Molex and each axis has the same configuration. The other two pins are left floating. This makes it such that if the user connects a coil into a connector for the wrong axis, there will be an open and a magnetic field will not be generated. Figure 31 shows the pin designations for the fail safe and controller board.

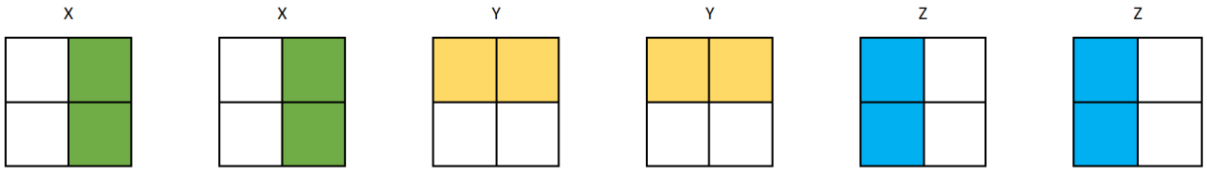

Figure 31. Connector Configuration

5.2 Software Development

The underlying architecture of the original GUI was developed using non-standard Python libraries. The bulk of the visual data processing was handled by the MayaVI engine, a scientific data visualization engine based on pipeline architecture similar to that used in Envisage. An unfortunate obstacle was encountered towards the end of the development process when it was discovered that VTK (an open-source visualization tool kit mandatory for MayaVI to properly function) is no longer in sync with MayaVI's build dependencies (i.e. the VTK module could be individually installed but would not be recognized by MayaVI even after PATH modifications). After several weeks of attempting to debug these two libraries' previously-nonexistent compatibility issues, it was determined that there was no longer any time left to be allocated towards debugging the build, and as such a less refined C program (Appendix C.4) was created to handle the calibration simulations. The functionality is the same, minus the visual feedback of the magnetic field in real time. Development took place on the Raspberry Pi 3 Model B.

In addition to the problems found with VTK, there were other problems found with the python Qt bindings. The UI prototypes were initially created with Python 3, PySide 2, and Qt 5.6. After porting the prototype code to the Raspberry Pi for a second stage of development, several issues were found with this approach. Firstly, the operating system chosen to run on the Pi did not have packages for the required version of Qt. The initial solution to this problem was to build the libraries from source. However, the Raspberry Pi took several hours to compile each library, and would not report failures until all steps had been processed. The next approach was to cross-compile the required libraries on a faster machine. While this was a viable solution for the Qt libraries, the PySide library had a much more complicated build process, and it was evident that creating a build procedure would take more time than was available.

After it was judged that there was not time to develop a build procedure, the versions used were downgraded. This form of the UI used Python 2.7, Qt 4.8, and PySide 1. This allowed development on the Raspberry Pi to proceed, but also required a re-configuration of all development environments. Ultimately, a visual layout for a UI was finalized, and functionality was added to load and display CSV files, and provide basic validation for the setting of a local offset. This UI can be seen in Due to time constraints, development was paused before there was time to create a communications module for the UI. A full repository with history for the UI is available on the Raspberry Pi.

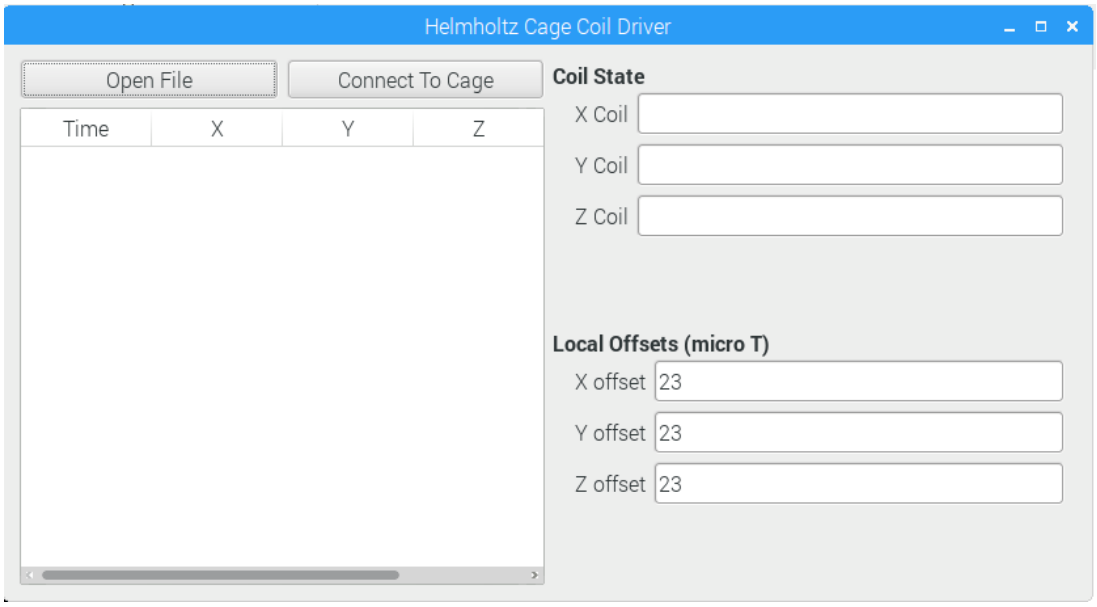

Figure 32. Qt Gui for driving coils

The aforementioned C program's design is as follows. The user runs an executable with a CSV file of the designated four column format. Any file extension not matching ".csv" will be rejected and prompt the user to fix it before using the interface. This is to prevent otherwise invalid files from sending potentially harmful data to the coils down the line. The CSV file is then analyzed line by line to scan each row of entries into a two-dimensional array. If any line is deemed to be of invalid format (less than or more than four entries), an appropriate error message is printed, and the program will continue to scan all further lines until the file has been thoroughly analyzed. If an error was encountered at any point, all error messages will have already been printed (to be subsequently fixed by the user) and the program will exit. At this point the CSV file stream is closed. The serial port for the Pi to communicate with the NUCLEO STM32F303ZE (the ST microcontroller) is then opened (/dev/ttyS0) with the appropriate termios options initialized and the baud rate synchronized to 57600. The program then enters a loop to scan the previously filled double array and analyze each entry of the line individually.

```
1,149.98,-150,125.01
2,-100,150,100
1,-100.001,-149.999,-126
```

Figure 33. Valid sample entry lines in a .csv file

The first number is set to be the time delay between current interpolations to be multiplied by 1000 to milliseconds. If at any point an invalid number is encountered in the second, third, or fourth column (not between -100 and -150 or 100 and 150 μT), the program will indicate the error (and which line it occurred on) and immediately exit. Each vector entry is first scanned to determine its negativity or positivity. A 0 is assigned to an 8-bit unsigned integer for a negative entry, or a 1 for a positive one. The magnitude itself is then linearly assigned a value between 0 and 1800 (hardware limited representation of the magnitude for the ST to read) from the determined scale limits of 100 and 150 into a 16-bit unsigned integer. The process is first conducted for the line's second entry (the X vector), then repeated for the third and fourth entries (the Y and Z vectors). The six integers are then consecutively sent to the ST for translation into a signal for the coils. The process as a whole then loops back until every line in the array has been fulfilled. Upon completion, the UART0 file stream is closed and the program exits successfully.

5.3 Microcontroller Development

The ST microcontroller receives a package of bits from the Pi according to the user's given vectors at an unspecified rate of time (each package is received at the user's specified time delay, so the coils can be fluctuated as fast or as

slow as desired). The microcontroller then translates the first 8-bit unsigned integer into a signal the X-axis motor controller will use to determine whether or not to flip the direction of the current (positive or negative). The microcontroller will then translate the first 16-bit unsigned integer (between 0 and 1800) into a magnitude for the motor controller to send to the X-coils (between 100 and 150 µT). The two previous steps are then repeated for the Y and Z coils, in that order. Once all six bit packages have been received, translated, and sent to the motor controller, the process will wait for the Pi's time delay to end and subsequently await the next packages of bits.

These magnitudes were translated into duty cycles of a 20 KHz PWM signal that was sent to the H Bridges. The direction was directly translated to an on/off signal sent to the direction pin on the H Bridges.

Development on the ST utilized the HAL libraries also provided by ST. These libraries were licensed for free user and distribution. However, as they are several thousand lines long, they were not included in the report, and were saved in a repository available on the Raspberry Pi.

5.4 CNC Manufacturing

During the manufacturing phase, we manufactured four distinct parts on the CNC machine. These parts included the translation brackets (two configurations), the aluminum pedestal base plates, and the clean room box base. The CAM'ing was done using the HSMWorks add-in for Solidworks, the standard software within the PolySat lab. The translation brackets were machined from 1.5" by 1" by 1/8" U channel. We only machined the bores on the base of the U, for the interference fits for the shafts and bushings, depending on the bracket. We made 9 of each to allow mistakes during the pressing or assembling process. We varied the diameter of the bore around the bushing until we got a good fit in the aluminum and were able to slide the shaft through with easy, a -.003" fit. We had to create a fixture to hold the brackets in place while machining. This was done with soft jaws as seen in Figure 34. We machined a channel into the soft jaws on the right side that we could slide the brackets into and indexed the inner corner of this fixture. This allowed us to quickly swap out brackets and not need to touch off on individual parts, saving lots of time off a run of 18 parts. We included a similar slot on the left side of the soft jaw to load a second part. While we did not machine the second part, it balanced the vice, ensuring we had a good grip on the part we were machining. If this second slot was not present, the vice would be torqued, meaning only a line of gripping force, rather than a plane.

Figure 34. Fixturing for the translation bracket.

We used the same soft jaws to do another operation on the brackets after attempting to assemble the cage. The U-Channel for the brackets got bent while doing the initial cutting on the chop saw. To correct this, we loaded the parts the other way in the soft jaw, such that the U was facing up, and used an end mill to clean up the sides. We ended up making the slot 1.308" in width, allowing for the thickness of the epoxy bonding the UHMWPE pads. These dimensions have been fixed in the drawings attached. With the soft jaws machined from the prior job, this adjustment was fairly quick to do, only a couple hours in shop. The finished parts can be seen in Figure 35.

Figure 35. Finished translation brackets

The remained of the parts involved machining 12” by 12” plates, so we completed the CNC’ing in one more day in the shop. A 12” by 12” plate does not typically fit in the jaws of a vise. The standard method for doing this would be clamping the part directly to the table. Being as both of the parts had through holes, we would have needed a sacrificial plate underneath it. Clamping to the table also requires you true each plate individually, a time-consuming process. To avoid this, we tried mounting the tall soft jaws to the backs of the vice rather than the front, meaning we could reference the true vice. Figure 36 shows the soft jaws loaded on the vise and Figure 37 shows the plate loaded on top of parallels. This fixturing worked as planned, and allowed us to machine the three plates in less than 4 hours.

Figure 36. Soft Jaws loaded on the reverse of the vise

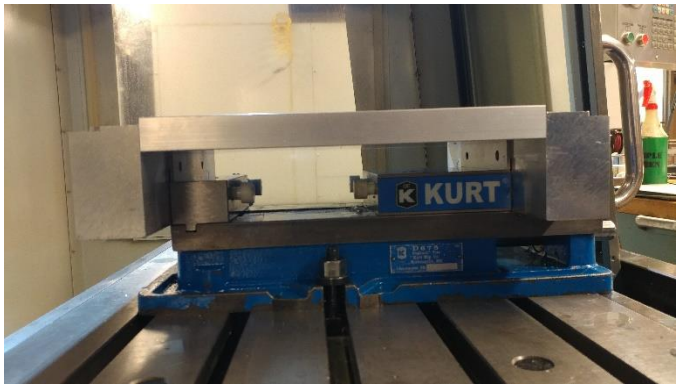

Figure 37. Side view of aluminum plate loaded in the vise.

The aluminum plate was a straight forward procedure. All features could be reached from one side, as designed. We started with the 4 mounting holes, being sure to center drill them first. This prevented wandering of the larger drill. Then we bored out the 6" counter bore. The bore was sized to a -.002" fit with the PVC pipe. The fit was very snug, but easy enough to do by hand, ensuring we were not stressing the PVC too much. If we were unable to fit it by hand we would have re-run the finishing pass with a slightly larger diameter until it fit as expected. Figure 38 shows the finished plate.

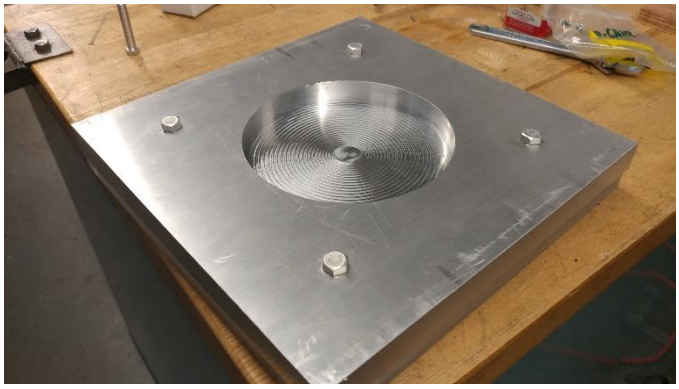

Figure 38. Completed aluminum plate with aluminum bolts in place.

The final CNC'ed part was the clean room base. This has the O-ring grove and the bolt pattern for mounting the spacecraft. The holes within the bolt pattern have counter bores on both sides, meaning we needed to flip the part during machining. We referenced the center of the plate to keep the features on the top and the bottom as aligned as possible. The cleanroom base is acrylic. For this reason, we bought a special, 62-degree drill bit made for acrylic to prevent cracking. We also ran to machine using shop air to remove chips rather than coolant, a usual procedure for acrylic. We opted to drill and tap the 3/8" holes by hand to keep cracking down. We used the CNC to drill a pilot hole with the special bit. From there I used a drill press and hand tap to finish the hole. Figure 39 and Figure 40 show the completed base, with hardware and satellite standoffs installed.

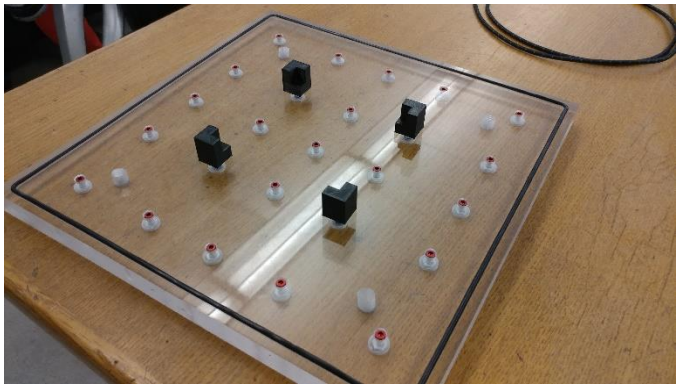

Figure 39. Top view of completed clean room base.

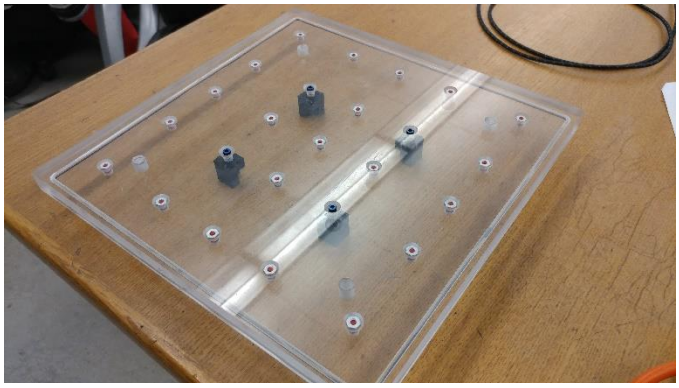

Figure 40. Bottom view of completed clean room base.

5.5 Cleanroom Box

Manufacturing the cleanroom box first involved laser cutting the walls and top of the lid from the stock extruded acrylic using the laser cutter in the Mustang ‘60 machine shop located at Cal Poly. The base of the cleanroom box was machined as detailed above using the CNC mills also in the Mustang ‘60 machine shop. To create the lid for the cleanroom box, epoxy was used to join the edges and top together. To make sure the lid had all right angles we first joined two sides then the top, which we knew were square. After the epoxy for the two sides and top had solidified, we continued to add the remaining two sides to create the full lid. With the lid assembled, small piece of laser cut acrylic were adhered to the walls of the lid at locations that would provide sufficient clamping for a seal. Repair putty was placed on top of the small acrylic pieces to create a surface and geometry that the clamps would hook onto well. The small acrylic pieces with putty can be seen in Figure 41. Foam strips were attached to bottom of the lid to assist in creating a seal when clamped.

Figure 41. Acrylic extrusions with putty attached to lid for clamps on base.

The only manufacturing to the base following the CNC'ing was attaching the clamps for maintaining a seal. The clamps were adhered to the base with epoxy and held to the top edge of the base for consistency. A portion of the mounts on the clamps were cut off with a band saw to make them shorter than height of the base or the clamps would interfere when placing the cleanroom box on the pedestal. A picture of the assembled cleanroom box is shown below in Figure 42.

Figure 42. Completely assembled cleanroom box.

5.6 Pedestal

The first part of the pedestal was the cut the base to 21.75” wide and 23.5” long to make it fit inside the cage with under .25” of clearance. Having the pedestal base fit closely inside the cage ensures the center of the base, which is where we’ll mount the satellite, be centered inside the cage. The corners of the base were cut off to eliminate interference with the brackets. 2x4’s had to be cut to make it interfere with the x-axis since it isn’t low enough to interfere with the base. The 2x4’s were cut to 20” and using wood glue were placed parallel to the 23.5” edge with an approximate 1/8” gap from the edge to allow room for the UHME PE bushing on the x-axis u-channel. The base with the 2x4’s attached can be seen in Figure 43. Holes were drilled into the base that would be used to mount the CNC’ed aluminum plate so that the center of the milled circle aligns in the center of the base. The full pedestal could then be assembled by inserting the PVC, shown in Figure 44, then inserting the top aluminum plate into the PVC. The mounting holes could then be used to fasten the cleanroom box to the Pedestal with aluminum bolts for testing. The completely assembled pedestal with cleanroom box can be seen in Figure 45.

Figure 43. Pedestal base with 2x4’s adhered using wood glue.

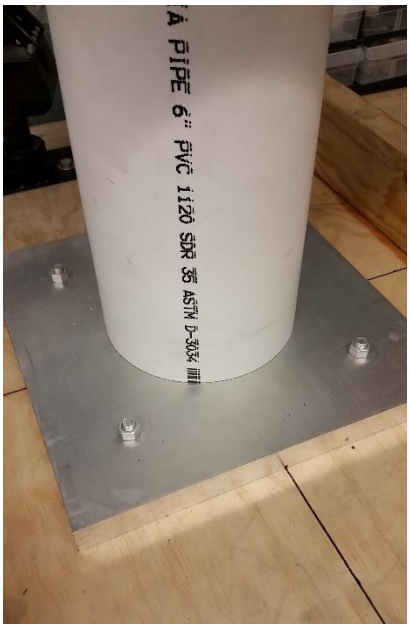

Figure 44. Pedestal base with mounted aluminum plate and PVC inserted.

Figure 45. Assembled pedestal and cleanroom box.

5.7 Cart

The cart was purchased from Costco Wholesale Warehouse in San Luis Obispo and assembled to allow storage and use of all components. The cart has 5 different levels that we spaced out so the pedestal, cleanroom box, power box, and monitor could be storage on different level. Components such as the monitor and power box were zip tied to the cage to prevent from tipping over during transport. The pedestal is stored on the bottom of the cart to add stability when moving the cart. Cut U-channels were zip tied to the top level of the cart to allow the cage to be hung off of the side of the cart when collapsed for easy transportation. Bungie cords will be used to secure the collapsed cage to the cart when stored. Electric tape was wrapped over the most outward edge of the U-channel attached to the top of the cart to cover sharp corners in case anyone was to hit their head. The completed cart can be seen in Figure 46

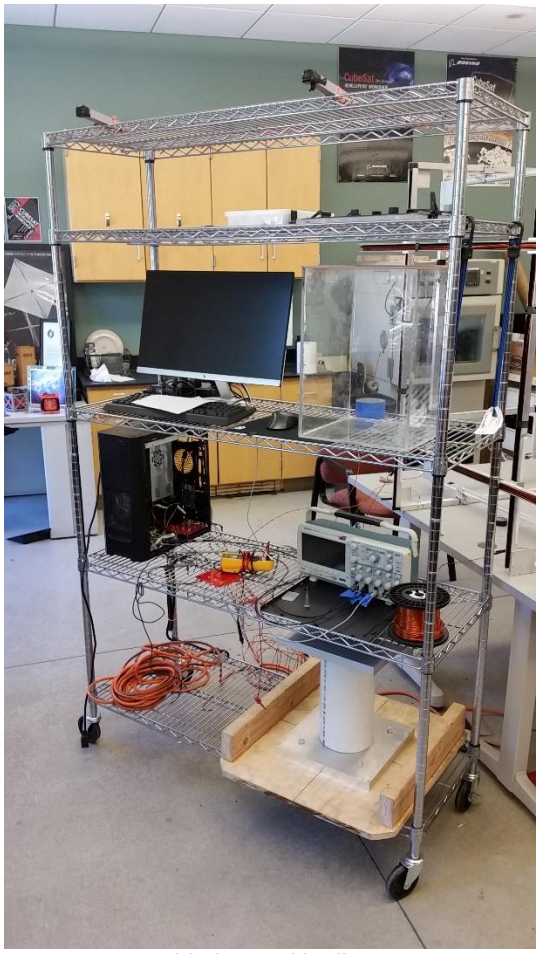

Figure 46. Assembled cart with all components stored.

5.8 Assembly

To begin the assembly, the translation brackets were CNC'ed from leftover U-channel as described previously in Section 6.2. The UHMW PE shaft bushings were shortened down to .125" on a lathe to fit inside the .378" hole without potentially interfering with cage coils. This shaft bushings were then press fit into translation bracket. Next, the aluminum shaft was cut down to .4" using a band saw. The .4" was critical as if the shaft was longer it would stick through the UHMW PE bushings and scrape on the coil's U-channel. So, the shaft had to be shorter than the bushing would provide between the two translation brackets. To help with press fitting the shaft, it was chamfered to approximately a 45° on a metal grinding wheel. Finally, the shaft was press fit into the translation bracket with the .247" hole using the manual press in the Mustang 60 machine shop. Spacers were made from leftover UHMW PE and cut to the width and length of the translation brackets using a handsaw. A hole slightly smaller than the shaft was then drilled into the center of the spacer to provide a slight interference fit into the shaft of the translation bracket. The spacer was placed in between the two translation brackets.

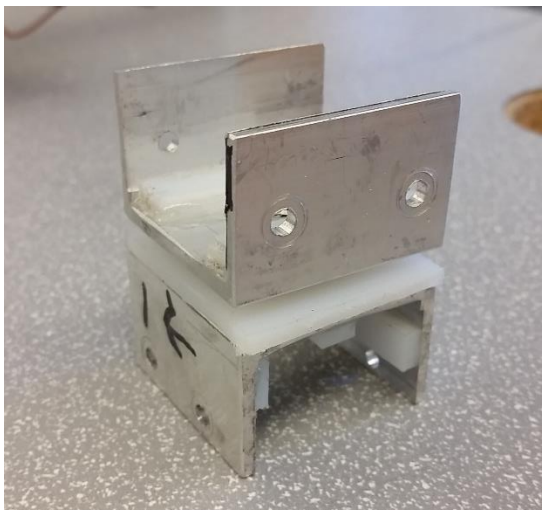

Figure 47. Assembled translation bracket with all UHMW PE bushings attached.

The next part of the assembly was the cage, which started by cutting the U-channels to appropriates lengths. 8 U-channels had to be cut for each length, 46.5”, 44.5”, and 42.375”, on the aluminum chop saw in the Mustang 60 machine shop at Cal Poly. Next, the corner brackets had to be cut from the aluminum sheet using the chop saw. With the U-channel and brackets the cage was ready to be assembled. To assemble the cage, masking tape and a right angle were used to make squares on the floor to make a template with equal sides and equal diagonalized for each of the pairs of coils. The appropriate U-channels were then lined up on the template and riveted one corner at a time with a single rivet to allow relative rotation but no translation, this help position the rest of the sides. Once all corners were riveted with a single rivet, a second rivet was placed to fix all sides of the coils. This was done for the remaining 7 coils and their respective sizes. For the Z-axis coils, translation brackets were riveted to the closed face on the outside of the U-channel so it can wrap around the Y-axis and be pinned to lock itself in place. The sharp corners of the brackets were grinded down with a Dremel to eliminate the hazard of someone hitting their head on it.

Figure 48. Cage coils assembled to perfect squares

With the coils assembled, UHMW PE was installed onto the sides of the coils and inside some of the translation brackets to help eliminate friction when collapsing. Adhering the UHMW PE to the aluminum U-channel was done using epoxy and clamps were used to apply pressure until the epoxy cured. UHMW PE was placed on two opposing

sides of the X-axis near the closed end of the U-channel, which is facing towards the center of the cage, so it wouldn't get in the way of the holes for the pins while not making the pins interfere with the wire. UHMW PE then was placed on two opposing sides of the Y-axis to help the Z-axis slide onto it. The UHMW PE also had to be placed nearest to the closed end of the U-channel for the same reasons previously stated. For 4 of the translation brackets with the shaft press fit, UHMW PE had to be placed on the inside bottom of the U-channel and the inside of the walls to constrain from side to side motion and to support the weight of the cage. For the other 4 translation brackets with the shaft press fit, UHMW PE was just put on the sides to constrain from side to side motion. No UHMW PE was placed on the bottom of the inside since it would be held up by the bottom brackets. For 4 of the translation brackets with the bushing press fit, two UHMW PE just had to be put on the corners of the inside bottom so the edges of the X-axis U-channel could rest on them. All side to side motion was already constrained with the UHMW PE on the X-axis. The other 4 translation brackets with the bushing press fit didn't need any UHMW PE adhered. All edges of the UHMW PE were sanded down with a Dremel to prevent collision when collapsing and expanding the cage. A summary of UHMW PE locations of the translation brackets can be seen in Table 7 earlier in this document.

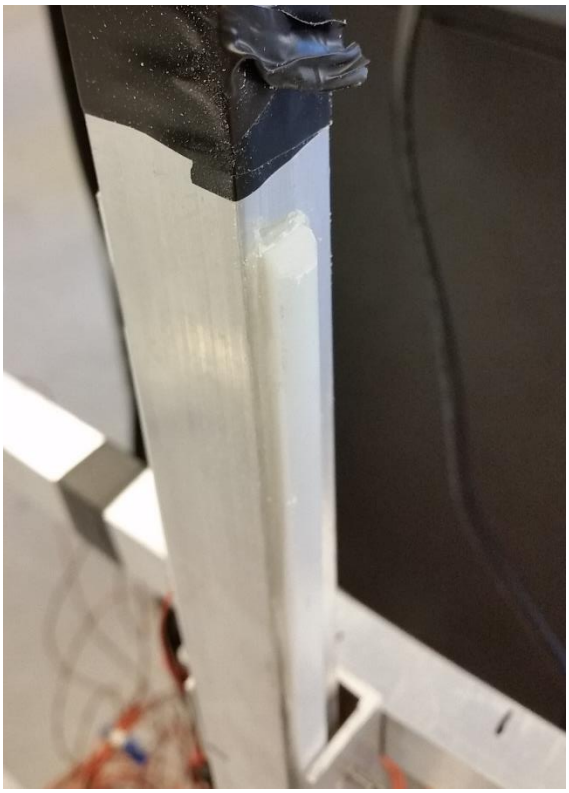

Figure 49. A close-up of the UHMW PE attached to the coil U-channels.

With all UHMW PE installed, the cage could be completely assembled and positioned to figure out locking pin locations. The cage was assembled and centered with the help of the pedestal and using the required position for the brackets taken from SolidWorks. Doing one at a time, the brackets were positioned in their appropriate locations, clamped then two holes were drilled completely through with a 3/8" drilled bit to make way for the pin. Two holes were drilled to prevent rotation of the coils relative to each other. Once the pin locations for X- and Y-axis coils and translation brackets the same procedure was performed on the Z-axis but only one pin hole was drilled.

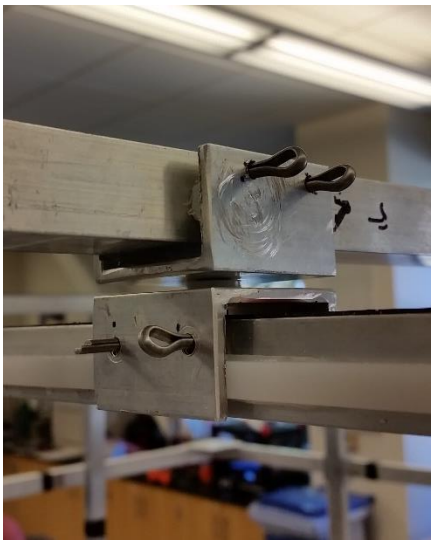

Figure 50. A close-up of the holes in the translation bracket and coil U-channel with pins installed.

Next to prepare the coil to be wrapped with magnet wire, the inside was covered in electrical tape to prevent the insulation from being scratched off. The coil was then wrapped with the required amount of magnet wire as determined in Section 4.3.2. Holes were drilled through the U-channel to allow the magnet wire to come through to the inside of the cage and have connectors attached.

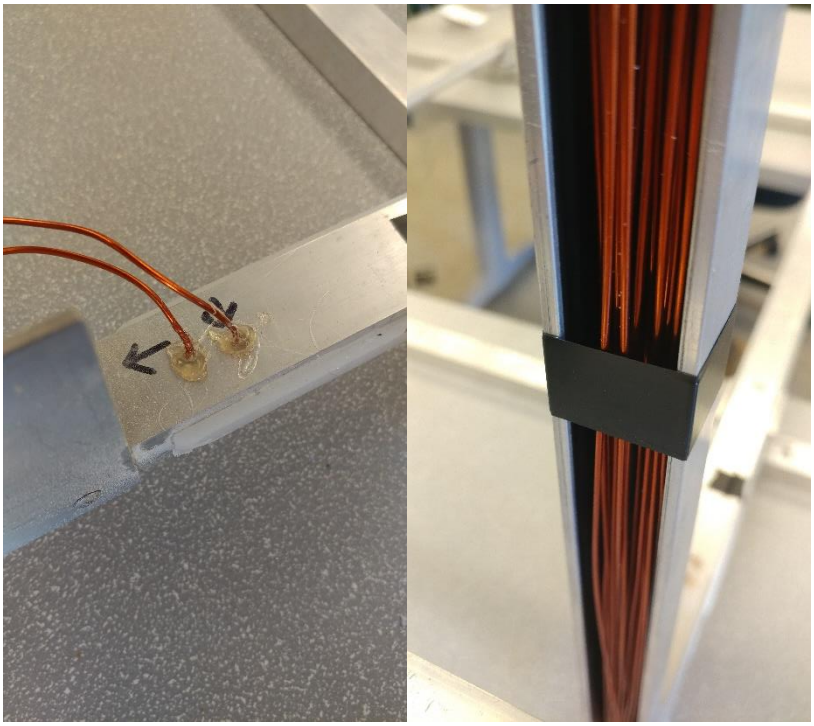

Figure 51. Magnet wire inside the coil with magnet wire sticking out for connectors to attach to.

With the coils assembled and wrapped then the translation brackets assembled the cage could be completely assembled. This required placing the translation brackets in their correct locations on the Y-axis first then sliding the X-axis coil onto the translation brackets inside the Y-axis. The X and Y axes were then aligned so the pin holes on the translation bracket were concentric with the pin holes in the U-channel. Once the holes were aligned, the pins were put into the holes to lock the X- and Y-axis to each other. With the X- and Y-axis assembled, the Z-axis was slid onto the Y-axis until the pin holes were aligned and pins were inserted to lock the position. To complete

assembly, the full cage was lifted and placed on top of the pedestal with the cleanroom box installed while aligning the pedestal base with the cage as this ensures the satellite is centered in the cage. The cart with the power and user equipment was then rolled over next to the cage and connectors from the power box were connected to the connectors on the cage.

To disassemble the cage, it is first lifted off of the pedestal and set on the ground by itself. Then the process outlined in Table 3 is followed to collapse the cage entirely. The Z-axis coils are stored on one side of the cart while the X- and Y-axis coils are stored on the other. The bungie cords are used to secure the coils to the cart. The cleanroom box is unscrewed from the pedestal and is taken back to the cleanroom if necessary to store the spacecraft and the cleanroom box is brought back to the cart for storage. The pedestal is placed on the bottom shelf of the cart for storage.

Figure 52. The assembled cage with X, Y, and Z-axes.

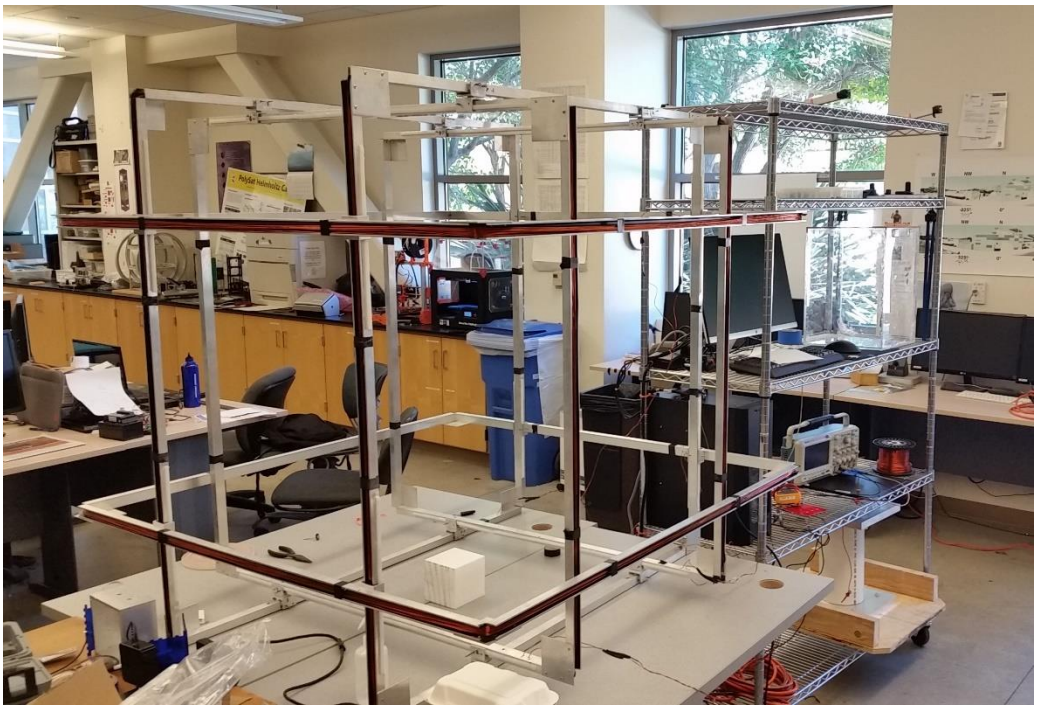

Figure 53. The complete assembly with the cage and cart with power and user equipment.

6.0 Testing Results

6.1 Testing Overview

To ensure that our cage meets the specifications derived at the beginning of the project, we created the following checklist to validate the final product, shown in Table 8. Most of the magnetic checkouts will be fully measured in the system testing phase previously described in 5.3.4 using PolySat's vector magnetometer, though this step was halted based on a ground looping issues on the H-bridge controllers. The field strength and accuracy will be measured in the center point calibration. The uniform field size will result from the spatial test. The budget presented in this report meets our cost maximum. The power requirement grew since the conceptual design review from 300W to 500W. Being as this is a safety issue, our system will be checked out be a certified electrician both in the design phase and before turning the cage on for the first time. The pedestal weight test will verify a max satellite with a factor of safety of 2.

Table 8. Verification Checklist

Spec #	Parameter Description	Requirement or Target (units)	Tolerance	Compliance Assurance
1	Generated Field Strength Range	100 µT	Min	Test with Calibrated Vector Magnetometer
2	Magnetic Vector Accuracy	+/- .5uT	N/A	Test with Calibrated Vector Magnetometer
3	Size	36cm Uniform Field	+/-1cm	Test with Calibrated Vector Magnetometer
4	Budget	$3800	Max	Well Documented Budget, BOM
5	Power	500 W	Max	Power Supply Limitations
6	Satellite Weight	60 lb	Min	Test with Mass Model
7	Tipping Resistance	50 lb	Min	Tip Test
8	Clean Room Held	Pass/Fail	N/A	Fully Enclosed Chamber

6.2 Structural Testing

6.2.1 Satellite Weight

We tested the pedestal with a 200 lb weight, a factor of safety of at least 3 over the 60 lb design specification. There were no visible deflections or failures of the pedestal. This test was a success.

6.2.2 Pedestal Tipping Test

We attempted to tip the pedestal by applying a force to the very top aluminum plate using a force gauge. On a concrete surface, it took 12 lb of force before the pedestal started to slip. There was no indication of tipping. On a carpet surface, it took 21 lb of force before the pedestal started to slip. There was no indication of tipping. Attempting to tip the pedestal with a fixed pivot point (not relying of friction), the force gauge maxed out at 50 pounds, meeting specification. This test was a success.

6.2.3 Clean Room Assurance

The validation of the cleanroom box is based off a visual inspction. All of the #6-32 holes in the mounting pattern can be plugged using aluminum #6-32 bolts and nuts, shown by the red bolts in the figure below. The larger 3/8"

threaded holes have been plugged using 3D printed plugs that were torqued then cut to be flush with the surface, the beige plugs in the figure below. The oring seal was presseded into the base, and a closed cell foam layed was added to the top. When the four clamps are closed, the foam is visably compressed, ensuring a tight seal.

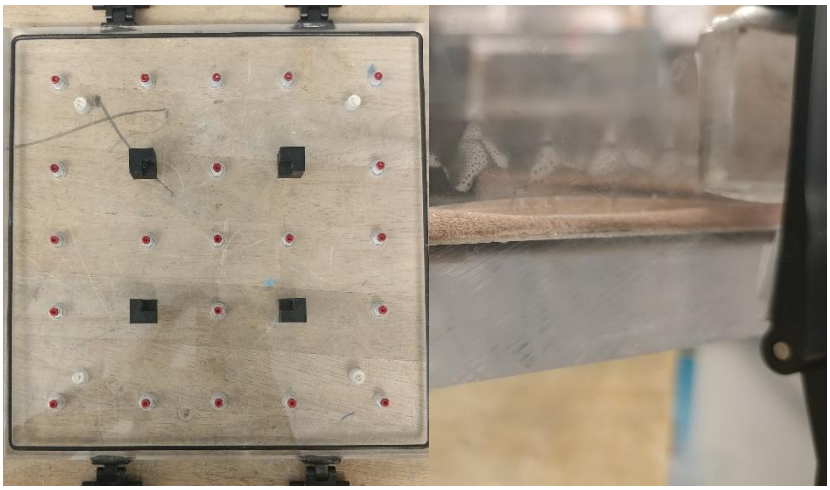

Figure 54. The complete assembly with the cage and cart with power and user equipment.

6.3 Electrical Testing

6.3.1 Concept Testing

Before assembling the entire electrical system, the development boards were configured in the proposed manner and tested on PolySat's existing Helmholtz cage. The ST Micro was configured to provide a PWM signal to the H-Bridge motor controller. The configuration successful generated a magnetic field with the existing Helmholtz cage. This test set-up consisted on a single power supply supplying the system. This test verified the functionality of the boards to generate a variable magnetic field.

6.3.2 Electrical System Testing, No Load

With the electrical system assembled, testing was conducted to verify that the PWM signal was successfully delivered to the connectors to the coils. The ST Microcontroller drove the H-Bridges and the H-Bridges were controlled by separate power supplies. Upon powering each H-Bridge, the PWM signal was successfully provided to the output of the fail safe and connector board.

6.3.3 Electrical System Testing, Load

The coils were connected to the electrical system for magnetic field generation testing. Original issues were a result of connecting the coils incorrectly to the controller board. The chosen Molex connectors were not ideal and did not consistently make electrical contact with the electronics box. The Molex connectors were removed and the coils were connected directly to the fail safe and connector board. This ensured an electrical connection.

Upon powering the system, the Helmholtz cage was able to generate a magnetic field. However, over time, one of the ground wires was determined to overheat, using a thermal camera. The ground wire would heat and smoke. After troubleshooting the issue, it was determined that the H-Bridge controller used in the design connects the grounds of all three power supplies to one common ground. This is not ideal because each power supply runs on its own ground. If one of the grounds on a power supply goes more negative or more positive than another power supply's ground, a potential difference is developed. Because the H-Bridge connected all three grounds together, the power supply tries to account for that difference, causing the ground line to overheat, as we observed. Solutions are suggested in Section 8.0.

6.4 Software Testing

6.4.1 File Format

Testing on the Pi's software began with self-contained formatting tests, with improper utilization verification ranging from files with non-csv extensions to files with non-compliant column formatting to files with out-of-bounds data in the second, third, or fourth columns. Any of the aforementioned were verified to print the respective error and subsequently quit when appropriate.

6.4.2 Pi UART Functionality

Pi testing then progressed to more self-contained verification, now looking at the proper opening of the Pi's serial communications ports. A female-to-female connector was used to connect the Pi's RX and TX pins, with an external program used to send bytes, receive said bytes, and verify that said bytes were received and in the proper order. Communication was conducted with the ST microcontroller's development process to verify the same baud rate of transmission and reception was being used. At this time, it was also verified that due to the Pi's little endianness, the sending and receiving of bytes were being read and written in the correct order (opposite configurations would have resulted in the order of the byte packages having to be reversed on either the Pi or the ST's side).

6.4.3 Pi to ST Communications

The next stage of testing moved to communication between the Pi and the ST but without the coils themselves (dummy loads of data). An oscilloscope was used to view if a current signal was properly pulsing on each respective axis. A sweeping data file was used with each axis being individually tested from 100 to 150 μT with increasing intervals of 1 while the other two axes remained constant at the lowest threshold. The pulses were then verified to progressively pulse at stronger rates. Because the only way to verify if the Pi's data was properly interpreted by the ST and subsequently sent to the coils with the proper magnitudes per axis, the testing could progress to full system testing, with the coils connected, a magnetometer placed at the center, and preparing the Pi to transmit data according to the data flow in Figure 29.

6.5 Thermal Testing

We ran a thermal test on the cage to ensure that the temperatures of the coils did not present a safety hazard. We conducted our testing on one of the Y-Axis coils using a constant current source. We set the current limit to 6.5 amps, the max design limit for the cage. A picture of the power supply setup can be seen below.

Figure 55. Thermal Test Power Supply.

We recorded the temperature of the coils every 15 seconds using a Etekcity Infrared Thermometer for 12 minutes. This is much longer than we anticipated for the cage to get to steady state, we expected it to only take 3 minutes. The transient response in these 12 minutes can be seen in the figure below. After the 12 minutes, we let the cage run. After 25 minutes the temperature had completely leveled out between 135°F and 140°F, or 60°C, varying along

the length. This is slightly higher than the 52.2°C prediction within Appendix F, as expected from the simplifications our model made. This temperature was not able to burn the user, verified by physically grabbing the copper wires with a bare hand.

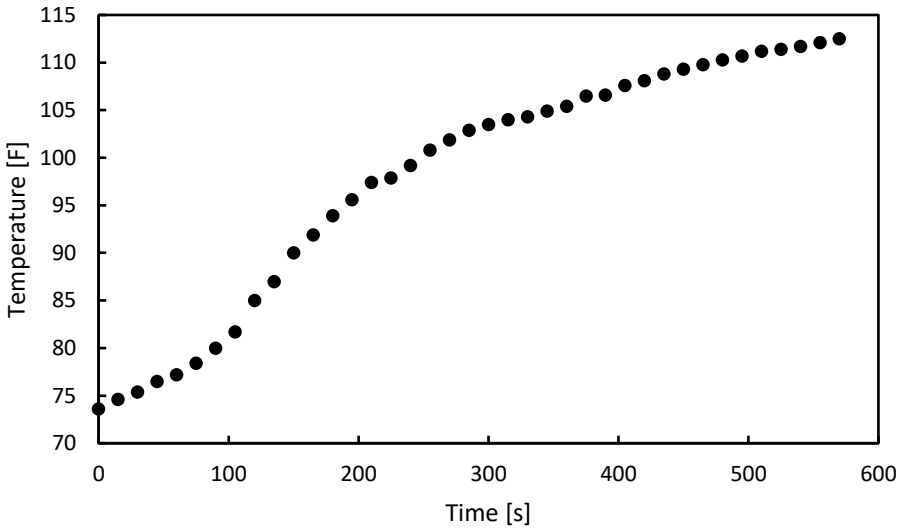

Figure 56. Transient Response of the coils.

Figure 57. Steady State Thermal Response.

7.0 Project Management Plan

7.1 Team Dynamic

The MagCal 5 Team is an interdisciplinary team, meaning we all worked towards creating a quality product for the PolySat lab. Sub-team consultants were as follows: Nicolas and Louie for software concerns, Alex and Jordan for mechanical/structural concerns, and Maddie for electrical/power concerns. With that said, all high-level design decisions were agreed upon as a group, rather than on a major by major basis, to help ensure that all subsystems are considered to be of optimal quality. The detailed design work primarily involved members working in their designated fields. Each team member agreed to put at least 7-10 hours a week towards this project during the research and design phase, and continued to dedicate that amount of time towards the final manufacturing phase. The MagCal 5 team will have weekly internal meetings on Thursdays to report research and designs to the group, and will schedule meetings as needed for special issues/deadlines. Deadlines for tasks will be determined by the entire team and each member is responsible for meeting the aforementioned deadlines.

Each member is responsible for bringing concerns to the attention of the rest of the team. After the concern is discussed, the member who brought up the concern is responsible for contacting the customer (Dr. Jordi Puig-Suari) via email (purpose being a paper trail). Contact will be conducted via the MagCal 5 email: polysat.magcal5@gmail.com. Weekly meetings with the advisor, Dr. Widmann, will be held to ensure that the project stays in the right direction.

7.2 Time Management

The Gantt chart is in Appendix G and shows our project timeline by month for the project. Once our CDR report was reviewed by our customer, we began to procure parts and quickly moved into the functionality, all the while documenting all technical specs and calibration procedures for the future members of the PolySat lab. A brief table of deadlines is shown in Table 8. All manufacturing was completed in time to display at Expo. We ran out of time for testing as we ran into previously described issues with the off-the-shelf components. We are still exploring the feasibility of design alternatives.

Table 9. Manufacturing and Testing Deadlines

Event	Deadlines
Acquire Parts	March 21st
Software Development	April 25th
PCB Fabrication/Testing	May 2nd
Manufacture Structure	May 5th
Full System Assembly/Testing	May 31st
Expo	June 2nd

8.0 Conclusions and Recommendations

The Helmholtz cage senior project is complete with its design and manufacturing phase, and has tested to the extent of its abilities that time has permitted. To show this, analyses have been performed and all designs have been documented with their respective justifications. This will also allow groups who want to improve upon our design to easily start at our report. CAD models and drawings have been developed for all parts and assemblies as well as manufacturing plans. A testing plan has also been developed for mechanical, electrical and software components. Generous time was given to manufacturing and testing to account for difficulties. From this experience, we recommend getting started on funding early to avoid any setbacks when purchasing parts. Getting started on analyses and having others double-check calculations will also prevent setbacks in design so we recommended this as well.

8.1 Electrical Recommendations

In order to resolve the ground loop issue, there are three recommended solutions. The first solution would be to purchase a new H-Bridge motor controller board that isolates the ground of the power supply from the controller ground. This would require little re-design. The new H-Bridge controller can drive 15A with an input voltage range of 3-36V. This board requires a 5V input from the controller, which the ST microcontroller provides. The new H-Bridge would be a drop-in replacement for the current H-Bridge controller. The information for the new H-Bridge controller can be found here: https://www.amazon.com/Quimat-H-Bridge-Circuit-Driving-Arduino/dp/B06X96MNQC/ref=sr_1_24?ie=UTF8&qid=1497023390&sr=8-24&keywords=dual+h+bridge+motor+driver.

A second solution is to keep the current Cytron motor controllers and use one power supply, instead of three separate modules, that can provide minimum 39A. The three axes can be wired in parallel and be driven off the same power supply. This is a more expensive option. The Pioneer Magnetics power supply is rated for 20V and can supply 40A. It is priced at $300. The original issue is that the H-Bridges connect the grounds for all three power supplies to one node. Therefore, when one of the grounds becomes more negative or more positive than another, there is a potential difference between the two grounds. This caused the ground wire between the two axes to heat up. Using one power supply for all three axes would put them on one common ground, which prevents a potential difference from developing between axes. The listing can be found here: http://www.ebay.com/itm/20V-40A-Pioneer-Magnetics-Tested-Power-Supply-20D40-PM2497A-2-Teradyne-404-936-/201453820905.

A third solution is to design a PCB that isolates the controller ground from the power ground of the power supplies. This option is potentially more expensive and will take more time to complete. The design uses optoisolators to separate the grounds. A 24V to 5V regulator would be necessary. A high-level block diagram is shown in Figure 55. This board would be placed in between the ST microcontroller and the H-Bridge DC motor controller.

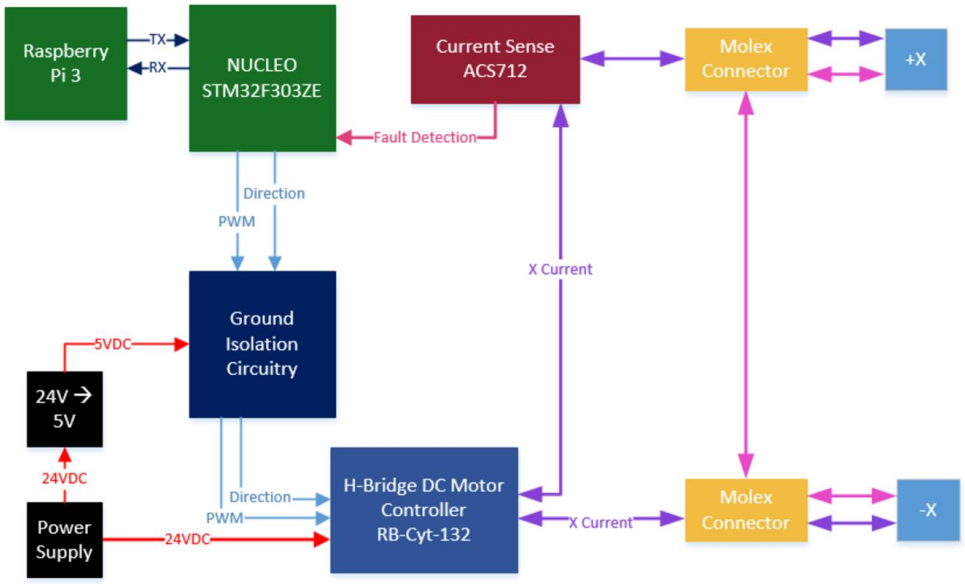

Figure 58. Suggested implementation of ground isolation circuitry.

8.2 Software Recommendations

The current C program being used to run simulations is fully capable of interpreting and sending all the requisite data required for the coils to run as intended. It is, however, terminal based and therefore not very user friendly for non-engineers. Should the user, for whatever reason, need to debug the C program, the source code has been provided. As described before, a fully functional GUI with a real-time magnetic field display of the current field being simulated and a CSV loading mechanism to potentially edit invalid data in real time was near the end of the development process before the module necessary (VTK) to build it was no longer properly supported by the toolkit (MayaVI) used to drive the display. From the standpoint of an optimal user experience, it is recommended that a user intuitive, non-terminal based, GUI be eventually implemented with the specifications. The only consideration to remember in keeping constant is the format of the data sent to the ST microcontroller (A 0/1 for the negativity/positivity of the magnitude sent as an 8-bit unsigned integer, a linearly mapped representation of the magnitude from 100-150 to 0-1800 sent as a 16-bit unsigned integer, and in the following order: X-signage, X-magnitude, Y-signage, Y-magnitude, Z-signage, Z-magnitude).

8.3 Mechanical Recommendations

All mechanical components worked as performed but some could be improved in hind sight. All recommendations have been mentioned in their respective sections. In summary, the U-channel corners could be cut at 45° angle and fastened to each other by riveting an L-bracket to the interior of the coil corners. Being more precise and taking time when drilling holes for pins and other components would smooth the functionality but isn't critical. Certain aspects of each component can also be redone for elegance.

Appendix A - References

[1] F. M. Poppenk, R. Amini, and G. F. Brouwer, "Design and Application of a Helmholtz Cage for Testing Nano-Satellites," in *ESA-ESTEC 6th International Symposium on Environmental Testing for Space Programmes*, 2015. [Online]. Available: http://www.lr.tudelft.nl/fileadmin/Faculteit/LR/Organisatie/Afdelingen_en_Leerstoelen/Afdeling_SpE/Space_Systems_Eng./Publications/2007/doc/Fedde_ESA_Environmental_Testing.pdf. Accessed: Oct. 12, 2016.

[2] Analytical Graphics Inc, "STK Engine 11.1 Programming Interface," in *AGI Systems Tool Kit*, 2015. [Online]. Available: http://help.agi.com/stkdevkit/index.html?page=source%2FcoreLibraries.htm. Accessed: Oct. 12, 2016.

[3] J. Foley, "Calibration and Characterization of CubeSat Magnetic Sensors Using a Helmholtz Cage," in *Cal Poly San Luis Obispo*, 2012. [Online]. Available: http://digitalcommons.calpoly.edu/cgi/viewcontent.cgi?article=1952&context=theses. Accessed: Oct. 12, 2016.

[4] M. Brewer, "CubeSat Attitude Determination and Helmholtz Cage Design," in *Department of the Air Force Institute of Technology*, 2012. [Online]. Available: http://www.dtic.mil/dtic/tr/fulltext/u2/a557488.pdf. Accessed: Oct. 13, 2016.

[5] B. Betts, "Sailing in Space," in *The Planetary Society*, 2016. [Online]. Available: http://propilotmag.com/archives/2016/July%2016/A4_Solar_p2.html. Accessed: Oct. 13, 2016.

[6] M. Prinkey, “Testing the Attitude Determination and Control of a CubeSat with Hardware-in-the-Loop,” in MIT, 2014 [Online]. Available: http://ssl.mit.edu/files/website/theses/SM-2014-PrinkeyMeghan.pdf Accessed: Oct. 13, 2016.

[7] Multiactive Software Inc. "HCS-01CL." HCS-01CL. Macintyre Electronics Design Associates, Inc., [Online]. Available: http://www.meda.com/catalog/item20.htm Accessed: Oct. 14 2016.

[8] N. Shetty, "Introduction to BSD Sockets," in *Treck User's Manual*, 2010. [Online]. Available: http://wiki.treck.com/Introduction_to_BSD_Sockets. Accessed: Oct. 20, 2016.

[9] IMS Nanofabrication GmbH, "Compensation of magnetic fields", US7436120B2, 2016.

[10] European Organization for Nuclear Research (CERN), "Device for calibration of magnetic sensors in three dimensions", US7259550B2, 2016.

[11] PNI Corp, "Automatic calibration of a three-axis magnetic compass." U.S. Patent No. 7,451,549. 18 Nov. 2008.

Appendix B – QFD, Decision Matrices

Appendix B.1 Complete Listing of Customer and Engineering Requirements

Customer Requirements	Engineering Requirements
Simulate earth's magnetic field	Shall be able to produce an equivalent magnetic field for a given orbit and time.
	Shall be able counter the local magnetic field and superimpose the orbital field
Simple to use	Shall support automatic calibration with magnetometer input
	Shall have a GUI with intuitive user interaction
Big enough to fit a CubeSat	Shall provide a volume large enough for a 12U CubeSat with uniform magnetic field
	Shall provide a uniform magnetic field within 0.1 uT of the commanded magnetic field
	Shall be able to support a 60lb satellite
Able to transport from room to room of ATL	Shall be mounted on wheels capable of carrying own weight plus satellite
	Shall fit through a 32" wide, 84" tall door frame
Easy to store	Shall collapse or easily disassemble for storage
Clean room safe	Shall use materials approved in a Class 100,000 clean room
Keep a satellite clean	Shall be able to be covered with clear sheeting
Affordable	Shall cost <$5,000
Calibrate multiple magnetometers at once	Shall spatially know the magnetic environment within the cage
	Shall be able to communicate with multiple magnetometers at any time
	Shall communicate with the satellite via the PolySat standard umbilical while testing.
Allow testing of magnetic actuators	Shall allow the cubesat to rotate in 1-3 rotational axes
	Shall align the COM of the CubeSat with the center of rotation
Be safe	Shall insulate any high current wire
	Shall rigidly hold the cubesat being tested
Reliable	Shall be operational for at least 10 years

Appendix B.2 Quality Function Deployment (QFD)

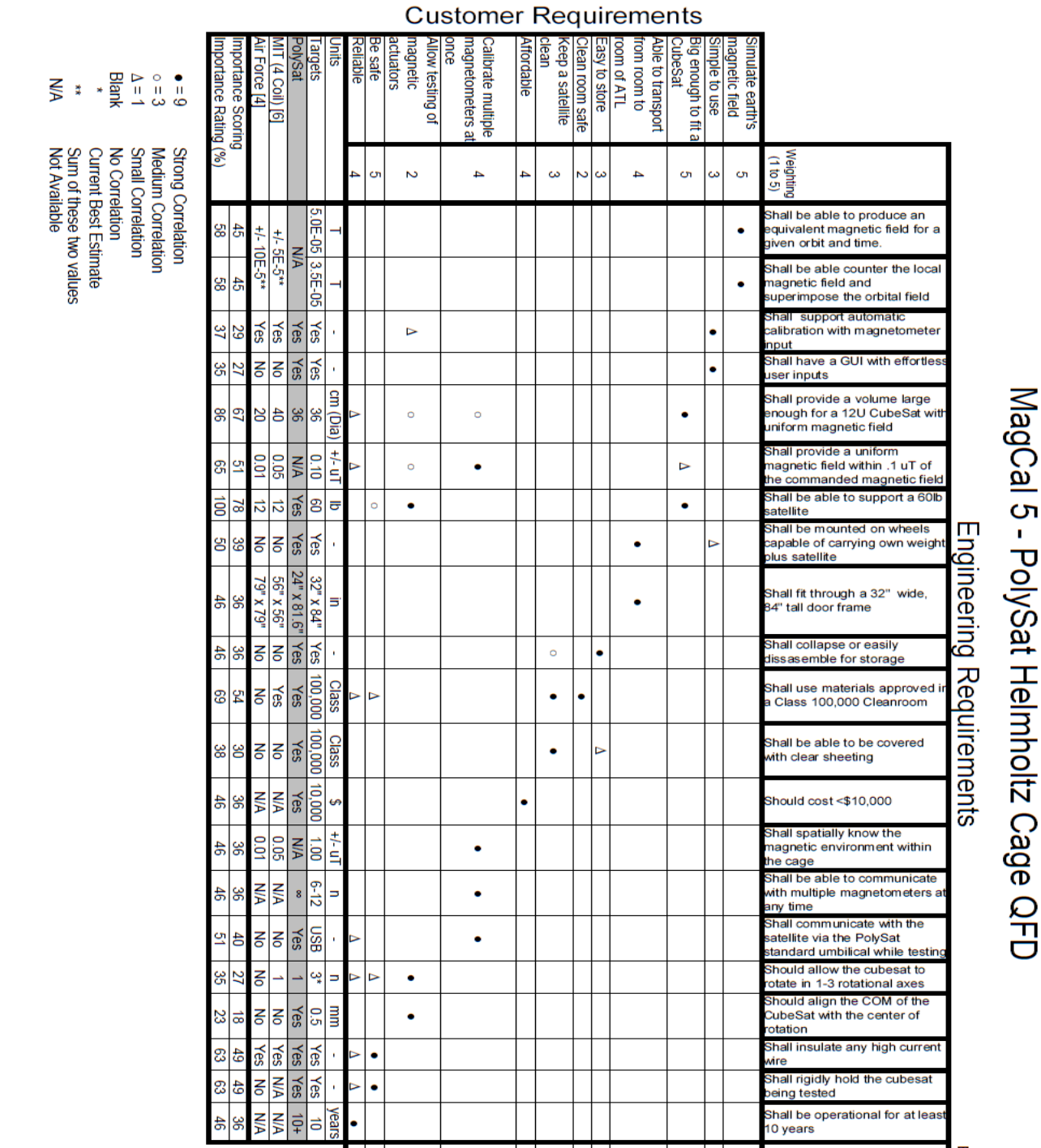

Appendix B.3 Decision Matrices

Concept Selection Legend	
Better	+
Same	S
Worse	-

Key Criteria	Importance Rating	Solution Alternatives								
		Design 5	Design 1	Design 2	Design 3	Design 4	Design 6	Design 7	Design 8	Design 9	Design 10
Able to transport	6		-	-	-	-	S	S	S	S	S
Easy to store	4		-	-	-	-	S	S	S	-	-
Clean room safe	5		S	S	S	S	S	S	S	S	S
Keep satellite clean	2		+	+	+	+	S	S	S	+	+
Inexpensive	7		-	-	-	-	+	+	+	-	-
Calibrate multiple magnetometers at once	8		-	-	S	-	S	-	-	+	-
Hazard free	5		+	+	+	+	S	S	S	-	-
Reliable	8		+	+	+	+	S	S	S	-	-
Big enough to fit CubeSat	10		S	S	S	S	S	S	S	S	S
Sum of Positives			3	3	3	3	1	1	1	2	1
Sum of Negatives			4	4	3	4	0	1	1	4	5
Sum of Sames			2	2	3	2	8	7	7	3	3

Pugh Matrix - Power Supply

Concept Selection Legend	
Better	+
Same	S
Worse	-

Key Criteria	Importance Rating	Benchmark Option	Solution Alternatives: Keysight E3604A	Keysight 34450A	BK 168A	CSI4010X	Hiltex
Amp Source	1	10	-	S	+	S	S
Volt Source	2	10	+	+	+	+	+
Cost	3	200 max	-	-	S	S	+
Dual Source	4	Y	+	-	-	-	-
Dimensions	5		S	S	S	S	+
Sum of Positives			2	1	2	1	3
Sum of Negatives			2	2	1	1	1
Sum of Sames			1	2	2	3	1

Pugh Matrix - Software

Concept Selection Legend	
Better	+
Same	S
Worse	-

Key Criteria	Importance Rating	Solution Alternatives: Java	Python	JavaScript	C++	Shell Script System
Fast	5		-	-	+	-
Fast Development Cycle	4		+	+	-	-
Testability	9		S	-	-	-
Handles Exceptions	8		S	-	-	-
Memory Safe	6		+	-	-	-
Easy to document	4		S	-	-	-
Reusability	5		+	-	-	+
Online Resources	7		S	-	-	-
Can interface with hardware	6		S	-	+	+
Ease of integration	5		S	-	-	-
Documentation available	2		S	-	S	+
Sum of Positives			3	1	2	3
Sum of Negatives			1	10	8	8
Sum of Sames			7	0	1	0

Pugh Matrix

Concept Selection Legend	
Better	+
Same	S
Worse	-

Key Criteria	Importance Rating	Flat Air Bearing	Petastool	OTS Spherical Air Bearing	Pinata	Roller Bearing Gimbal	Homemade Spherical Air Bearing
			Solution Alternatives				
# DOF	N/A		-	+	S	+	+
Frictional Losses	N/A		-	S	S	-	S
Rigidly Hold Satelitte	N/A		+	S	-	S	S
Ease to Insert	N/A		+	-	-	S	-
Ability to Adjust COM	N/A		+	-	S	-	+
Security of satellite	N/A		+	+	-	-	+
Travel in each DOF	N/A		_	S	S	S	+
Ability to route wires to satellite	N/A		+	S	-	-	-
Ability to lock a satellite in a given orientation	N/A		+	S	-	-	-
Effect on satellite Inertia	N/A		+	-	+	-	S
Manufacturability	N/A		+	S	+	-	-
Cost	N/A		+	-	+	S	-
Sum of Positives			9	2	3	1	4
Sum of Negatives			2	4	5	7	5
Sum of Sames			0	6	4	4	3

Pugh Matrix

Concept Selection Legend	
Better	+
Same	S
Worse	-

Key Criteria	Importance Rating	Cubic	Circular	Cubic, 4 Coils	Octahedral
			Solution Alternatives		
Uniformity of Field	N/A		+	+	S
Strength of Field	N/A		S	+	S
Ease of Assembly	N/A		-	-	-
Ease of Machining	N/A		-	-	-
Ability to Compress	N/A		-	-	-
Sum of Positives			1	2	0
Sum of Negatives			3	3	3
Sum of Sames			1	0	2

Appendix C – Detailed Deign

Appendix C.1 – Mechanical Drawings

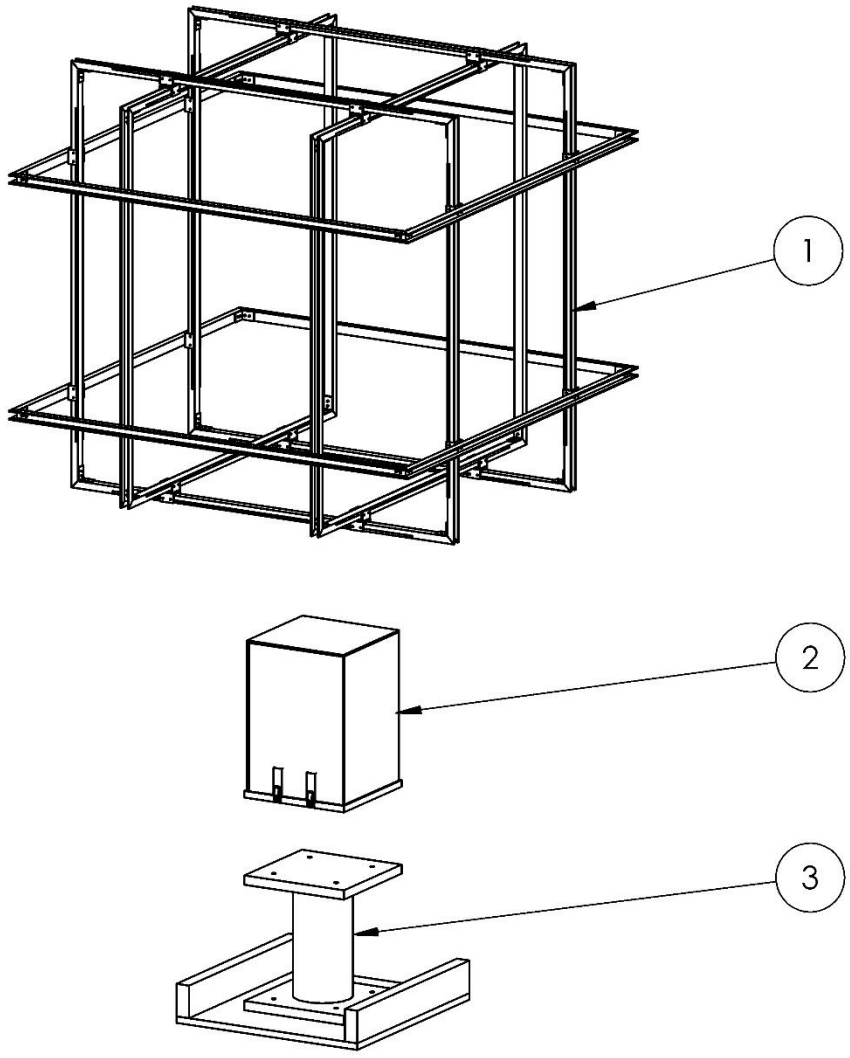

ITEM NO.	DESCRIPTION	PART NUMBER	QTY.
1	COIL ASSEMBLY	101000, 102000	1
2	CLEAN ROOM BOX	103000	1
3	PEDESTAL	104000	1

	NAME	DATE
Drwn. By:	A. NICHOLS	6/7/17
Chkd. By:	J. SKARO	6/7/17
Q.A.		

COMMENTS

PolySat

PART NAME
HELMHOLTZ CAGE ASSEMBLY

SIZE	DRAWING NUMBER	REV.
A	100000	1

SCALE: 1=20 | SHEET: 1 OF 1

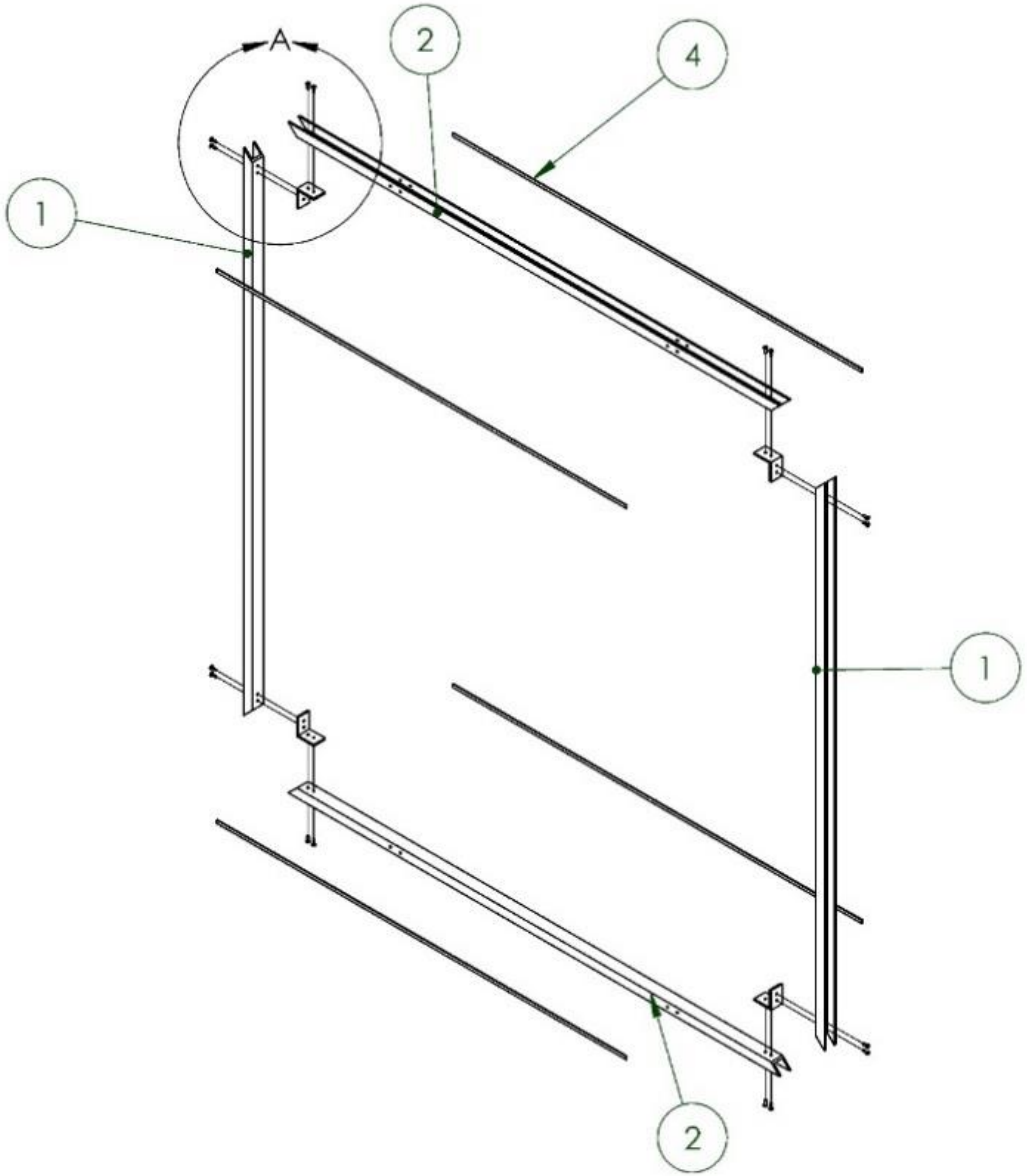

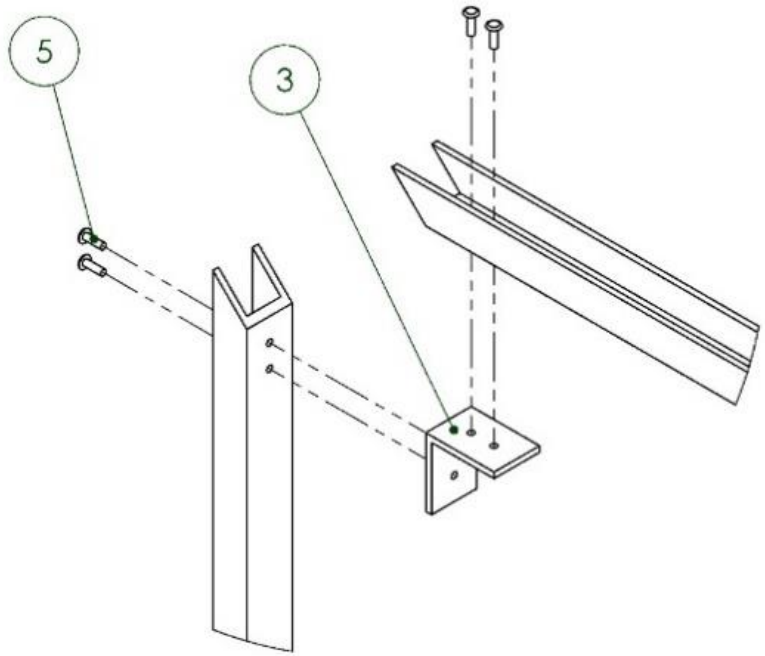

DETAIL A
SCALE 1 : 3

ITEM NO.	DESCRIPTION	PART NUMBER	MATERIAL	QTY.
1	SMALL RAIL	101001	ALUMINUM	2
2	SMALL RAIL - M	101002	ALUMINUM	2
3	CORNER BRACKET	101007	ALUMINUM	4
4	LINEAR BUSHING	101008	DELRIN	4
5	1/8"X5/16 RIVET	MC-97447A125	ALUMINUM	16

	NAME	DATE
Drwn. By:	A. NICHOLS	2/10/17
Chkd. By:	J. SKARO	2/11/17
Q.A.		

COMMENTS

PolySat

PART NAME
SMALL COIL ASSEMBLY

SIZE	DRAWING NUMBER	REV.
A	101000-1	1

SCALE: 1=12 | SHEET: 1 OF 1

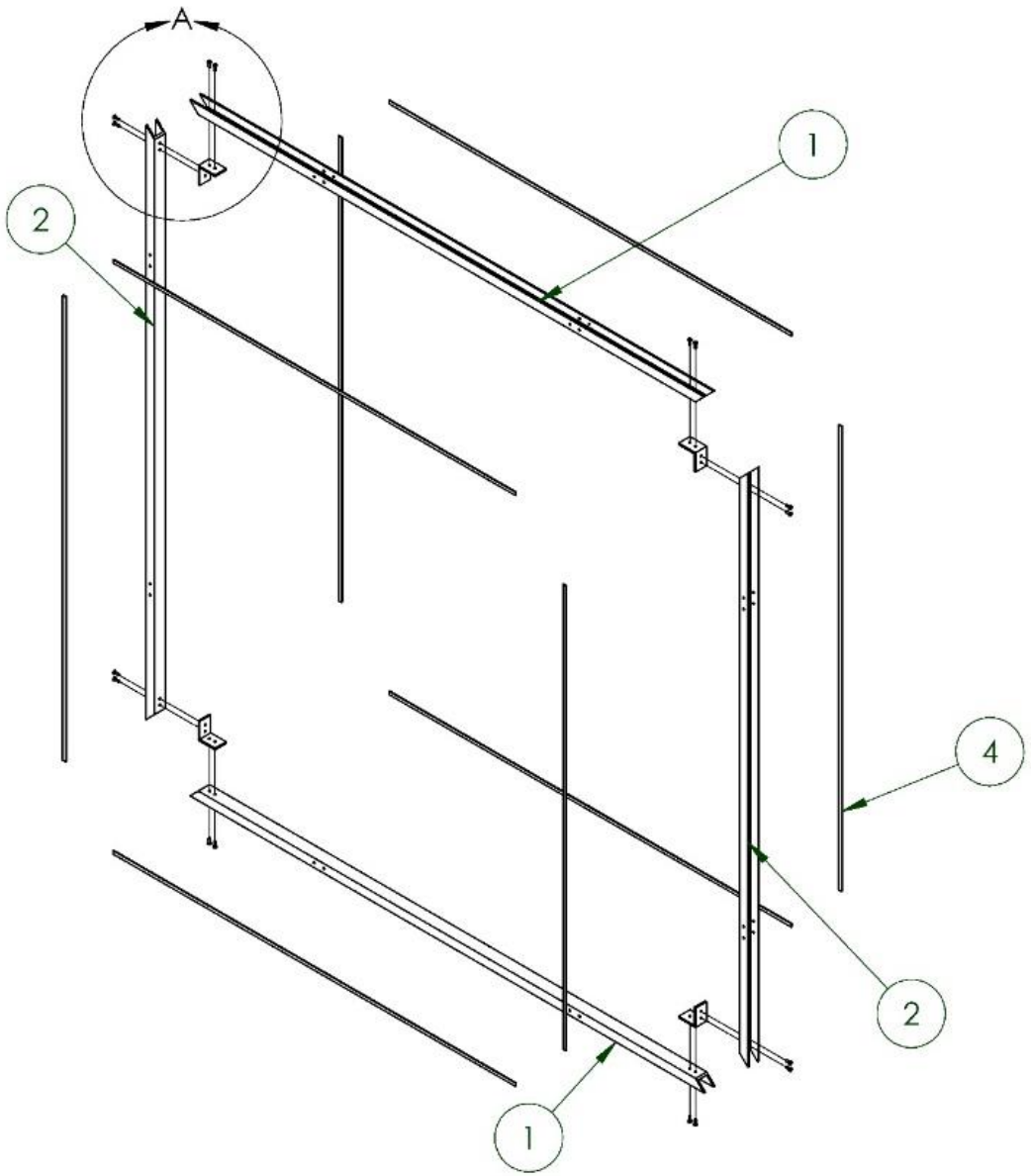

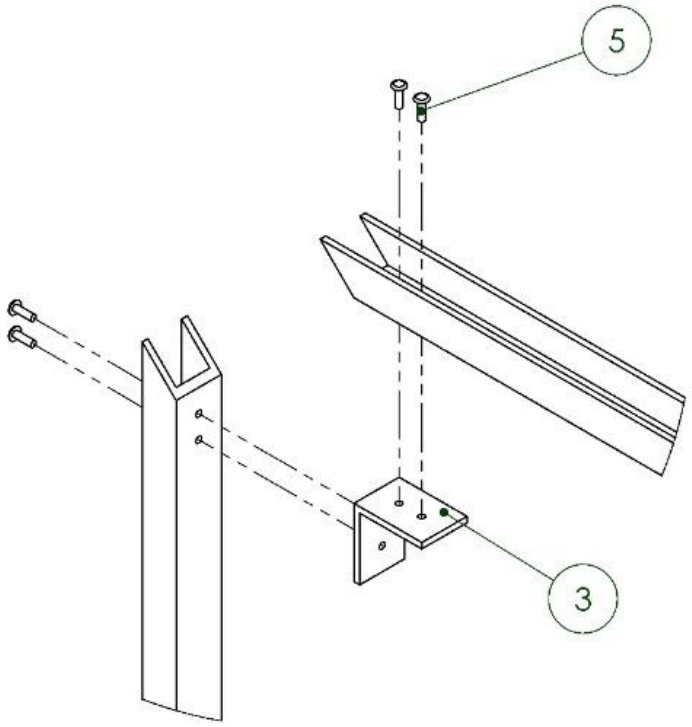

DETAIL A
SCALE 1 : 3

ITEM NO.	DESCRIPTION	PART NUMBER	MATERIAL	QTY.
1	MED. RAIL -S	101003	ALUMINUM	2
2	MED. RAIL - L	101004	ALUMINUM	2
3	TRANSLATION BRACKET	101007	ALUMINUM	4
4	LINEAR BUSHING	101008	DELRIN	8
5	1/8"X5/16 RIVET	MC-97447A125	ALUMINUM	16

	NAME	DATE
Drwn. By:	A. NICHOLS	2/10/17
Chkd. By:	J. SKARO	2/11/17
Q.A.		

COMMENTS

PolySat

PART NAME
MEDIUM COIL ASSEMBLY

SIZE	DRAWING NUMBER	REV.
A	101000-2	1

SCALE: 1=12 | SHEET: 1 OF 1

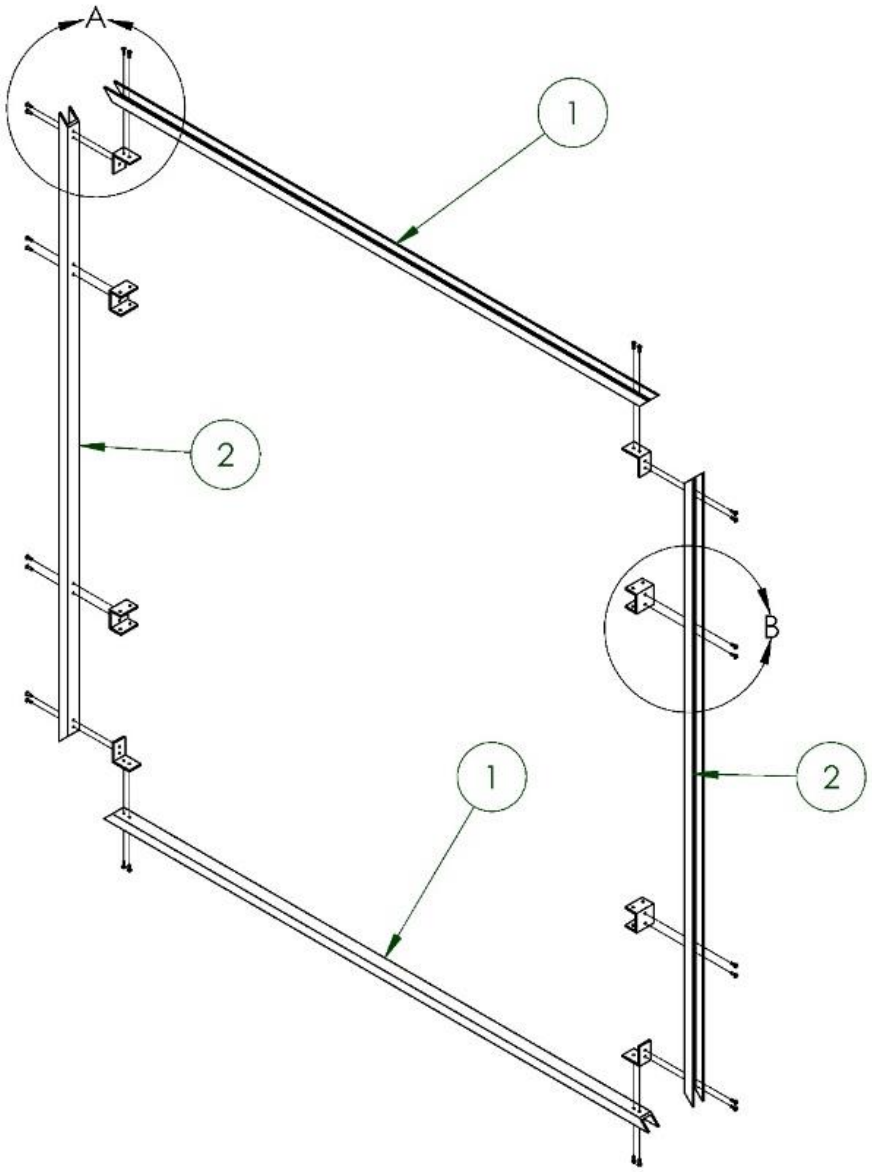

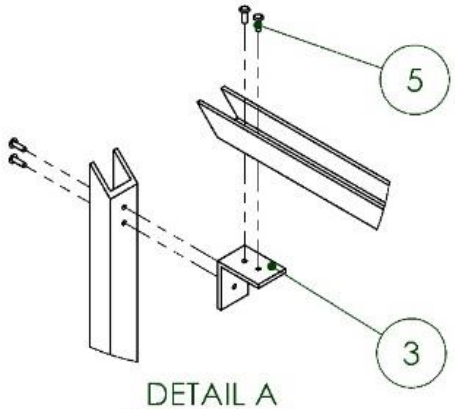

DETAIL A
SCALE 1 : 5

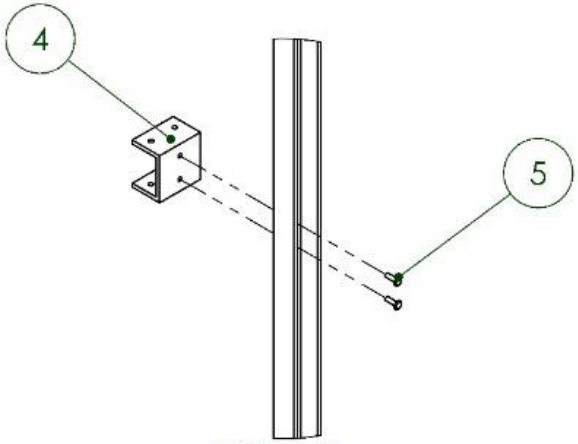

DETAIL B
SCALE 1 : 5

ITEM NO.	DESCRIPTION	PART NUMBER	MATERIAL	QTY.
1	LARGE RAIL	101005	ALUMINUM	2
2	LARGE RAIL - M	101006	ALUMINUM	2
3	CORNER BRACKET	101007	ALUMINUM	4
4	Z MOUNTING BRACKET	101009	ALUMINUM	4
5	1/8"X5/16 RIVET	MC-97447A125	ALUMINUM	24

	NAME	DATE
Drwn. By:	A. NICHOLS	2/10/17
Chkd. By:	J. SKARO	2/11/17
Q.A.		

COMMENTS

PolySat

PART NAME
LARGE COIL ASSEMBLY

SIZE	DRAWING NUMBER	REV.
A	101000-3	1

SCALE: 1=12 | SHEET: 1 OF 1

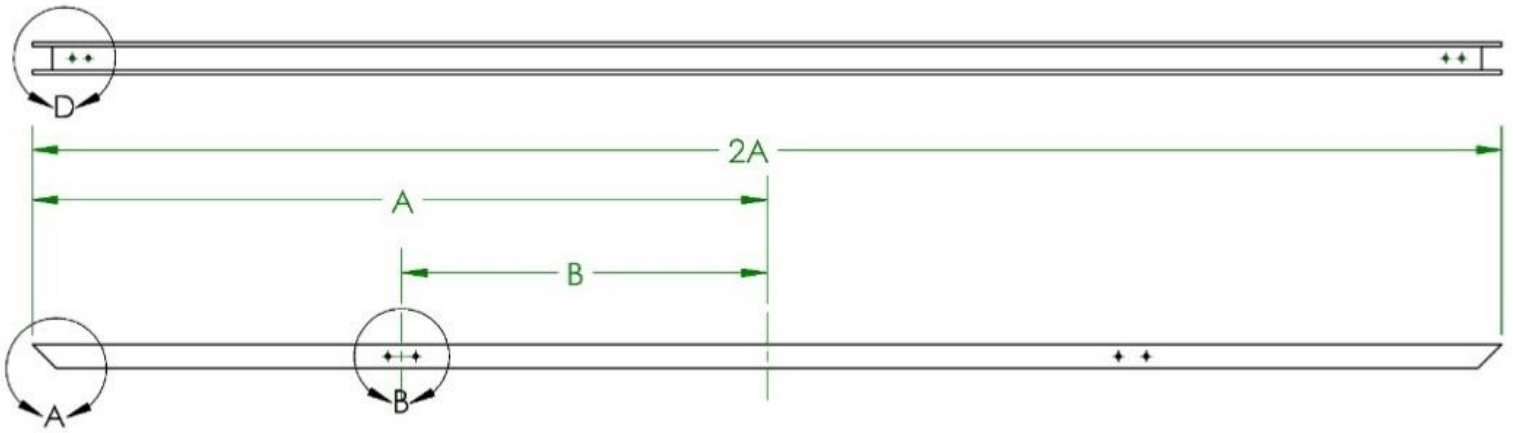

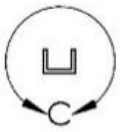

DETAIL A
SCALE 1 : 1

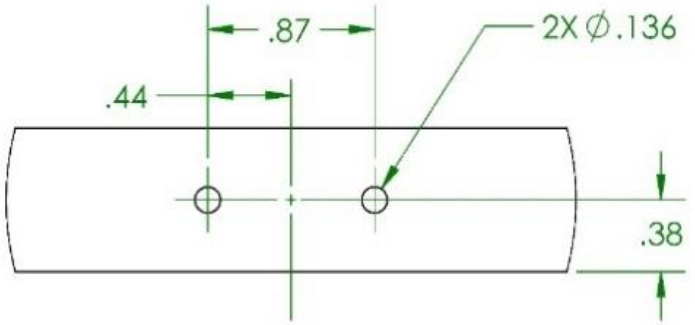

DETAIL B
SCALE 1 : 1

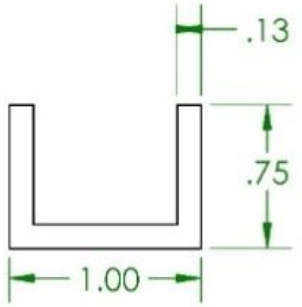

DETAIL C
SCALE 1 : 1

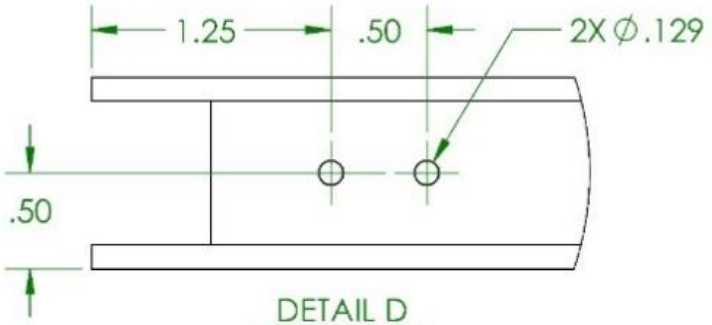

DETAIL D
SCALE 1 : 1

PART NUMBER	2A	A	B
101001	43.25	21.63	N/A
101002	43.25	21.63	12.18
101003	46.00	23.00	12.73
101004	46.00	23.00	11.44
101005	48	24	N/A

UNLESS OTHERWISE SPECIFIED:
DIMENSIONS ARE IN INCHES
DIMENSIONS: X.XX ± .01
DIMENSIONS: X.XXX ±.005
ANGULAR: MACH ± 1°
BREAK ALL EDGES AND SHARP
CORNERS .005 IN

	NAME	DATE
Drwn. By:	A. NICHOLS	2/11/17
Chkd. By:	J. SKARO	2/11/17
Q.A.		

MATERIAL: ALUMINUM 6061

FINISH: 63 MICRONS

COMMENTS
SYMETRIC ABOUT CENTER LINE
MACHINED FROM 1"X.75"X1/8" U-CHANNEL
(ORANGE ALUMINUM 0A8107-M)
B DIMENSION N/A = NO PIN HOLES REQUIRED

PolySat

PART NAME: COIL RAILS

SIZE	DRAWING NUMBER	REV.
A	101001-101005	1

SCALE: 1=6 | SHEET: 1 OF 2

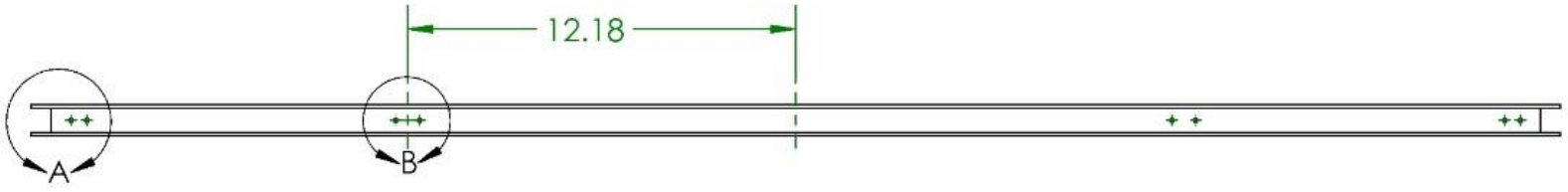

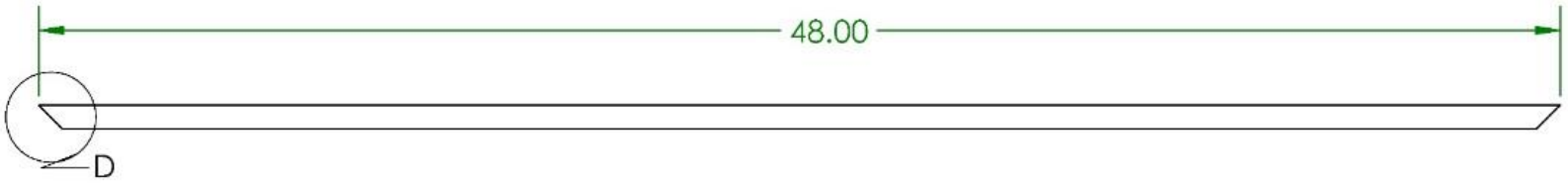

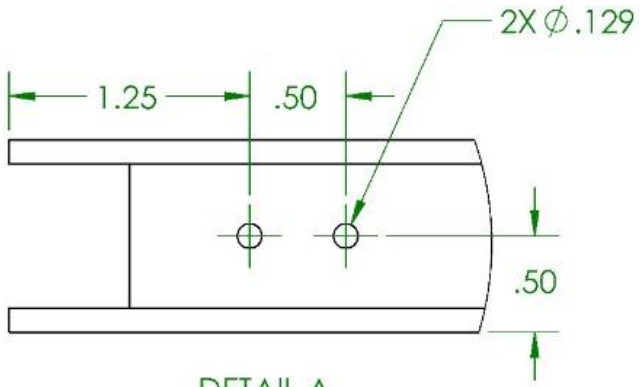

DETAIL A
SCALE 1 : 1

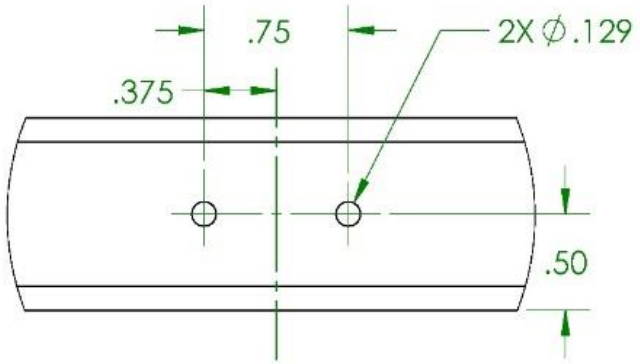

DETAIL B
SCALE 1 : 1

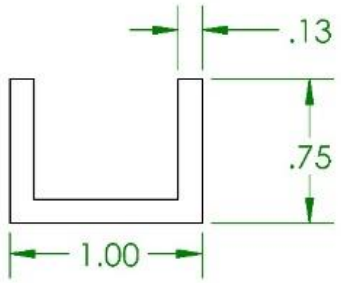

DETAIL C
SCALE 1 : 1

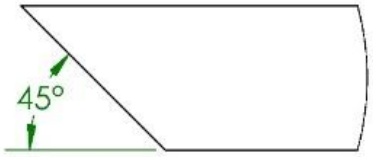

DETAIL D
SCALE 1 : 1

UNLESS OTHERWISE SPECIFIED:
DIMENSIONS ARE IN INCHES
DIMENSIONS: X.XX ± .01
DIMENSIONS: X.XXX ±.005
ANGULAR: MACH ± 1°
BREAK ALL EDGES AND SHARP
CORNERS .005 IN

	NAME	DATE
Drwn. By:	A. NICHOLS	2/11/17
Chkd. By:	J. SKARO	2/11/17
Q.A.		

MATERIAL: ALUMINUM 6061

FINISH: 63 MICRONS

COMMENTS
SYMETRIC ABOUT CENTER LINE
MACHINED FROM 1"X.75"X1/8" U-CHANNEL
(ORANGE ALUMINUM 0A8107-M)

PolySat

PART NAME: COIL RAILS

SIZE	DRAWING NUMBER	REV.
A	101006	1

SCALE: 1=6 | SHEET: 2 OF 2

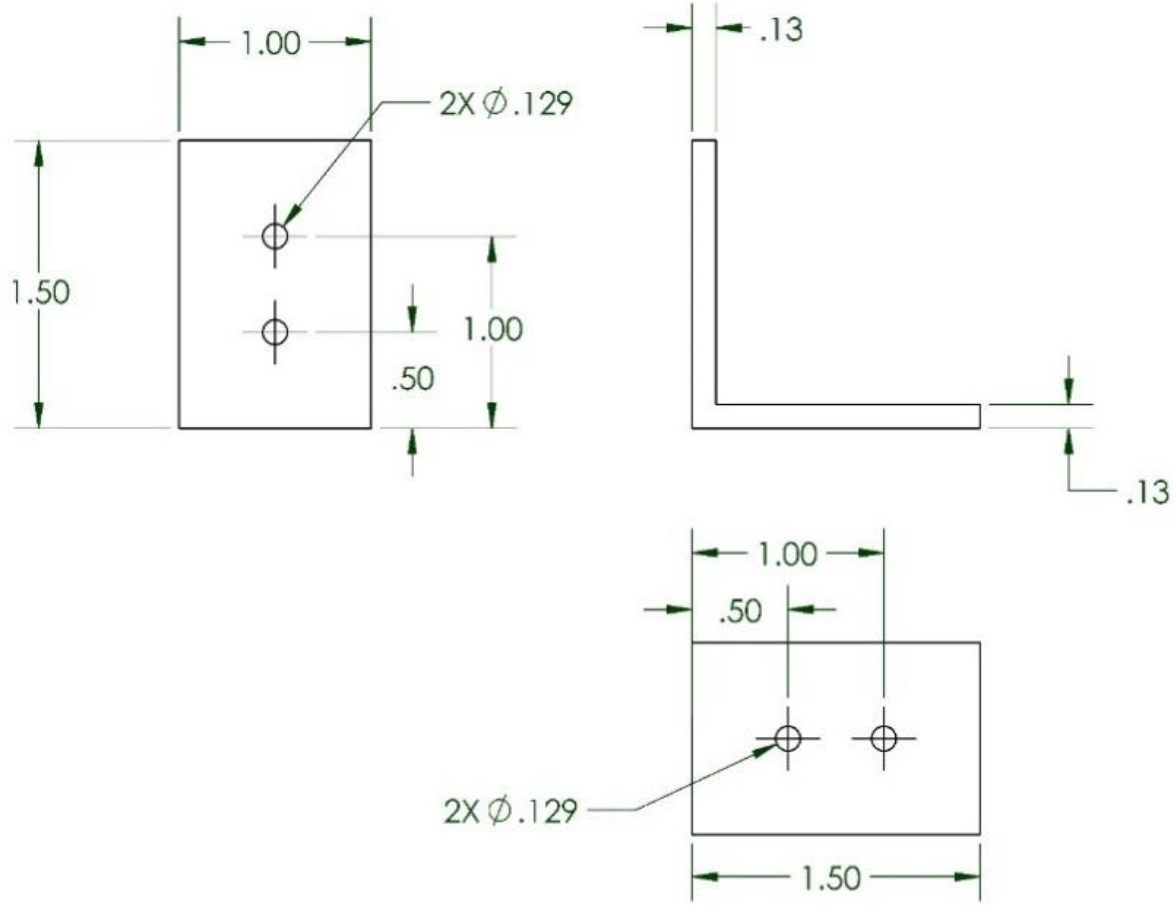

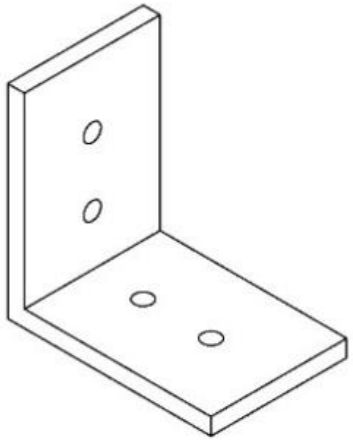

UNLESS OTHERWISE SPECIFIED:		NAME	DATE
DIMENSIONS ARE IN INCHES DIMENSIONS: X.XX ± .01 DIMENSIONS: X.XXX ±.005 ANGULAR: MACH ± 1° BREAK ALL EDGES AND SHARP CORNERS .005 IN	Drwn. By:	A. NICHOLS	2/11/17
	Chkd. By:	J. SKARO	2/11/17
	Q.A.		
MATERIAL: ALUMINUM 6061	COMMENTS: MACHINED FROM 1.5X1.5X.125" L-CHANNEL STOCK		
FINISH: 63 MICRONS			

PolySat

PART NAME: CORNER BLOCK

SIZE	DRAWING NUMBER	REV.
A	101007	1

SCALE: 1=1 | SHEET: 1 OF 1

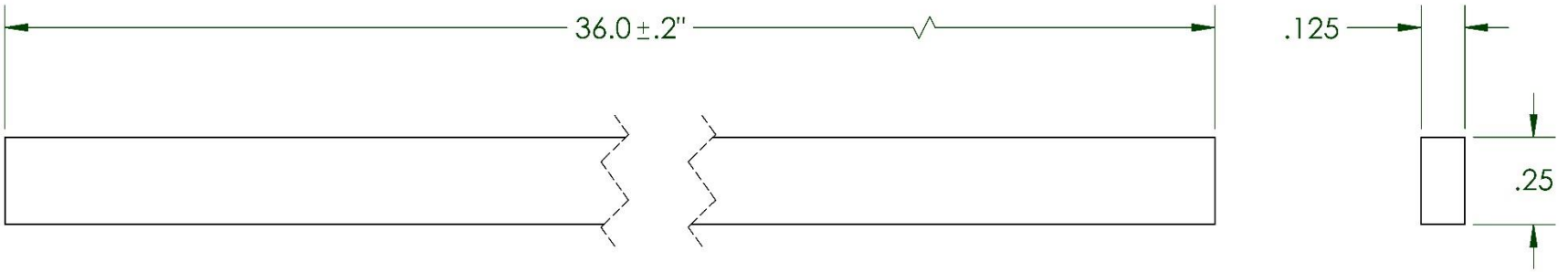

UNLESS OTHERWISE SPECIFIED:		NAME	DATE
DIMENSIONS ARE IN INCHES DIMENSIONS: X.XX ± .01 DIMENSIONS: X.XXX ±.001 ANGULAR: MACH ± 1° BREAK ALL EDGES AND SHARP CORNERS .005 IN	Drwn. By:	A. NICHOLS	6/7/17
	Chkd. By:	J. SKARO	6/7/17
	Q.A.		
MATERIAL: UHWM PE	COMMENTS: CUT FROM 1/8" SHEET OF DELRIN, (~2'X4')		
FINISH: 63 MICRONS			

PolySat

PART NAME: LINEAR BUSHING

SIZE	DRAWING NUMBER	REV.
A	101008	1

SCALE: 2=1 | SHEET: 1 OF 1

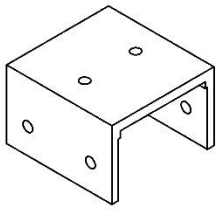

PN: 102001
SCALE 1=2

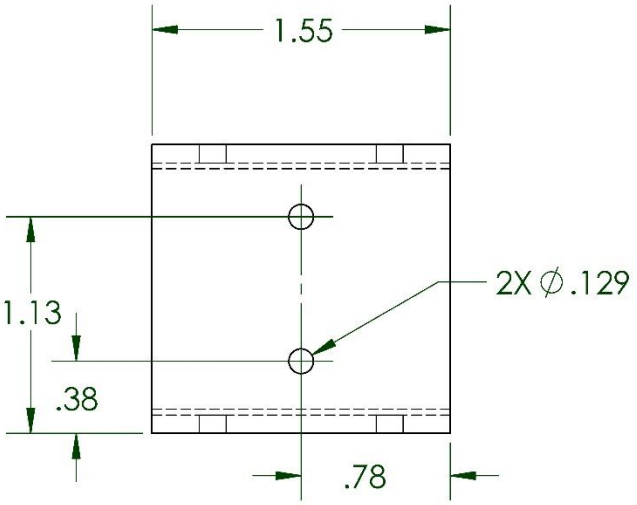

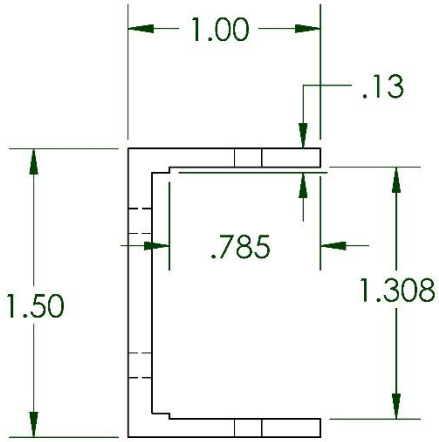

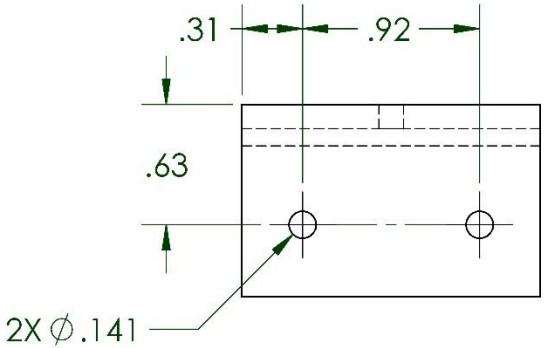

UNLESS OTHERWISE SPECIFIED:
DIMENSIONS ARE IN INCHES
DIMENSIONS: X.XX ± .01
DIMENSIONS: X.XXX ±.005
ANGULAR: MACH ± 1°
BREAK ALL EDGES AND SHARP CORNERS .005 IN

	NAME	DATE
Drwn. By:	A. NICHOLS	6/7/17
Chkd. By:	J. SKARO	6/7/17
Q.A.		

MATERIAL: ALUMINUM 6061
FINISH: 63 MICRONS
COMMENTS: MACHINED FROM 1.5"X1"X.125" U CHANNEL

PolySat

PART NAME: Z - BRACKET

SIZE	DRAWING NUMBER	REV.
A	101009	1

SCALE: 1=1 | SHEET: 1 OF 1

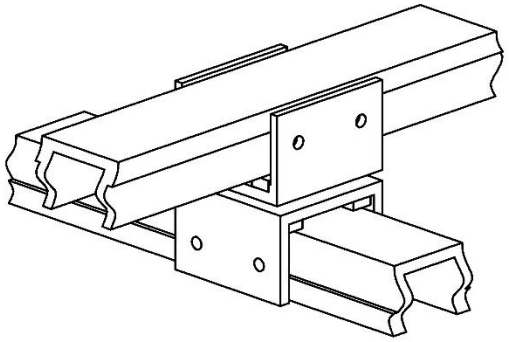

NOTE: SCALE 1:2

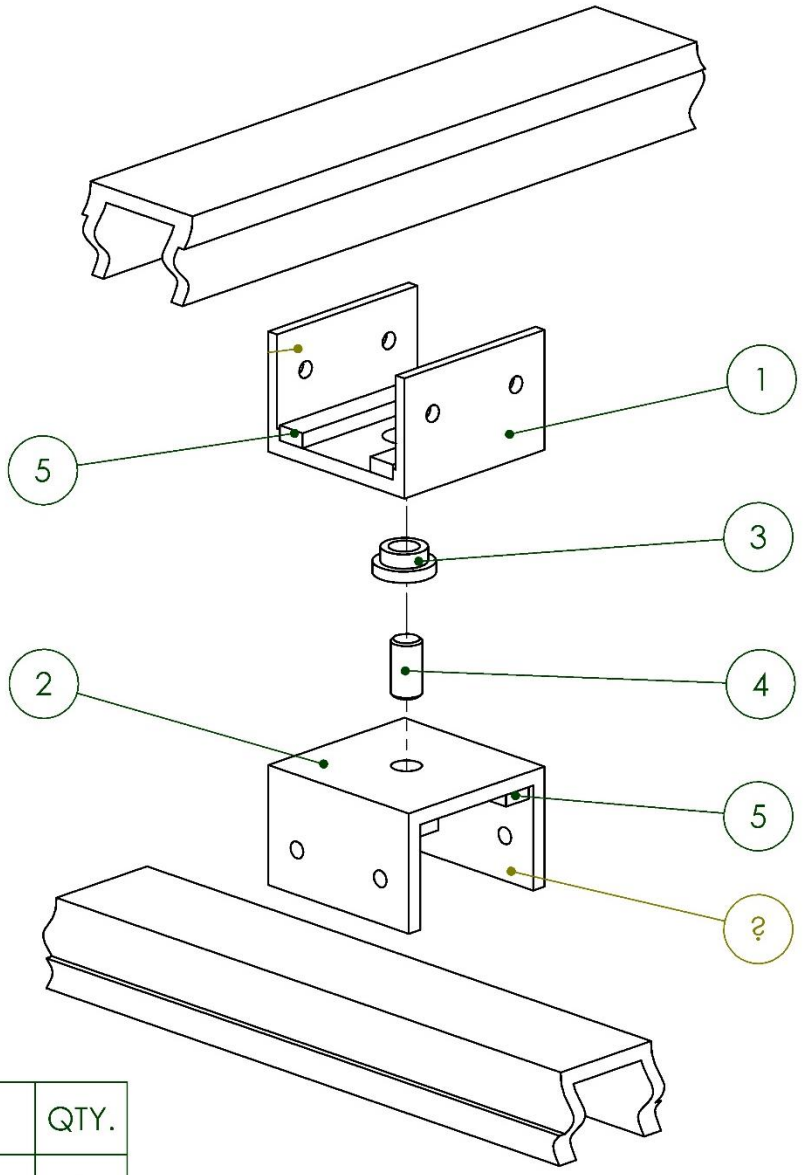

ITEM NO.	PART NUMBER	DESCRIPTION	MATERIAL	QTY.
1	102001	TRANSLATION BRACKET - BSHG	ALUMINUM	1
2	102002	TRANSLATION BRACKET - SHFT	ALUMINUM	1
3	102003	DELRIN BUSHING	DELRIN	1
4	102004	1/4 IN SHAFT	ALUMINUM	1
5	102005	1/8 IN DELRIN PAD	DELRIN	4

	NAME	DATE
Drwn. By:	A. NICHOLS	2/10/17
Chkd. By:	J. SKARO	2/11/17
Q.A.		

COMMENTS

PolySat

PART NAME
BUSHING ASSEMBLY

SIZE	DRAWING NUMBER	REV.
A	102000	1

SCALE: 2=3 | SHEET: 1 OF 1

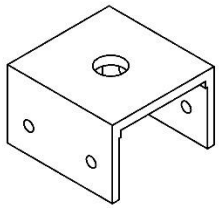

PN: 102001
SCALE 1=2

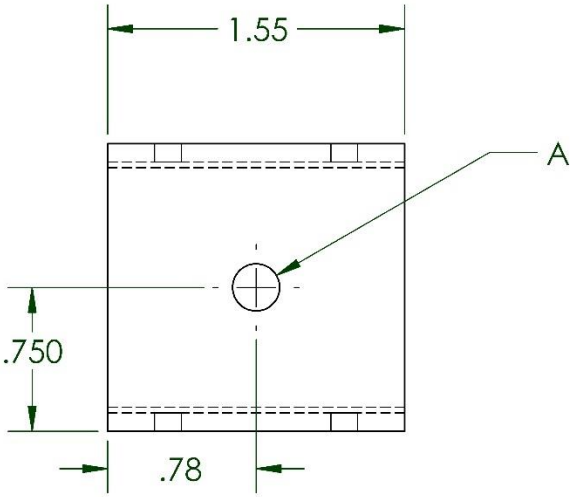

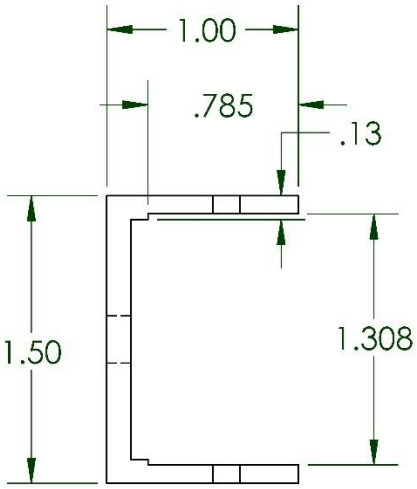

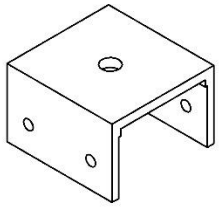

PN: 102002
SCALE 1=2

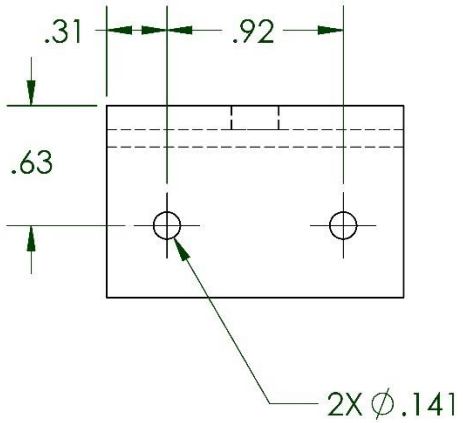

PART NUMBER	A	MATING PART
102001	∅.378±.002	BUSHING
102002	∅.247±.002	SHAFT

UNLESS OTHERWISE SPECIFIED:
DIMENSIONS ARE IN INCHES
DIMENSIONS: X.XX ± .063
DIMENSIONS: X.XXX ±.005
ANGULAR: MACH ± 1°
BREAK ALL EDGES AND SHARP
CORNERS .005 IN

	NAME	DATE
Drwn. By:	A. NICHOLS	6/7/17
Chkd. By:	J. SKARO	6/7/17
Q.A.		

MATERIAL: ALUMINUM 6061
FINISH: 63 MICRONS
COMMENTS: MACHINED FROM 1.5"X1"X.125" U CHANNEL

PolySat

PART NAME: TRANSLATION BRACKET

SIZE	DRAWING NUMBER	REV.
A	102001-102002	1

SCALE: 1=1 | SHEET: 1 OF 1

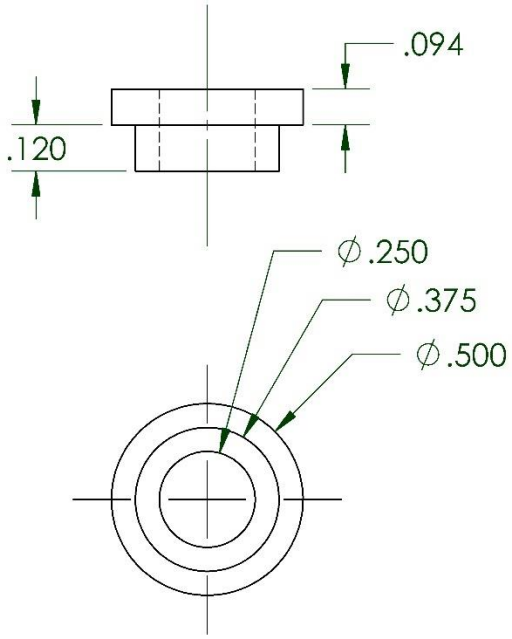

PN: 102003
STOCK: MC 2705T14
(FLANGED BUSHING)

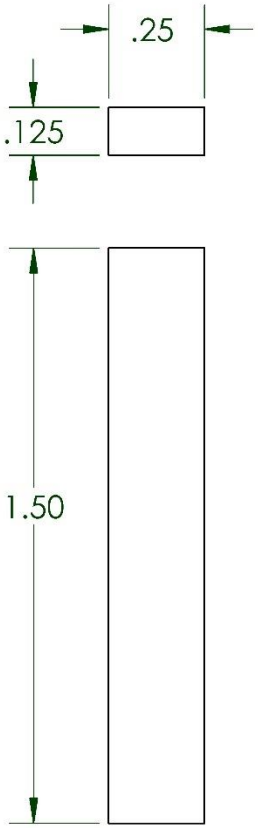

PN: 102005
STOCK: 1/8" DELRIN SHEET

UNLESS OTHERWISE SPECIFIED:
DIMENSIONS ARE IN INCHES
DIMENSIONS: X.XX ± .01
DIMENSIONS: X.XXX ±.005
ANGULAR: MACH ± 1°
BREAK ALL EDGES AND SHARP CORNERS .005 IN

	NAME	DATE
Drwn. By:	A. NICHOLS	6/7/17
Chkd. By:	J. SKARO	6/7/17
Q.A.		

MATERIAL: DELRIN
FINISH: 63 MICRONS
COMMENTS:

PolySat

PART NAME: DELRIN BUSHINGS

SIZE	DRAWING NUMBER	REV.
A	102003, 12005	1

SCALE: 2=1 | SHEET: 1 OF 1

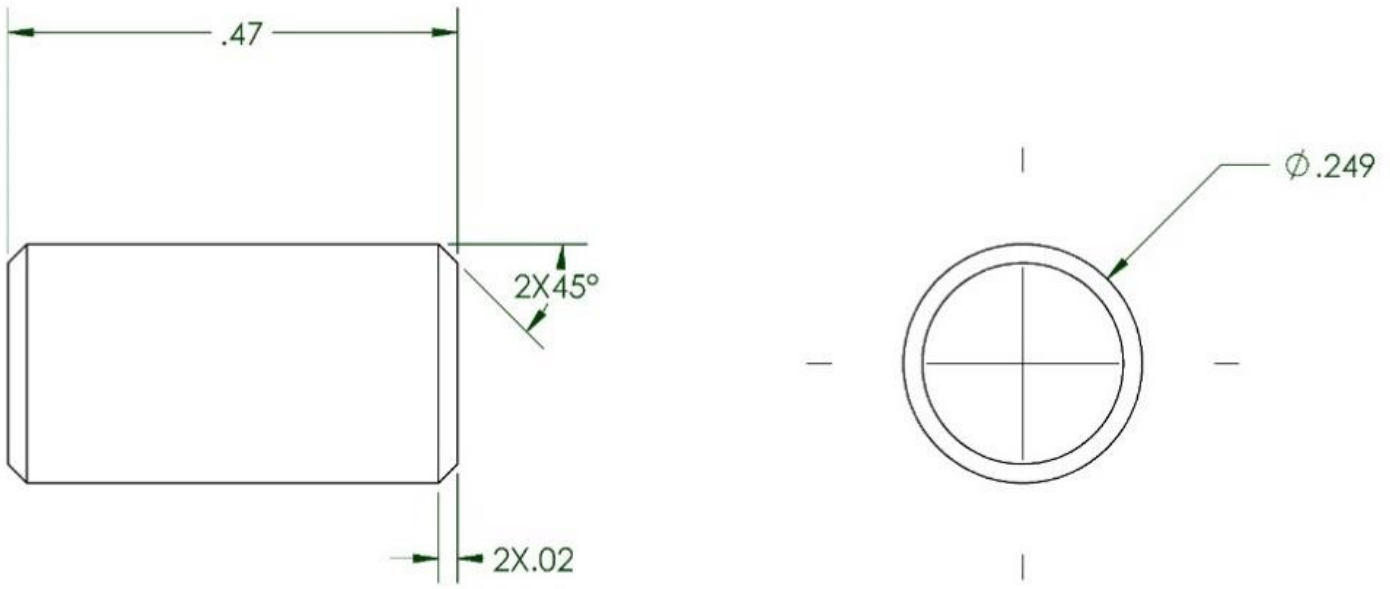

UNLESS OTHERWISE SPECIFIED:
DIMENSIONS ARE IN INCHES
DIMENSIONS: X.XX ± .01
DIMENSIONS: X.XXX ±.005
ANGULAR: MACH ± 1°
BREAK ALL EDGES AND SHARP
CORNERS .005 IN

	NAME	DATE
Drwn. By:	A. NICHOLS	2/11/17
Chkd. By:	J. SKARO	2/11/17
Q.A.		

MATERIAL: ALUMINUM 6061
FINISH: 63 MICRONS

COMMENTS
CUT FROM 1/4 ALUMINUM SHAFT (MC-5911K41)
CHAMFER BY HAND WITH GRINDER

PolySat

PART NAME: ALUMINUM SHAFT

SIZE	DRAWING NUMBER	REV.
A	102004	1

SCALE: 5=1 | SHEET: 1 OF 1

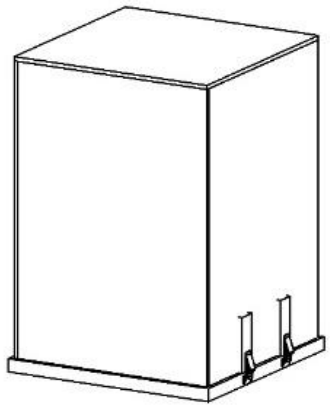

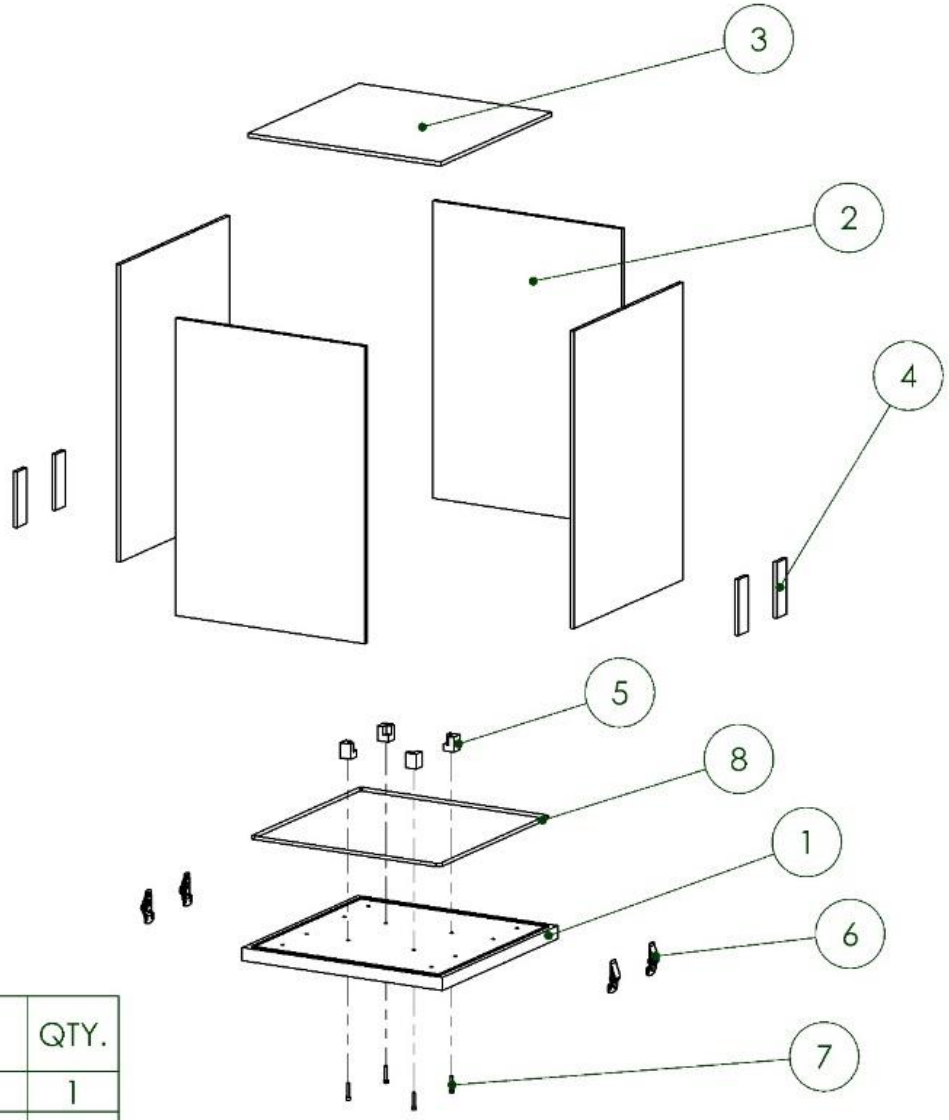

ITEM NO.	DESCRIPTION	PART NUMBER	MATERIAL	QTY.
1	BASE	103001	ACRYLLIC	1
2	WALL	103002	ACRYLLIC	4
3	TOP	103003	ACRYLLIC	1
4	CLIP EXTENDER	103004	ACRYLLIC	4
5	CORNER BLOCK	103005	PLA	4
6	LATCH	WS-H05021	PLASTIC	4
7	6-32 SCREW, 1"	MC-95868A154	NYLON	4
8	O-RING	MC-9452K491	RUBBER	1

	NAME	DATE
Drwn. By:	A. NICHOLS	2/10/17
Chkd. By:	J. SKARO	2/11/17
Q.A.		

COMMENTS

PolySat

PART NAME
CLEAN ROOM BOX ASSEMBLY

SIZE	DRAWING NUMBER	REV.
A	103000	1

SCALE: 1=10 | SHEET: 1 OF 1

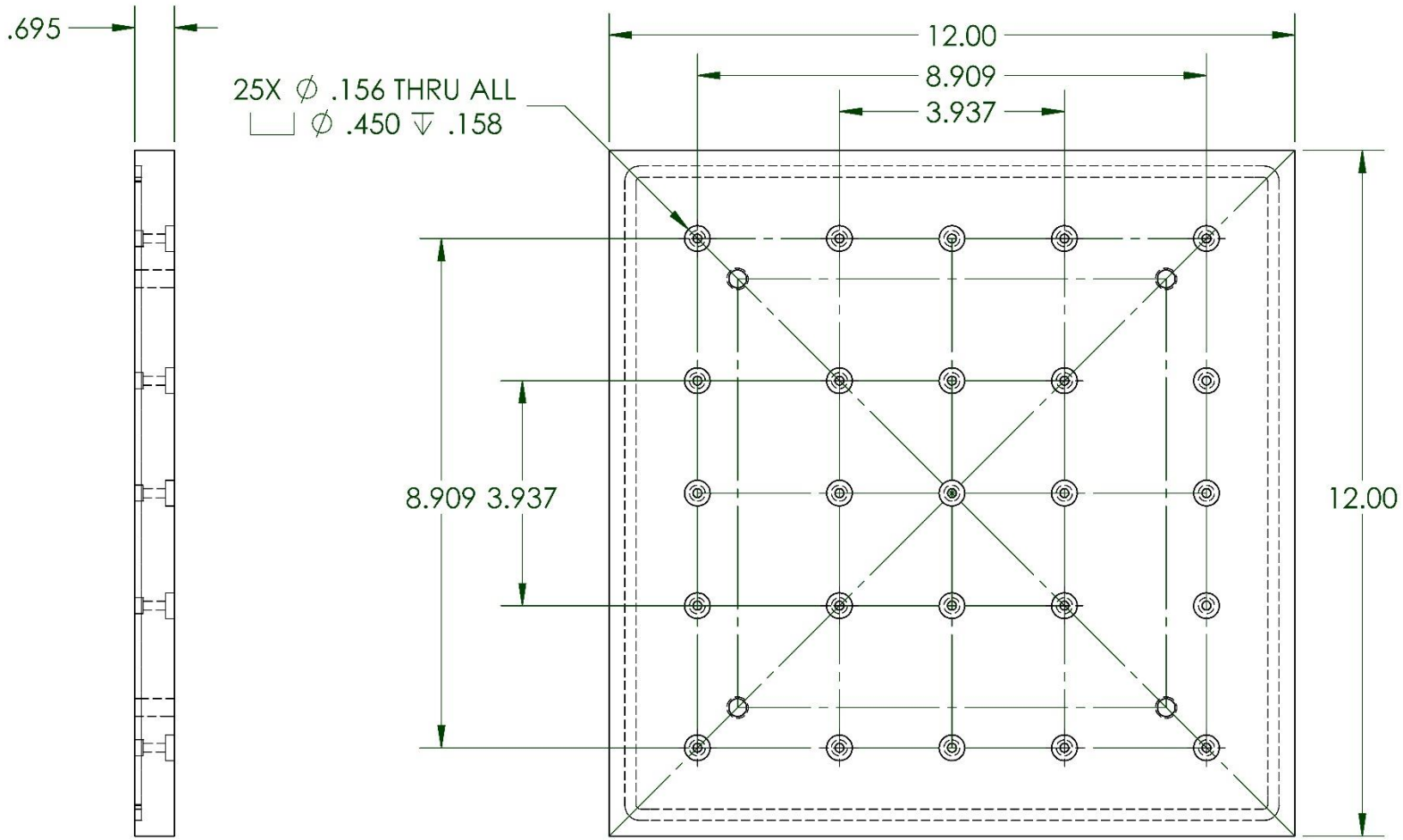

UNLESS OTHERWISE SPECIFIED:		NAME	DATE
DIMENSIONS ARE IN INCHES DIMENSIONS: X.XX ± .01 DIMENSIONS: X.XXX ±.005 ANGULAR: MACH ± 1° BREAK ALL EDGES AND SHARP CORNERS .005 IN	Drwn. By:	A. NICHOLS	6/7/17
	Chkd. By:	J. SKARO	6/7/17
	Q.A.		
MATERIAL: ACRYLLIC	COMMENTS MACHINED FROM 12"X12"X18MM ACRYLLIC ALL HOLE PATTERNS CENTERED ON PLATE		
FINISH: 63 MICRONS			

PolySat

PART NAME: BASE

SIZE	DRAWING NUMBER	REV.
A	103001	1

SCALE: 1=3 | SHEET: 1 OF 1

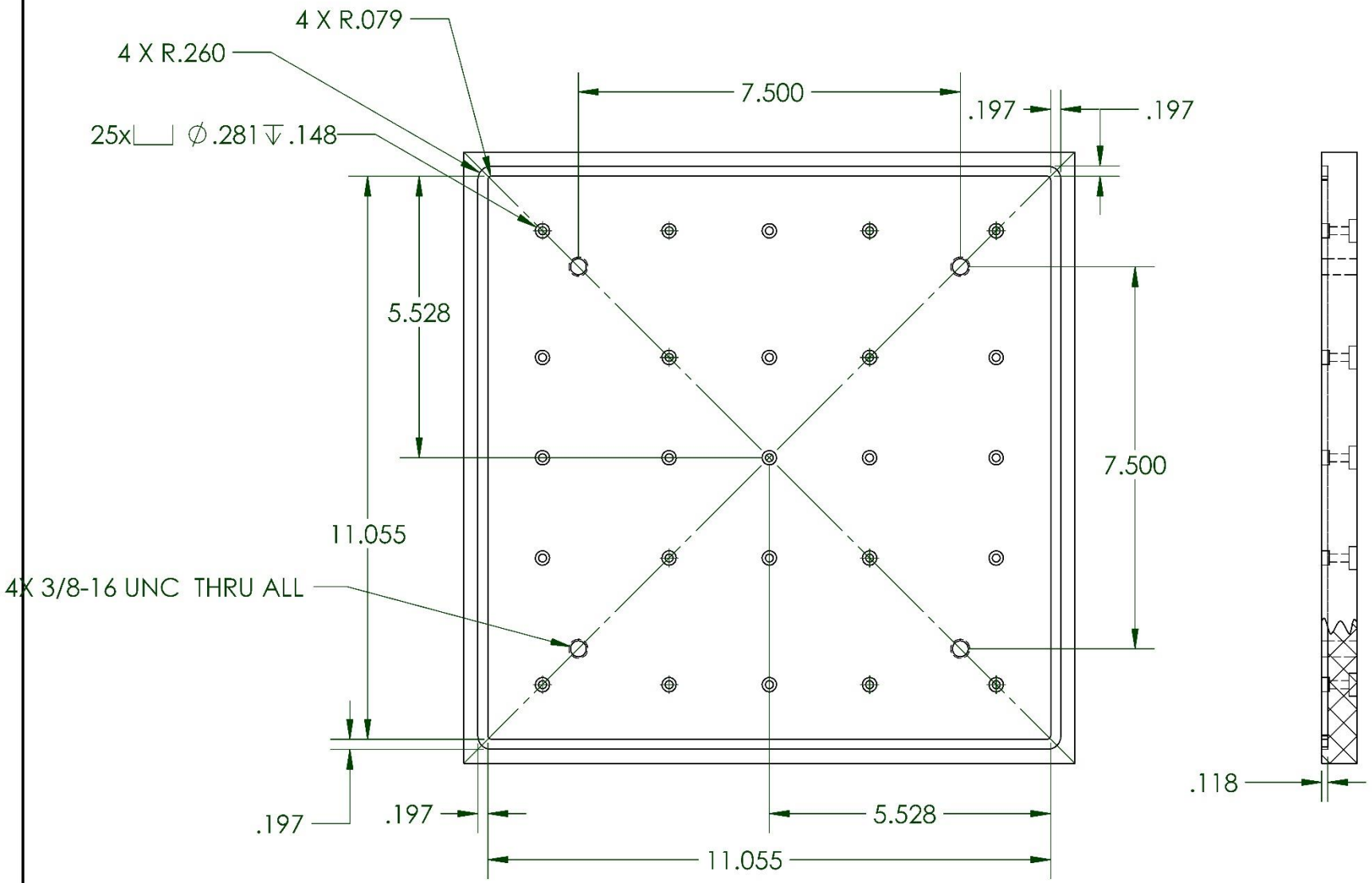

UNLESS OTHERWISE SPECIFIED:
DIMENSIONS ARE IN INCHES
DIMENSIONS: X.XX ± .01
DIMENSIONS: X.XXX ±.005
ANGULAR: MACH ± 1°
BREAK ALL EDGES AND SHARP
CORNERS .005 IN

	NAME	DATE
Drwn. By:	A. NICHOLS	6/7/17
Chkd. By:		
Q.A.		

MATERIAL: ACRYLLIC
FINISH: 63 MICRONS
COMMENTS: O-RING SLOT CENTERED ON PLATE

PolySat

PART NAME: BASE

SIZE	DRAWING NUMBER	REV.
A	103001	1

SCALE: 1=3 | SHEET: 2 OF 2

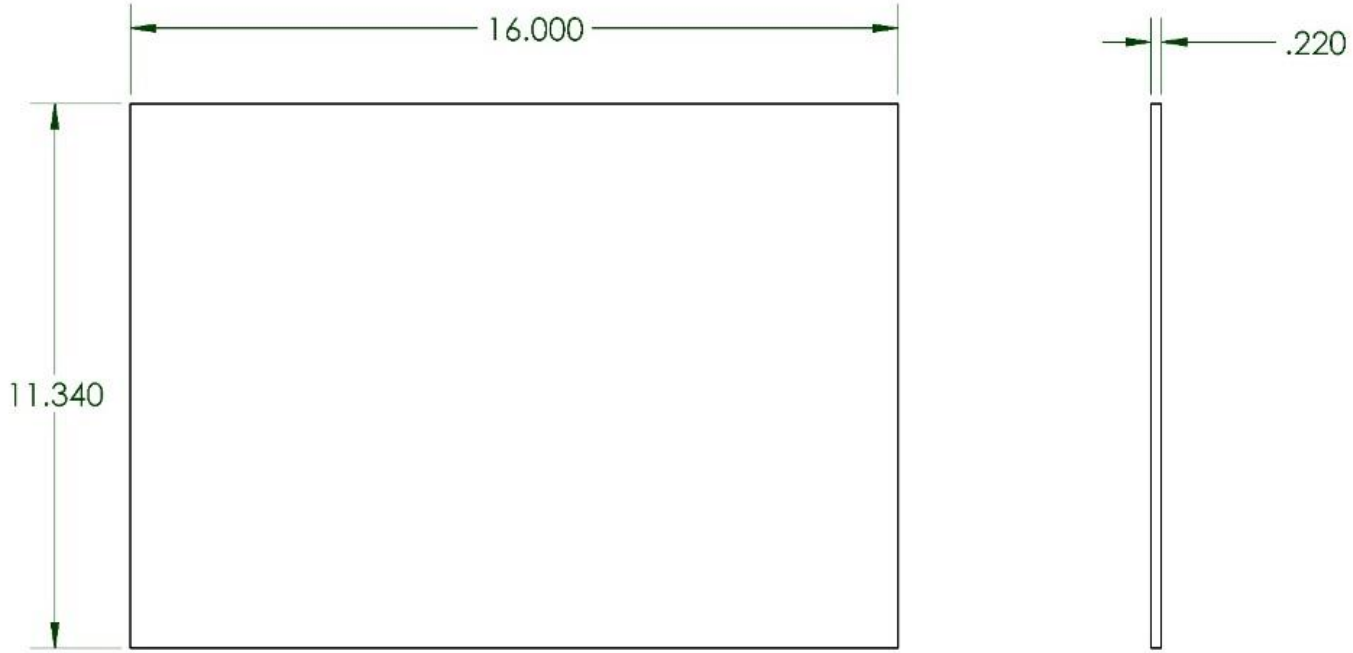

UNLESS OTHERWISE SPECIFIED:
DIMENSIONS ARE IN INCHES
DIMENSIONS: X.XX ± .01
DIMENSIONS: X.XXX ±.005
ANGULAR: MACH ± 1°
BREAK ALL EDGES AND SHARP
CORNERS .005 IN

MATERIAL: ACRYLLIC

FINISH: 63 MICRONS

	NAME	DATE
Drwn. By:	A. NICHOLS	2/11/17
Chkd. By:	J. SKARO	2/11/17
Q.A.		

COMMENTS
CUT FROM 5.6MM ACRYLLIC,
LASER CUT FINAL DIMENSIONS

PolySat

PART NAME: WALL

SIZE	DRAWING NUMBER	REV.
A	103002	1

SCALE: 1=4 | SHEET: 1 OF 1

UNLESS OTHERWISE SPECIFIED:
DIMENSIONS ARE IN INCHES
DIMENSIONS: X.XX ± .01
DIMENSIONS: X.XXX ±.005
ANGULAR: MACH ± 1°
BREAK ALL EDGES AND SHARP
CORNERS .005 IN

	NAME	DATE
Drwn. By:	A. NICHOLS	2/11/17
Chkd. By:	J. SKARO	2/11/17
Q.A.		

MATERIAL: ACRYLLIC
FINISH: 63 MICRONS
COMMENTS: CUT FROM 5.6MM ACRYLLIC, LASER CUT FINAL DIMENSIONS

PolySat

PART NAME: TOP

SIZE	DRAWING NUMBER	REV.
A	103003	1

SCALE: 1=3 | SHEET: 1 OF 1

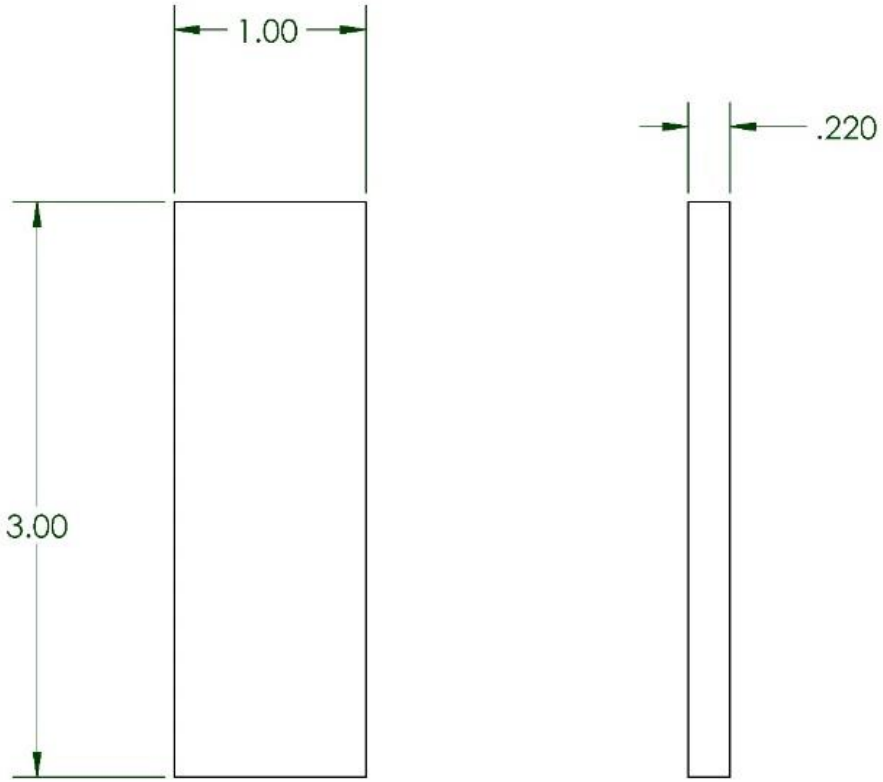

UNLESS OTHERWISE SPECIFIED:
DIMENSIONS ARE IN INCHES
DIMENSIONS: X.XX ± .01
DIMENSIONS: X.XXX ±.005
ANGULAR: MACH ± 1°
BREAK ALL EDGES AND SHARP
CORNERS .005 IN

	NAME	DATE
Drwn. By:	A. NICHOLS	2/11/17
Chkd. By:	J. SKARO	2/11/17
Q.A.		

MATERIAL: ACRYLLIC
FINISH: 63 MICRONS
COMMENTS: CUT FROM 5.6MM ACRYLLIC, LASER CUT FINAL DIMENSIONS

PolySat

PART NAME: CLIP EXTENDER

SIZE	DRAWING NUMBER	REV.
A	103004	1

SCALE: 1=1 | SHEET: 1 OF 1

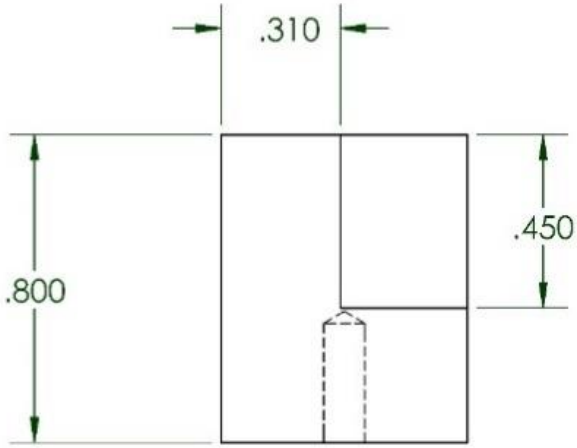

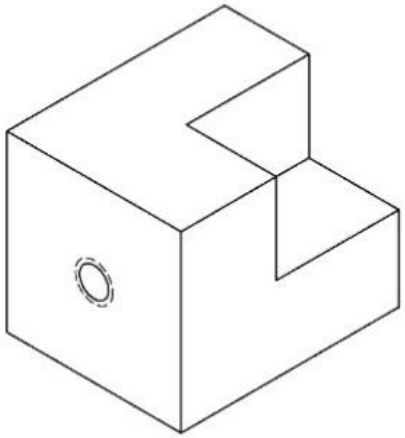

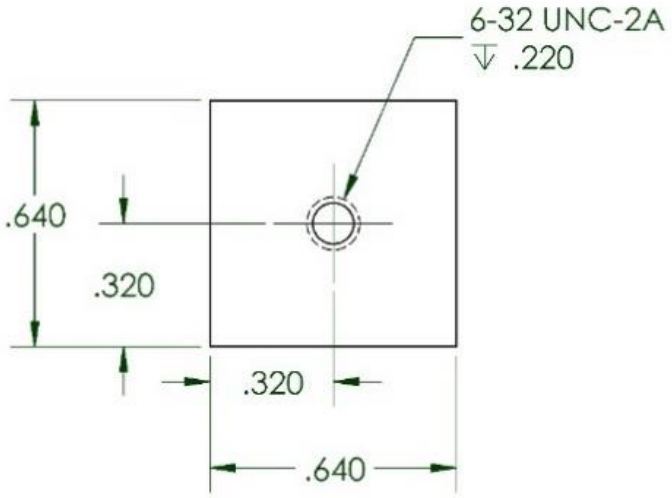

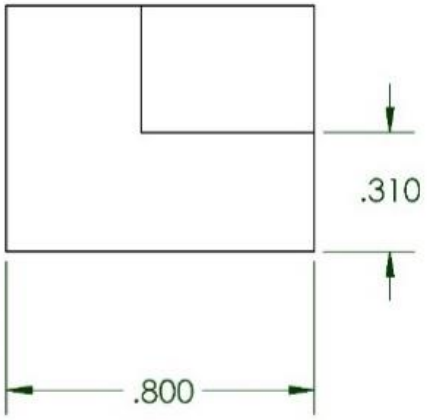

UNLESS OTHERWISE SPECIFIED:
DIMENSIONS ARE IN INCHES
DIMENSIONS: X.XX ± .01
DIMENSIONS: X.XXX ±.005
ANGULAR: MACH ± 1°
BREAK ALL EDGES AND SHARP
CORNERS .005 IN

	NAME	DATE
Drwn. By:	A. NICHOLS	2/11/17
Chkd. By:	J. SKARO	2/11/17
Q.A.		

MATERIAL: PLA
FINISH: 63 MICRONS
COMMENTS: TO BE 3D PRINTED USING POLYSAT'S MAKERBOT

PolySat

PART NAME: CORNER BLOCKS

SIZE	DRAWING NUMBER	REV.
A	103005	1

SCALE: 2=1 | SHEET: 1 OF 1

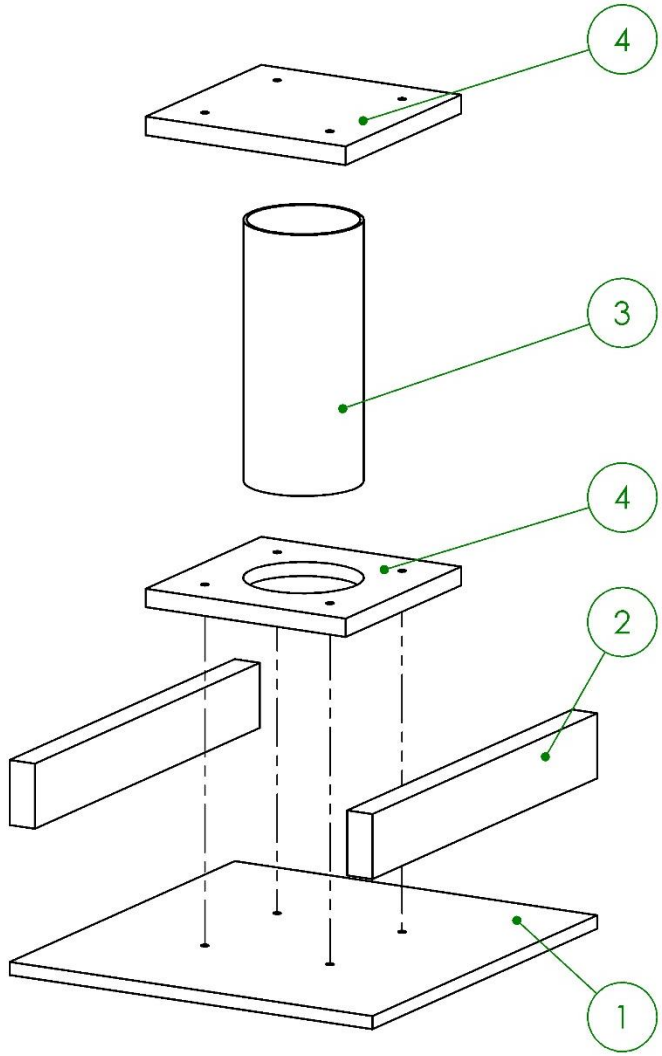

ITEM NO.	DESCRIPTION	PART NUMBER	MATERIAL	QTY.
1	ROD FIXTURE BASE	104001	PLYWOOD	1
2	2x4	104003	PINE	2
3	PVC_Pipe	104005	PVC	1
4	Aluminum Plate	104006	ALUMINUM	2

	NAME	DATE
Drwn. By:	J. SKARO	6/7/17
Chkd. By:	A. NICHOLS	6/7/17
Q.A.		

COMMENTS

PolySat

PART NAME
PEDESTAL ASSEMBLY

SIZE	DRAWING NUMBER	REV.
A	104000	1

SCALE: 1=6 | SHEET: 1 OF 1

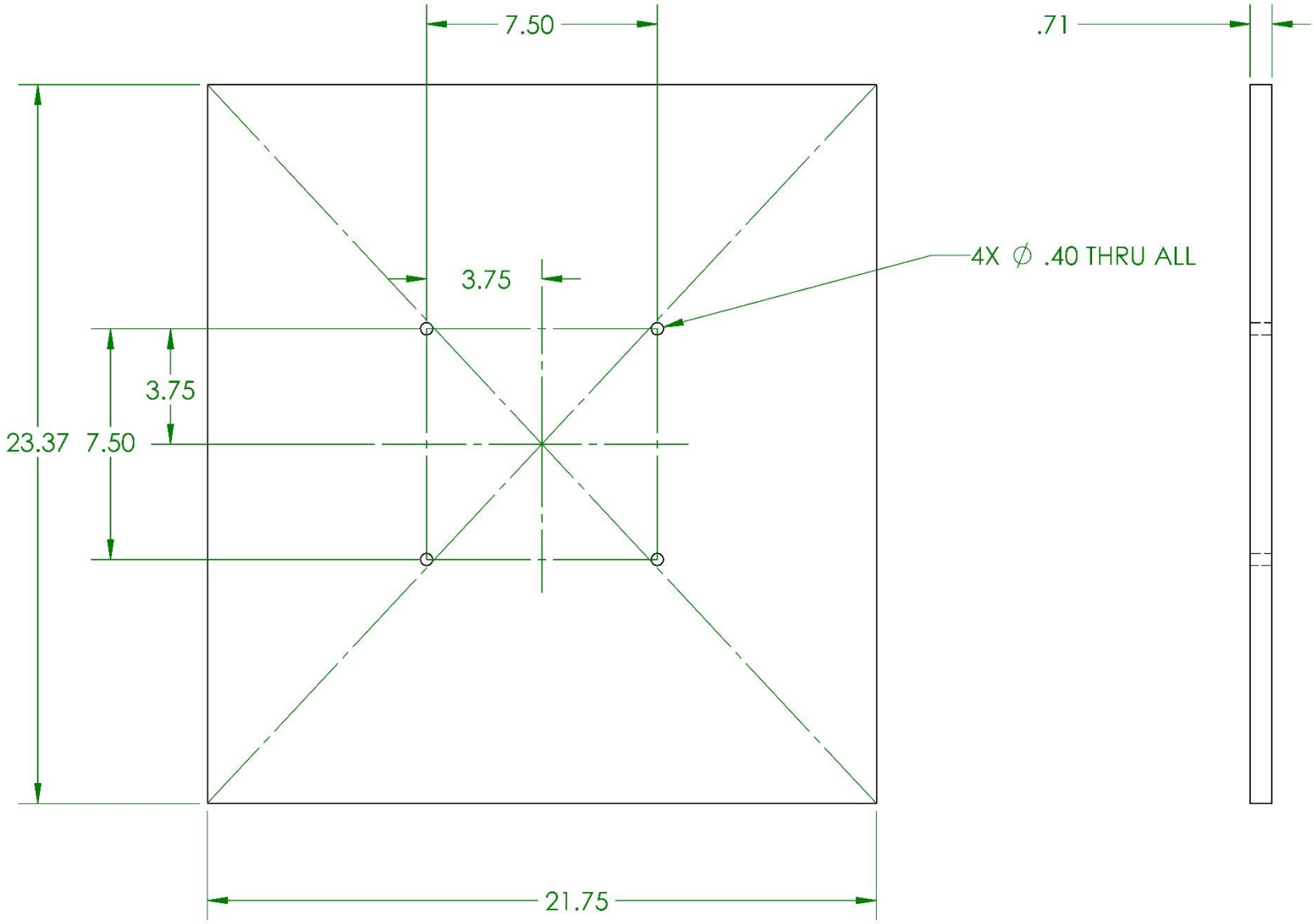

UNLESS OTHERWISE SPECIFIED:		NAME	DATE
DIMENSIONS ARE IN INCHES DIMENSIONS: X.XX ± .01 DIMENSIONS: X.XXX ±.005 ANGULAR: MACH ± 1° BREAK ALL EDGES AND SHARP CORNERS .005 IN	Drwn. By:	J. SKARO	6/7/17
	Chkd. By:	A. NICHOLS	6/7/17
	Q.A.		
MATERIAL PINE PLYWOOD	COMMENTS		
FINISH 63 MICRONS			

PolySat

PART NAME: ROD FIXTURE BASE

SIZE	DRAWING NUMBER	REV.
A	104001	1

SCALE: 1=5 | SHEET: 1 OF 1

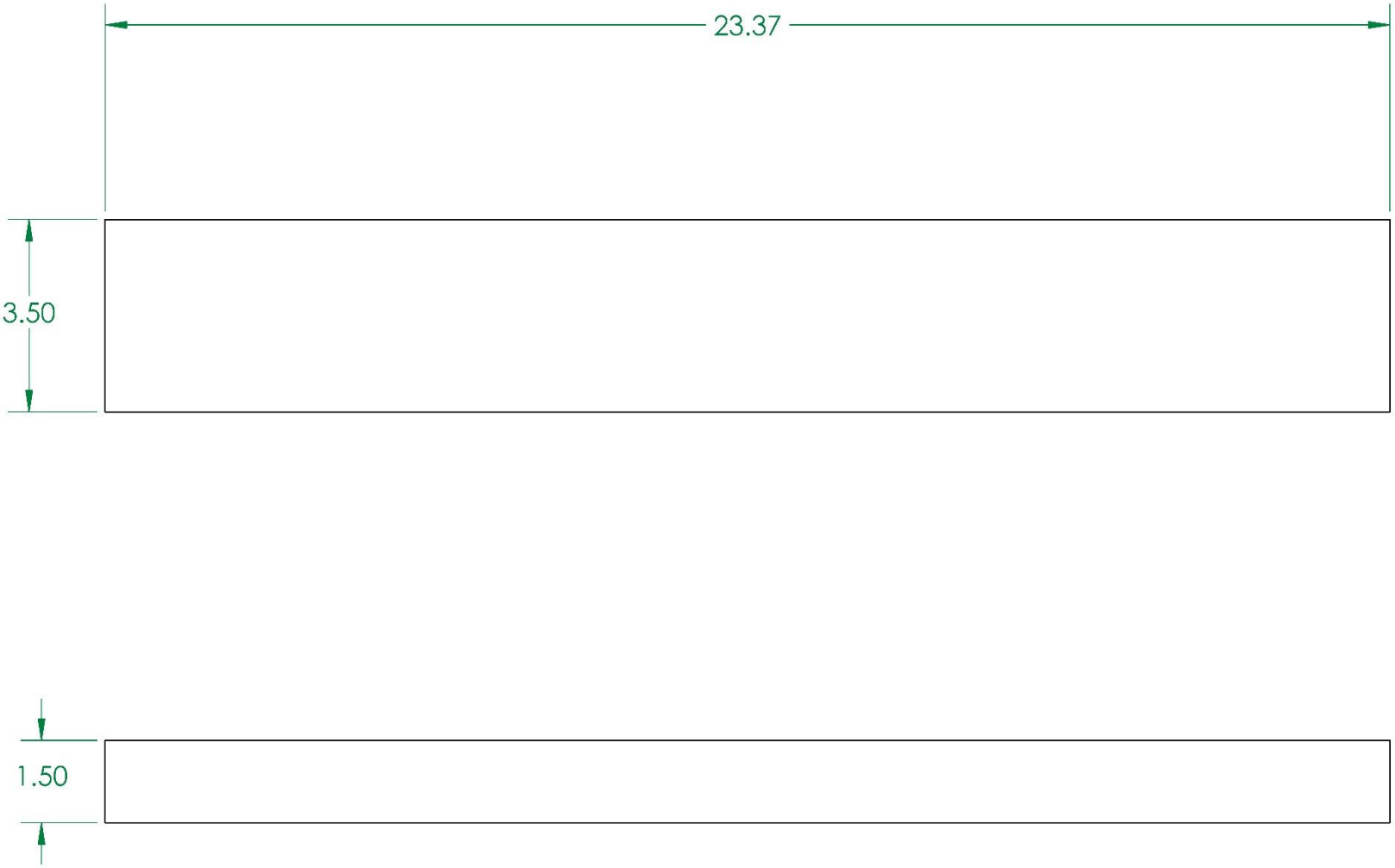

UNLESS OTHERWISE SPECIFIED:		NAME	DATE
DIMENSIONS ARE IN INCHES DIMENSIONS: X.XX - .25 DIMENSIONS: X.XXX ±.005 ANGULAR: MACH ± 1° BREAK ALL EDGES AND SHARP CORNERS .005 IN	Drwn. By:	J. SKARO	6/7/17
	Chkd. By:	A. NICHOLS	6/7/17
	Q.A.		
MATERIAL: PINE WOOD	COMMENTS		
FINISH: 63 MICRONS			

PolySat

PART NAME: 2X4

SIZE	DRAWING NUMBER	REV.
A	104003	1

SCALE: 1=1 | SHEET: 1 OF 1

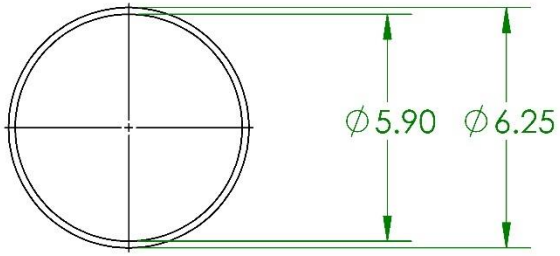

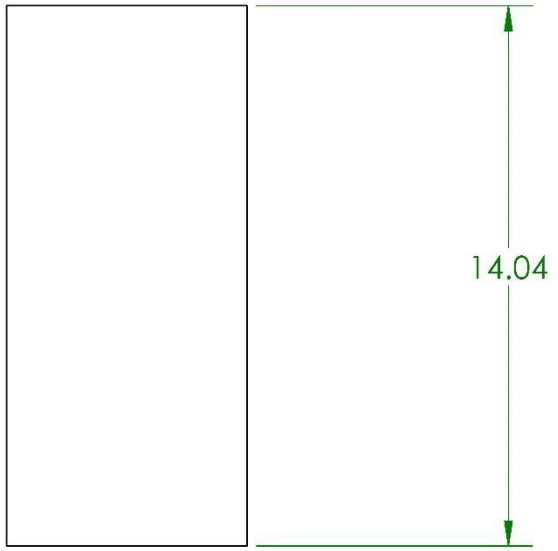

UNLESS OTHERWISE SPECIFIED:
DIMENSIONS ARE IN INCHES
DIMENSIONS: X.XX ± .063
DIMENSIONS: X.XXX ±.005
ANGULAR: MACH ± 1°
BREAK ALL EDGES AND SHARP
CORNERS .005 IN

	NAME	DATE
Drwn. By:	J. SKARO	6/7/17
Chkd. By:	A. NICHOLS	6/7/17
Q.A.		

MATERIAL: PVC

FINISH: 63 MICRONS

COMMENTS

PolySat

PART NAME: PVC PIPE

SIZE	DRAWING NUMBER	REV.
A	104005	1

SCALE: 1=5 | SHEET: 1 OF 1

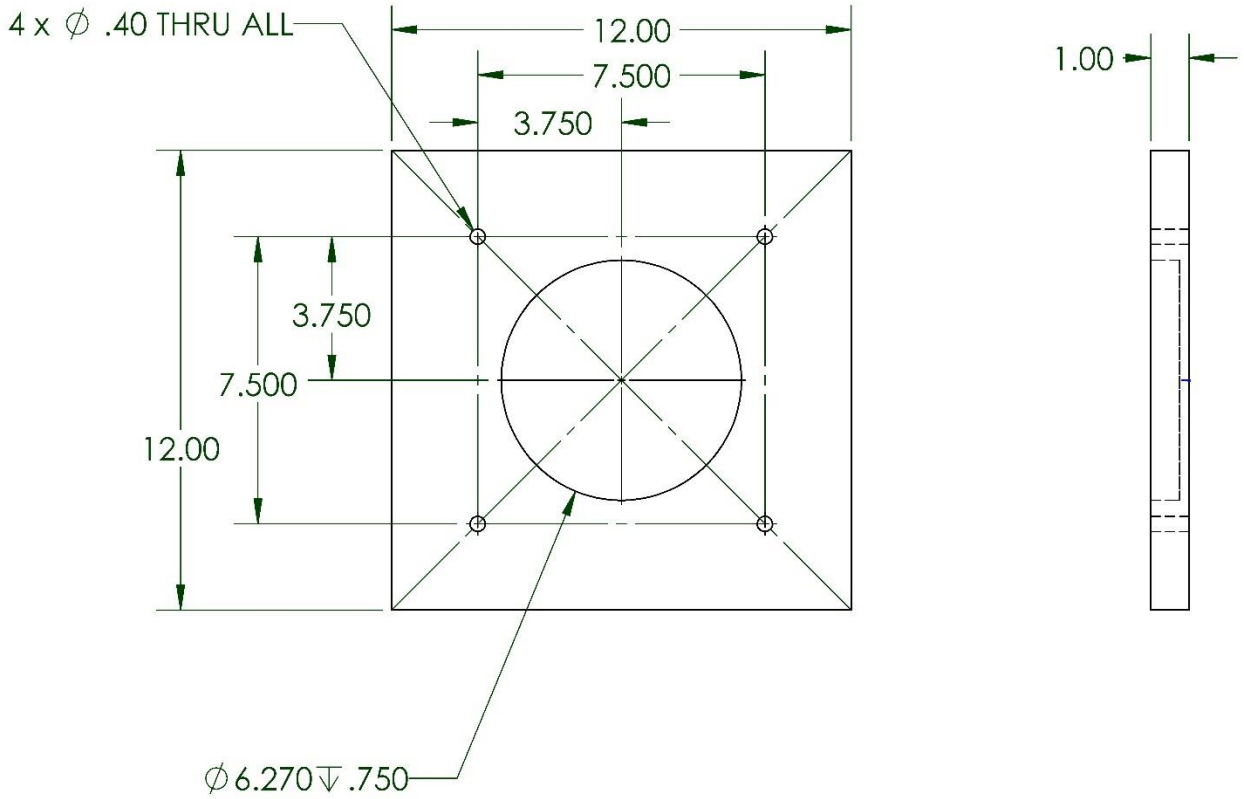

UNLESS OTHERWISE SPECIFIED:
DIMENSIONS ARE IN INCHES
DIMENSIONS: X.XX ± .05
DIMENSIONS: X.XXX ±.005
ANGULAR: MACH ± 1°
BREAK ALL EDGES AND SHARP
CORNERS .01 MM

	NAME	DATE
Drwn. By:	A. NICHOLS	6/7/17
Chkd. By:	J. SKARO	6/7/17
Q.A.		

MATERIAL: ALUMINUM 6061
FINISH: 32 MICRONS
COMMENTS:

PolySat

PART NAME: ALUMINUM PLATE

SIZE	DRAWING NUMBER	REV.
A	104006	1

SCALE: 1=5 | SHEET: 1 OF 1

Appendix C.2 – Electrical Schematics

Complete Controller Board High-Level Block Diagram

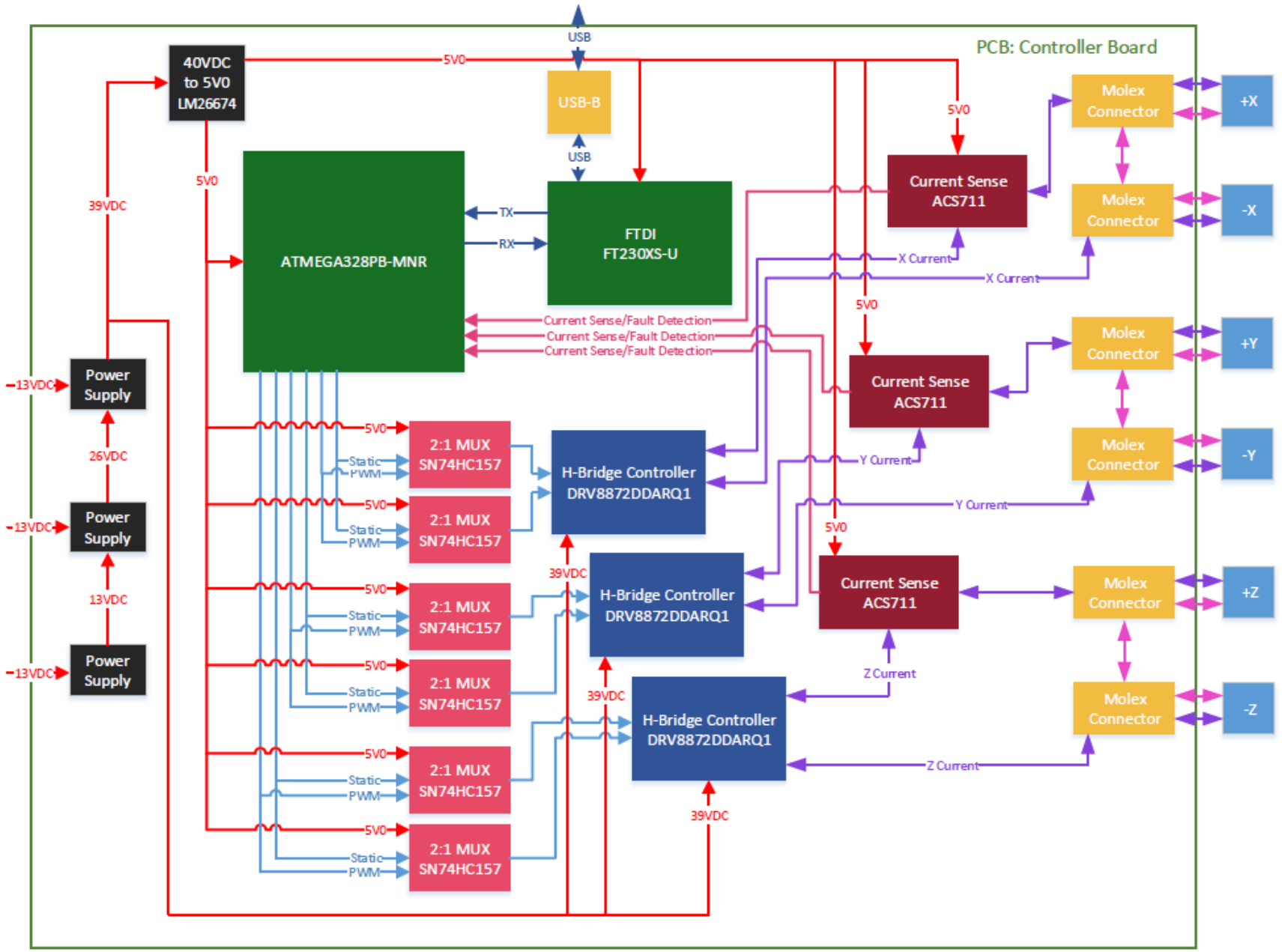

Final Block Diagram

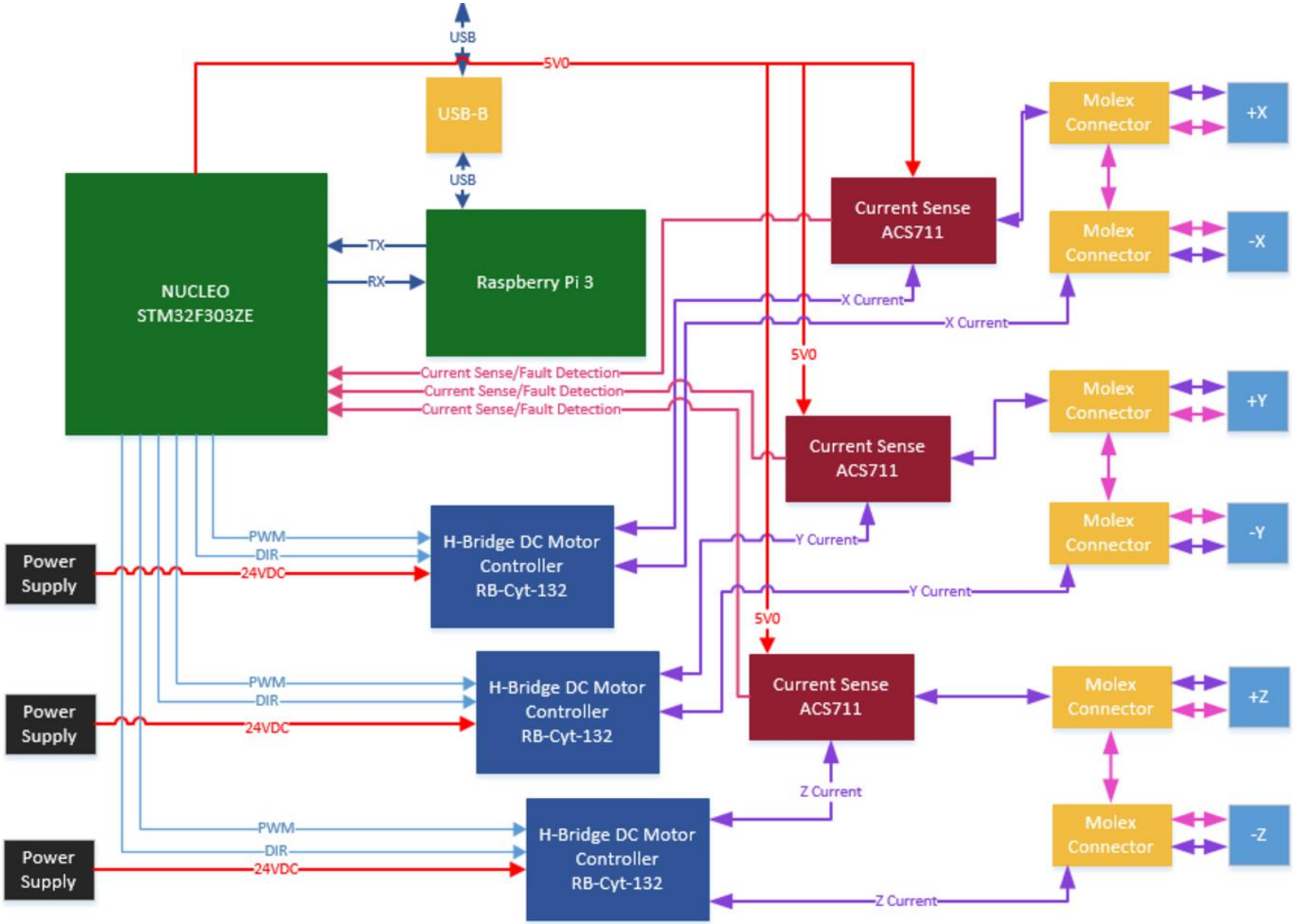

Pin	*Notes	5V0	GND	PWM_X	PWM_Y	PWM_Z	DIR_X	DIR_Y	DIR_Z	STATIC	RX	TX	CTS	RTS	ISENSE_X	ISENSE_Y	ISENSE_Z	RESET	MISO	MOSI	SCK	XTAL1	XTAL2
PB0							x	x	x	x			x	x									
PB1				xOC1A			x	x	x	x			x	x									
PB2	NC			xOC1B			x	x	x	x			x	x									
PB3	Double Booked!						x	x	x	x		x1	x	x						x0			
PB4	Double Booked!						x	x	x	x	x1		x	x					x0				
PB5							x	x	x	x			x	x							x0		
PB6							x	x	x	x			x	x								x	
PB7							x	x	x	x			x	x									x
PC0	NC						x	x	x	x			x	x	x	x	x						
PC1							x	x	x	x			x	x	x	x	x						
PC2							x	x	x	x			x	x	x	x	x						
PC3							x	x	x	x			x	x	x	x	x						
PC4	NC						x	x	x	x			x	x	x	x	x						
PC5	NC						x	x	x	x			x	x	x	x	x						
PC6 / RST	ACTIVE LOW RST	x					x	x	x	x			x	x				x					
PD0					xOC3A		x	x	x	x	x0		x	x									
PD1						xOC4A	x	x	x	x		x0	x	x									
PD2	NC				xOC4B	xOC4B	x	x	x	x			x	x									
PD3							x	x	x	x			x	x									
PD4							x	x	x	x			x	x									
PD5							x	x	x	x			x	x									
PD6							x	x	x	x			x	x									
PD7							x	x	x	x			x	x									
PE0	NC						x	x	x	x			x	x									
PE1	NC						x	x	x	x			x	x									
PE2	NC						x	x	x	x			x	x									
PE3	NC						x	x	x	x			x	x	x	x	x						
AVCC		x																					
VCC		x																					
GND			x																				
AREF		x																					

Helmholtz Cage Controller Board

Connectors
- Power jack connections to three 13.8V 12A power supplies
- USB-B Connection to Raspberry Pi
- 4 pin Molex connectors to each coil (total of 6 Molex connectors)
    * Coils per axis connected in series
    * Axes connected in parallel

Interface
- USB connection to the FTDI
- FTDI communicates to the ATMEGA * RX/TX
- LED indicators for programming

Current Control
- Data delivered from ATMEGA
- H-Bridge controlled by 2 to 1 multiplexers
- One H-Bridge for each axes
- H-Bridge controls forward and reverse current through the coils
- Current sensor to check for mismatched connectors or faults in the coils

Parts
- ATMEGA328PB-MNR : Microcontroller
- FT230XS-U : FTDI
- TPS7A6601QDGNRQ1 : Voltage Regulator
- DRV8872DDARQ1 : H-Bridge
- ACS711ELCTR-12AB-T : Current Sensor
- SN74HC157PWR : 2 to 1 Multiplexer
- 39-01-2040 : 4 pin Molex Female
- PJ-025 : Female Power Jack
- 217-36CTE6 : Heat Sink

Title: Overview		
Size: A	Document Number: M Tran	Rev: 0
Date: Tuesday, February 14, 2017	Sheet 1 of 5	

Power Jacks

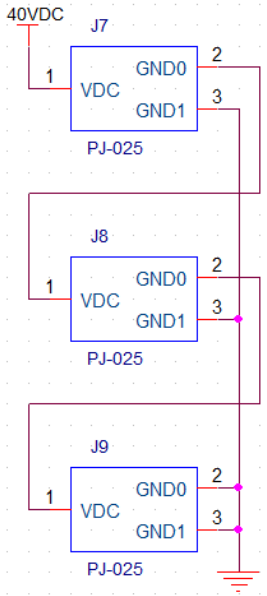

USB-B

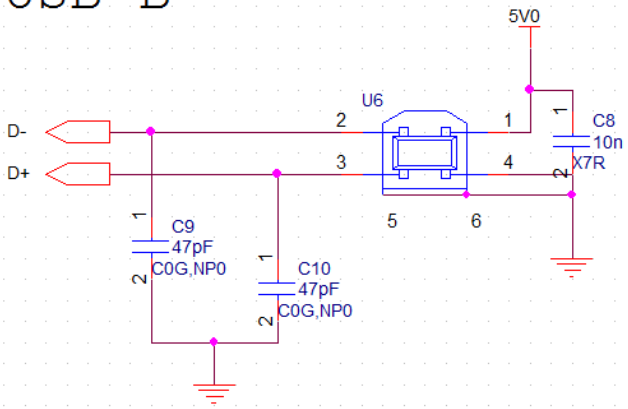

Molex Connectors Coils

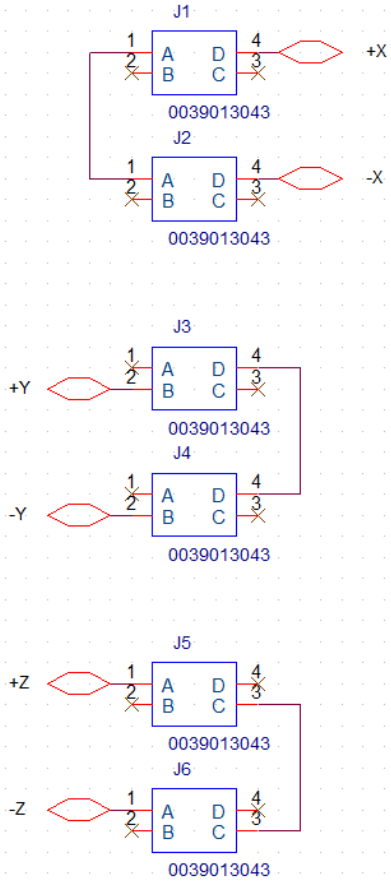

Coils connected in series.
Axes connected in parallel.

Title: Connectors			
Size: A	Document Number: M Tran		Rev: 0
Date: Tuesday, February 14, 2017		Sheet 2 of 5	

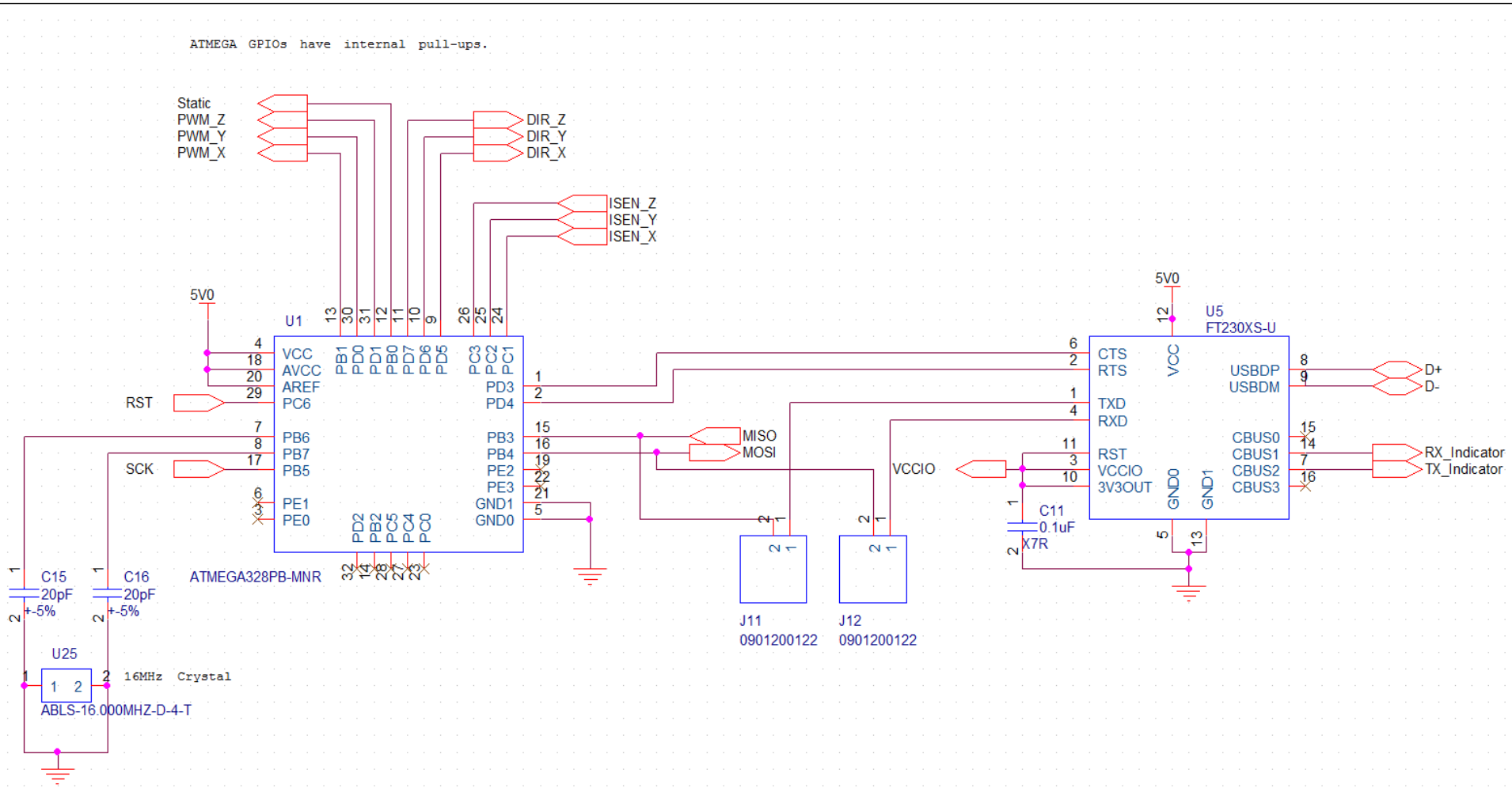

Title	Microcontroller and FTDI	
Size A	Document Number M Tran	Rev 0
Date: Tuesday, February 14, 2017	Sheet 3 of 5	

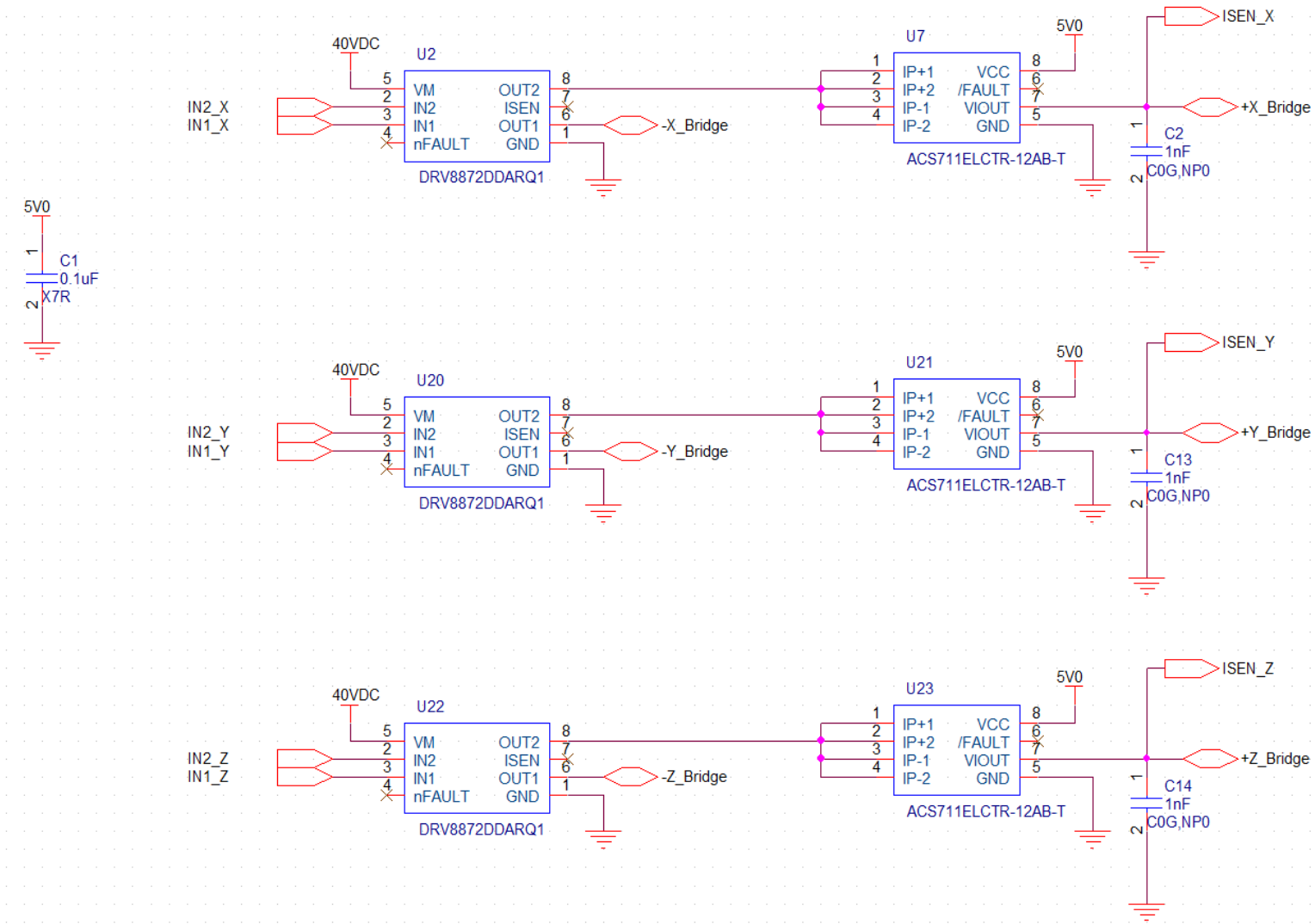

Title	Current Sense & Control	
Size A	Document Number M Tran	Rev 0
Date: Tuesday, February 14, 2017	Sheet 4 of 5	

Current Logic (Multiplexers) H-Bridge Control

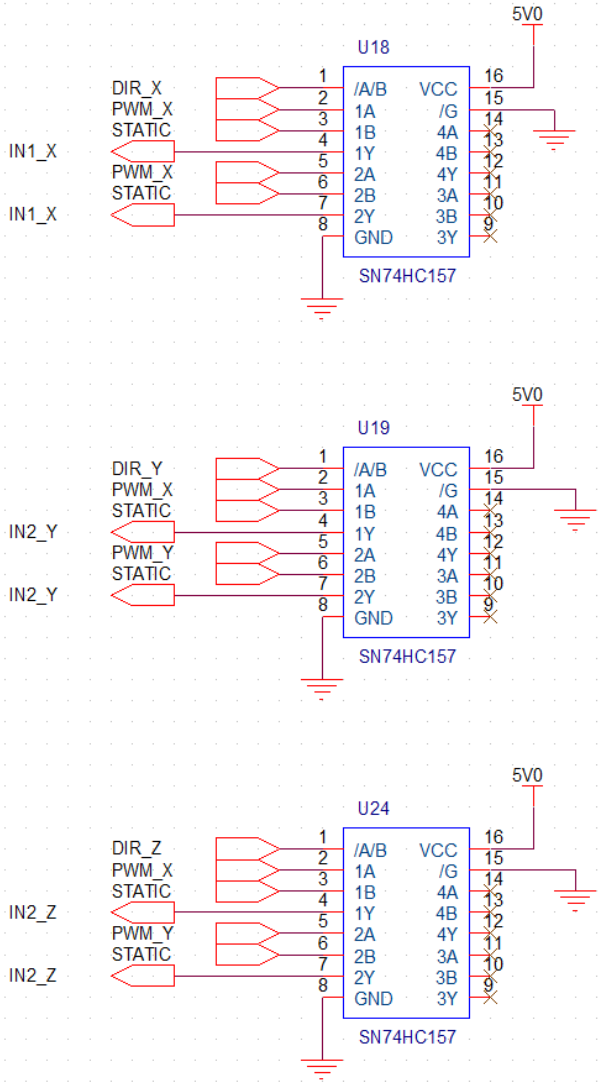

LED Indicators

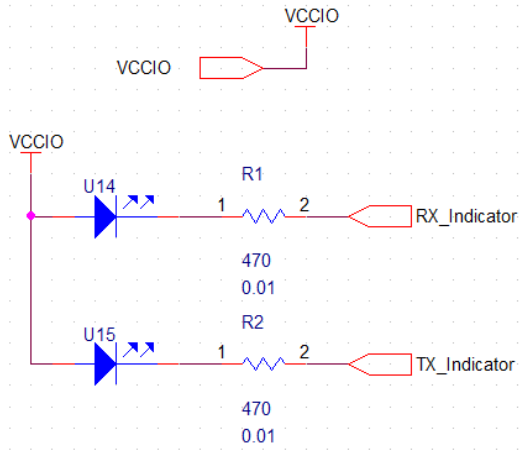

Voltage Regulation

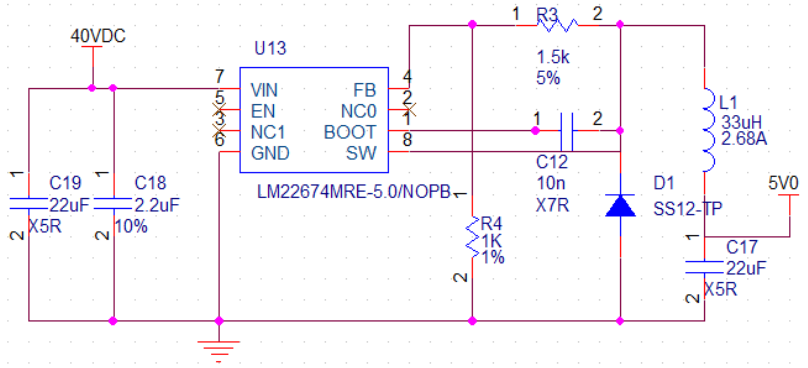

EN is internally pulled-up.
Pull-up to a voltage greater than 2.2 V or leave
EN floating to turn the regulator on.
Pull EN to GND to turn regulator off. Pull-up
voltage should never exceed 6 V.

Title: Regulation / Logic / LED Indicators		
Size: A	Document Number: M Tran	Rev: 0
Date: Tuesday, February 14, 2017	Sheet 5 of 5	

Fail Safe and Connector Board

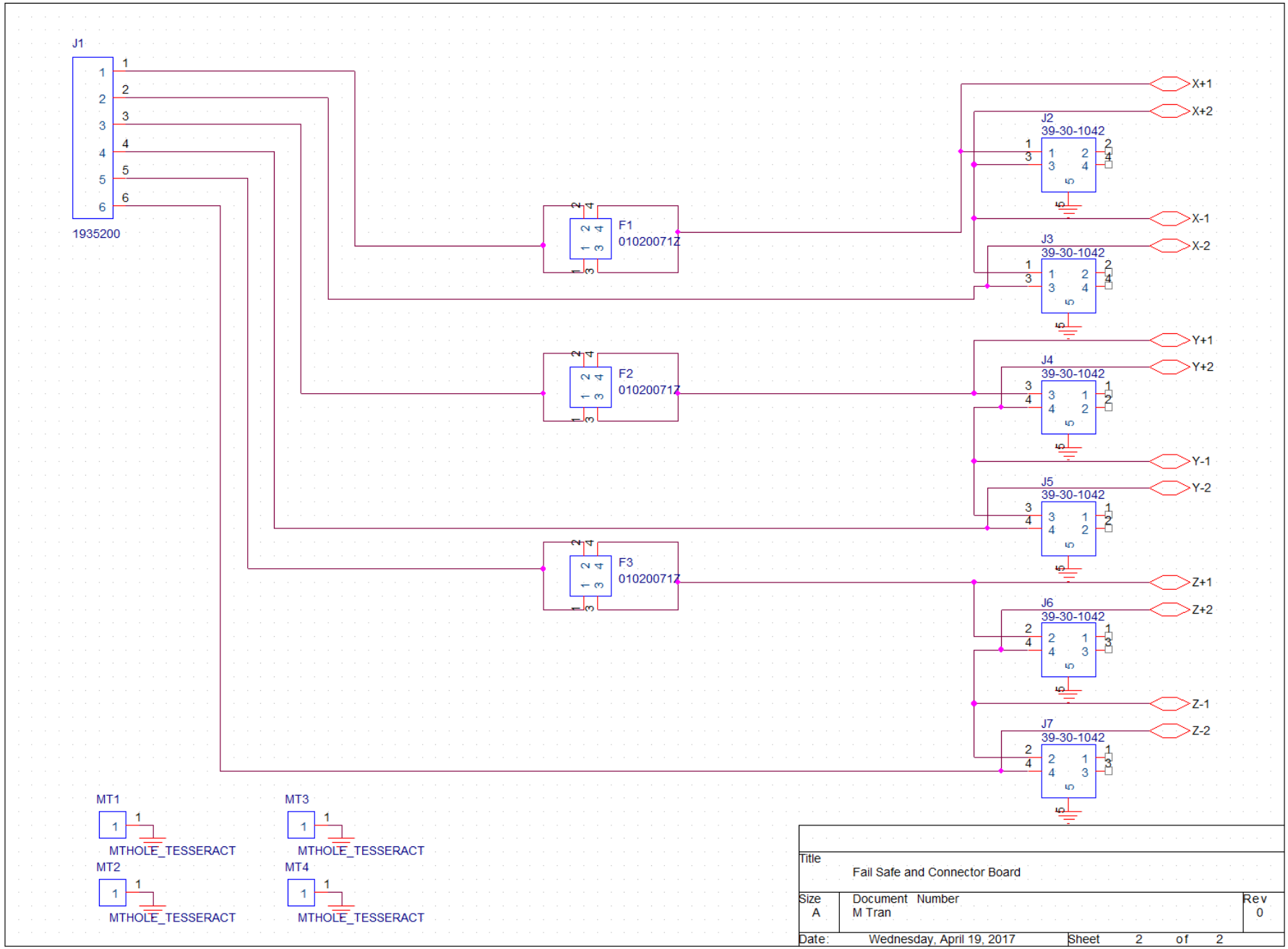

Appendix C.3 – Software Diagrams

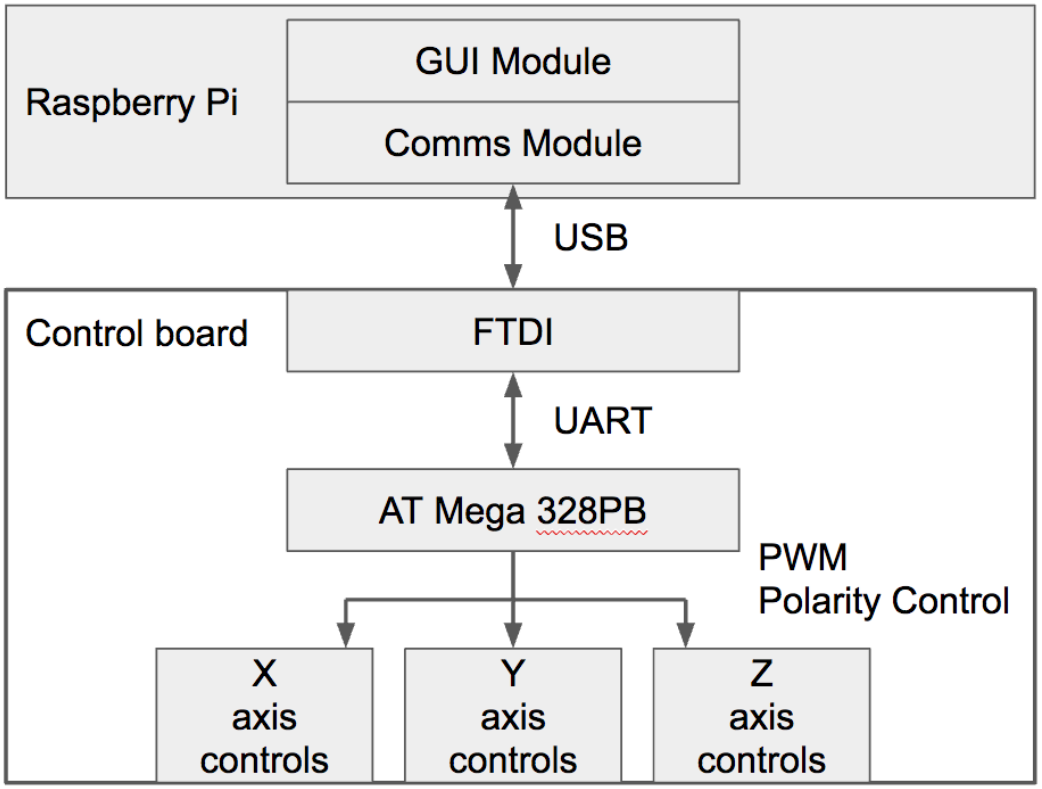

Appendix C.4 – Source Code

```
/*
* AUTHOR: Nicolas Le Renard
* START DATE: 19 May 2017
*/

#include <stdio.h>
#include <stdlib.h>
#include <string.h>
#include <unistd.h>
#include <ctype.h>
#include <math.h>
#include <fcntl.h>
#include <stdint.h>
#include <errno.h>
#include <termios.h>
#include <sys/stat.h>
#include <time.h>

#define MIN_ENTRY 100.0
#define MAX_ENTRY 150.0
#define MAX_UINT16 1800

void commandLineCheck(int, char *);
void usageError();
const char *getFileNameExt(const char *);
void scanLine(char *, int *, int *, double [][4], int *);
void checkLine(int *, int *, int *);
void delay(double);
void analyzeValidity(double, int, int, int);
uint8_t analyzeFlag(double);
uint16_t analyzeMagnitude(double);

int main(int argc, char **argv) {
    FILE *stream;
    char line[1024];
    int lineNumber = 0, entryNumber = 0;
    double entries[1024][4];
```

```
38.     int badFlag = 0;
39.
40.     int uart0_filestream = -1;
41.     struct termios options;
42.
43.     int lineIndex;
44.     uint8_t xFlag, yFlag, zFlag;
45.     uint16_t xMag, yMag, zMag;
46.
47.     commandLineCheck(argc, argv[1]);
48.     stream = fopen(argv[1], "r");
49.     if (stream == NULL)
50.         usageError();
51.     while (fgets(line, sizeof line, stream) != NULL) {
52.         scanLine(line, &entryNumber, &lineNumber, entries, &badFlag);
53.         checkLine(&entryNumber, &lineNumber, &badFlag);
54.     }
55.     fclose(stream);
56.     if (badFlag == 1)
57.         exit(EXIT_FAILURE);
58.     uart0_filestream = open("/dev/ttyS0", O_RDWR | O_NOCTTY | O_NDELAY);
59.     if (uart0_filestream == -1) {
60.         fprintf(stderr, "Unable to open UART\n");
61.         exit(EXIT_FAILURE);
62.     }
63.     tcgetattr(uart0_filestream, &options);
64.     options.c_iflag = 0;
65.     options.c_oflag = 0;
66.     options.c_lflag = 0;
67.     options.c_cflag = 0;
68.     options.c_cc[VMIN] = 0;
69.     options.c_cc[VTIME] = 0;
70.     options.c_cflag = B57600 | CS8 | CREAD;
71.     tcsetattr(uart0_filestream, TCSANOW, &options);
72.     for (lineIndex = 0; lineIndex < lineNumber; lineIndex++) {
73.         delay(entries[lineIndex][0] * 1000);
74.         analyzeValidity(entries[lineIndex][1], lineIndex + 1, 1, uart0_filestream);
75.         analyzeValidity(entries[lineIndex][2], lineIndex + 1, 2, uart0_filestream);
76.         analyzeValidity(entries[lineIndex][3], lineIndex + 1, 3, uart0_filestream);
```

```
            xFlag = analyzeFlag(entries[lineIndex][1]);
            yFlag = analyzeFlag(entries[lineIndex][2]);
            zFlag = analyzeFlag(entries[lineIndex][3]);
            xMag = analyzeMagnitude(entries[lineIndex][1]);
            yMag = analyzeMagnitude(entries[lineIndex][2]);
            zMag = analyzeMagnitude(entries[lineIndex][3]);
            printf("Sending... %d ", xFlag);
            write(uart0_filestream, &xFlag, sizeof(uint8_t));
            printf("%hu ", xMag);
            write(uart0_filestream, &xMag, sizeof(uint16_t));
            printf("%d ", yFlag);
            write(uart0_filestream, &yFlag, sizeof(uint8_t));
            printf("%hu ", yMag);
            write(uart0_filestream, &yMag, sizeof(uint16_t));
            printf("%d ", zFlag);
            write(uart0_filestream, &zFlag, sizeof(uint8_t));
            printf("%hu\n", zMag);
            write(uart0_filestream, &zMag, sizeof(uint16_t));
        }
        close(uart0_filestream);
        exit(EXIT_SUCCESS);
    }

void delay(double milli) {
    long pause;
    clock_t now, then;

    pause = milli * (CLOCKS_PER_SEC / 1000);
    now = then = clock();
    while ((now - then) < pause) {
        now = clock();
    }
}

void analyzeValidity(double entry, int line, int which, int fd) {
    double min = MIN_ENTRY;
    double max = MAX_ENTRY;

    if (entry >= MIN_ENTRY && entry <= MAX_ENTRY) {
```

```
116.     }
117.     else if (entry <= MIN_ENTRY * -1 && entry >= MAX_ENTRY * -1) {
118.     }
119.     else {
120.         if (which == 1) {
121.             fprintf(stderr, "X vector out of bounds on line %d\n", line);
122.             fprintf(stderr, "Magnitude must be between %.1f and %.1f or -%.1f and -%.1f\n", min, max, min, max);
123.             close(fd);
124.             exit(EXIT_FAILURE);
125.         }
126.         else if (which == 2) {
127.             fprintf(stderr, "Y vector out of bounds on line %d\n", line);
128.             fprintf(stderr, "Magnitude must be between %.1f and %.1f or -%.1f and -%.1f\n", min, max, min, max);
129.             close(fd);
130.             exit(EXIT_FAILURE);
131.         }
132.         else {
133.             fprintf(stderr, "Z vector out of bounds on line %d\n", line);
134.             fprintf(stderr, "Magnitude must be between %.1f and %.1f or -%.1f and -%.1f\n", min, max, min, max);
135.             close(fd);
136.             exit(EXIT_FAILURE);
137.         }
138.     }
139. }
140.
141. uint8_t analyzeFlag(double entry) {
142.     if (entry < 0)
143.         return 0;
144.     else
145.         return 1;
146. }
147.
148. uint16_t analyzeMagnitude(double oldEnt) {
149.     double entry = fabs(oldEnt);
150.
151.     return (entry - MIN_ENTRY) / (MAX_ENTRY - MIN_ENTRY) * (MAX_UINT16);
152. }
153.
154. void commandLineCheck(int argc, char *filename) {
```

```
155.     if (argc < 2) {
156.         fprintf(stderr, "Executable (./helmholtz) requires .csv file as argument\n");
157.         exit(EXIT_FAILURE);
158.     }
159.     if (strcmp("csv", getFileNameExt(filename)) != 0) {
160.         fprintf(stderr, "File extension must be .csv\n");
161.         exit(EXIT_FAILURE);
162.     }
163. }
164.
165. void usageError() {
166.     fprintf(stderr, "Usage: ./helmholtz *.csv\n");
167.     fprintf(stderr, "4 entries per line separated by commas\n");
168.     fprintf(stderr, "Entry 1: Time\n");
169.     fprintf(stderr, "Entry 2: X vector\n");
170.     fprintf(stderr, "Entry 3: Y vector\n");
171.     fprintf(stderr, "Entry 4: Z vector\n");
172.     fprintf(stderr, "Example: 1,150,-100.01,125.99\n");
173.     exit(EXIT_FAILURE);
174. }
175.
176. const char *getFileNameExt(const char *filename) {
177.     const char *dot = strrchr(filename, '.');
178.     if (!dot || dot == filename)
179.         return "";
180.     return dot + 1;
181. }
182.
183. void scanLine(char *line, int *entryNumber, int *lineNumber, double entries[][4], int *badFlag) {
184.     char *pt;
185.     double entry;
186.
187.     pt = strtok(line, ",");
188.     while (pt != NULL) {
189.         entry = atof(pt);
190.         if (*entryNumber > 3) {
191.             fprintf(stderr, "Too many entries on line %d\n", *lineNumber + 1);
192.             *badFlag = 1;
193.             return;
```

```
194.         }
195.         entries[*lineNumber][*entryNumber] = entry;
196.         (*entryNumber)++;
197.         pt = strtok(NULL, ",");
198.     }
199. }
200.
201. void checkLine(int *entryNumber, int *lineNumber, int *badFlag) {
202.     if (*entryNumber == 0) {
203.         fprintf(stderr, "Line %d is empty\n", *lineNumber + 1);
204.         *badFlag = 1;
205.     }
206.     else if (*entryNumber < 4) {
207.         fprintf(stderr, "Too few entries on line %d\n", *lineNumber + 1);
208.         *badFlag = 1;
209.     }
210.     *entryNumber = 0;
211.     (*lineNumber)++;
212. }
```

Appendix C.5 – Bill of Materials

Component	Subsystem	Price	Part Number	Source
Aluminum Channeling	Structure	400	Various	Orange Aluminum
Rivets	Structure	15	97447A015	McMaster Carr
2in Cotter Pins	Structure	25	B00HYK7M14	Amazon
Delrin Sheeting	Strcture	50	8573K27	McMaster Carr
Plastic Cart	Structure	85	73002	Amazon
Bushings	Structure	70	2705T14	McMaster Carr
Shaft	Structure	30	5911K41	McMaster Carr
Plastic Clips	Cleanroom Box	20	H05021	Webstaurant
O Rings	Cleanroom Box	20	9452K491	McMaster Carr
12" x 24" x 5.6 mm Acrylic	Cleanroom Box	55	44352	US Plastics
12" x 12" x 5.6 mm Acrylic	Cleanroom Box	7	44350	US Plastics
12" x 12" x 18 mm Acrylic	Cleanroom Box	25	44402	US Plastics
23/32" x 4 ft x 8 ft Pine Plywood	Pedestal	30	-	Home Depot
2" x 4" x 8 ft Pine	Pedestal	3	-	Home Depot
PVC	Pedestal	12	8749K11	McMaster Carr
Aluminum Box	PCB Housing	35	-	Amazon
Adhesive	General	20	TBD	TBD
Shipping Costs	General	148	-	-
Replacement Parts/Other	General	500	-	-
20 AWG Magnet wire (3000 ft)	Electrical	300		
PCB Components (x10 for 5 assemb	Electrical			
Microcontroller		30	ATMEGA328PB-MNR	Digi-Key
FTDI		30	FT230XS-U	Digi-Key
Voltage Regulator		30	LM22674MRE-5.0/NOPB	Digi-Key
DC Motor Driver/H-Bridge		90	DRV8872DDARQ1	Digi-Key
Current Sensor		80	ASC711	Digi-Key
2:1 Multiplexer		15	SN74HC157	Digi-Key
Molex Connectors Male		10	39013043	Digi-Key
Molex Connectors Female		10	39-01-2040	Digi-Key
Power Jack Male		20	PP-016	Digi-Key
Power Jack Female		30	PJ-025	Digi-Key
Heat Sinks		15	217-36CTE6	Digi-Key
PCB Fabrication and Assembly5 PCI	Electrical	420	-	PCB Way
PCB Fabrication and Assembly5 PCI	Electrical	420	-	PCB Way
13.8V, 12A power supply (x3)	Electrical	400	TP1863	Amazon
Raspberry Pi 3 Model B	Computer	100	RASPBERRYPI3-MODB-1GB	Amazon
Logitech M500	Computer Acces.	30	910-001204	Amazon
Steelseries QcK	Computer Acces.	10	63004	Amazon
HP 24ea	Computer Acess.	165	24ea	Amazon
Havit HV-KB380L	Computer Acess.	45	HV-KB380L	Amazon
	Total	**3800**		

Appendix C.6 – Manufacturing Checklist

Helmholtz Cage Manufacturing Guide																
Assembly	Drawing	Checked	Sub Assembly	Drawing	Checked	Assembled	Part	Configuration	Number	Material	Special Tooling	Quantity	Drawing	Checked	Stock Recieved	Manufactured
Helmholtz Cage (100000)	Alex	Jordan	Coils (101000-1) (101000-2) (101000-3)	Alex	Jordan		Aluminum Rail	Large Rail	101005	Aluminum	-	4	Alex	Jordan		
								Large Rail - M	101006	Aluminum	-	4		Jordan		
								Med. Rail - S	101003	Aluminum	-	4		Jordan		
								Med. Rail - L	101004	Aluminum	-	4		Jordan		
								Small Rail	101001	Aluminum	-	4		Jordan		
								Small Rail - M	101002	Aluminum	-	4	Alex	Jordan		
							Corner Brackets	Default	101007	Aluminum	CNC	24	Alex	Jordan		
							Linear Bushing	Default	101008	Delrin	-	32	Alex	Jordan		
			Bushing Assembly (102000)	Alex	Jordan		Translation Bracket	BSHG	102001	Aluminum	CNC	8	Alex	Jordan		
								Shaft	102002	Aluminum	CNC	8		Jordan		
								Z-Axis	101009	Aluminum	CNC	8	Alex	Jordan		
							1/4in Shaft	Default	102004	Aluminum	-	8	Alex	Jordan		
							1/8" Delrin Pad	Default	102005	Delrin	-	48		Jordan		
							1/16" Delrin Pad	Default	102006	Delrin	-	48		Jordan		
							Bushing	Default	102003	Delrin	Mill	8		Jordan		
			Clean Room Box (103000)	Alex	Jordan		Wall	Default	103002	Acryllic	Laser Engraver	4	Alex	Jordan		
							Base	Default	103001	Acryllic	CNC	1	Alex	Jordan		
							Top	Default	103003	Acryllic	Laser Engraver	1	Alex	Jordan		
							Clip Extender	Default	103004	Acryllic	Laser Engraver	4	Alex	Jordan		
							Corner Blocks	Default	103005	PLA/ABS	3D Printer	4	Alex	Jordan		
			Pedastal (104000)	Jordan	Alex		Aluminum Angle	Default	104004	Aluminum	-	4	Jordan	Alex		
							Rod Fixture	Top	104002	Pine	-	1	Jordan	Alex		
								Base	104001	Pine	-	1	Jordan	Alex		
							PVC Pipe	Default	104005	PVC	-	1	Jordan	Alex		
							2X4X37	Default	104003	Pine	-	2	Jordan	Alex		

Appendix D – Vendor Information

Distributor	Contact: E-mail	Contact: Phone	Address	Website
Digi-Key Electronics	sales@digikey.com	218-681-6674	701 Brooks Avenue South, Thief River Falls, MN 56701 USA	http://www.digikey.com/
Manufacturer	**Contact E-mail**	**Contact: Phone**	**Address**	**Website**
Allegro MicroSystems, LLC Caltron Components Corp.	jmorgese@caltroncomponents.com	408-748-2140	3350 Scott Blvd. Bldg. 31 Santa Clara, CA 95054	http://www.allegromicro.com/
CUI Inc.	Form must be filled out for e-mail support	503-612-2300	20050 SW 112th Avenue Tualatin, OR 97062	http://www.cui.com/
Future Technology Devices International Ltd.	sales1@ftdichip.com support1@ftdichip.com	+44 (0) 141-429-2777	Unit 1, 2 Seaward Place Centurion Business Park, Glasgow G41 1HH United Kingdom	http://www.ftdichip.com/
Microchip Technology	Account needed for e-mail support	949-462-9523	25950 Acero St. Suite 200 Mission Viejo, CA 92692 USA	http://www.microchip.com/
Molex	Form must be filled out for e-mail support	630-969-4550	2222 Wellington Court, Lisle, IL 60532-1682	http://www.molex.com/molex/home
Tekpower	info@tekpower.us	909-628-6088	5185 Cliffwood Dr. Montclair, CA 91763 USA	http://tekpower.us/
Texas Instruments	Account needed for product support	972-995-2011	Dallas, TX 75226-0199	http://www.ti.com/
Wakefield-Vette	Form must be filled out for e-mail support	603-635-2800	33 Bridge St, Pelham, NH 03076	http://www.wakefield-vette.com/

Appendix E – Vendor Specification Sheets

8-bit AVR Microcontroller

ATmega328PB

DATASHEET COMPLETE

Introduction

The Atmel® ATmega328PB is a low-power CMOS 8-bit microcontroller based on the AVR® enhanced RISC architecture. By executing powerful instructions in a single clock cycle, the ATmega328PB achieves throughputs close to 1MIPS per MHz. This empowers system designer to optimize the device for power consumption versus processing speed.

Feature

High Performance, Low Power Atmel®AVR® 8-Bit Microcontroller Family

- Advanced RISC Architecture
  - 131 Powerful Instructions
  - Most Single Clock Cycle Execution
  - 32 x 8 General Purpose Working Registers
  - Fully Static Operation
  - Up to 20 MIPS Throughput at 20MHz
  - On-chip 2-cycle Multiplier
- High Endurance Non-volatile Memory Segments
  - 32KBytes of In-System Self-Programmable Flash program memory
  - 1KBytes EEPROM
  - 2KBytes Internal SRAM
  - Write/Erase Cycles: 10,000 Flash/100,000 EEPROM
  - Data retention: 20 years at 85°C/100 years at 25°C(1)
  - Optional Boot Code Section with Independent Lock Bits
    - In-System Programming by On-chip Boot Program
    - True Read-While-Write Operation
  - Programming Lock for Software Security
- Peripheral Touch Controller
  - Capacitive touch buttons, sliders and wheels
  - 24 Self-cap channels and 144 mutual cap channels
- Peripheral Features
  - Two 8-bit Timer/Counters with Separate Prescaler and Compare Mode

  - Three 16-bit Timer/Counter with Separate Prescaler, Compare Mode, and Capture Mode
  - Real Time Counter with Separate Oscillator
  - Ten PWM Channels
  - 8-channel 10-bit ADC in TQFP and QFN/MLF package
  - Two Programmable Serial USART
  - Two Master/Slave SPI Serial Interface
  - Two Byte-oriented 2-wire Serial Interface (Philips I^2C compatible)
  - Programmable Watchdog Timer with Separate On-chip Oscillator
  - On-chip Analog Comparator
  - Interrupt and Wake-up on Pin Change
- Special Microcontroller Features
  - Power-on Reset and Programmable Brown-out Detection
  - Internal Calibrated Oscillator
  - External and Internal Interrupt Sources
  - Six Sleep Modes: Idle, ADC Noise Reduction, Power-save, Power-down, Standby, and Extended Standby
  - Unique Device ID
- I/O and Packages
  - 27 Programmable I/O Lines
  - 32-pin TQFP and 32-pin QFN/MLF
- Operating Voltage:
  - 1.8 - 5.5V
- Temperature Range:
  - -40°C to 105°C
- Speed Grade:
  - 0 - 4MHz @ 1.8 - 5.5V
  - 0 - 10MHz @ 2.7 - 5.5.V
  - 0 - 20MHz @ 4.5 - 5.5V
- Power Consumption at 1MHz, 1.8V, 25°C
  - Active Mode: 0.2mA
  - Power-down Mode: 0.2µA
  - Power-save Mode: 1.3µA (Including 32kHz RTC)

2. Configuration Summary

Features	ATmega328PB
Pin count	32
Flash (KB)	32
SRAM (KB)	2
EEPROM (KB)	1
General Purpose I/O pins	27
SPI	2
TWI (I^2C)	2
USART	2
ADC	10-bit 15ksps
ADC channels	8
AC propagation delay	400ns (Typical)
8-bit Timer/Counters	2
16-bit Timer/Counters	3
PWM channels	10
PTC	Available
Clock Failure Detector (CFD)	Available
Output Compare Modulator (OCM1C2)	Available

4. Block Diagram

Figure 4-1 Block Diagram

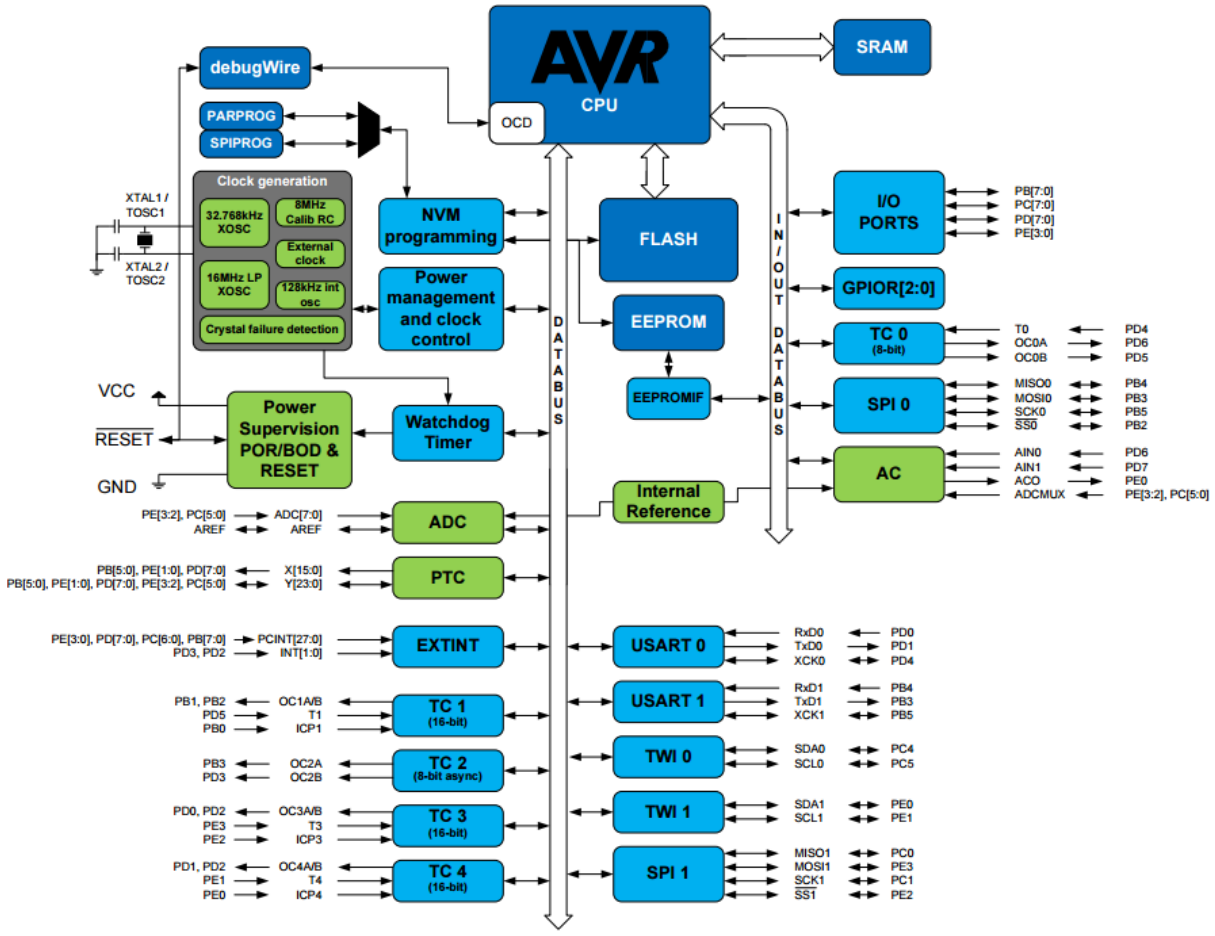

5. Pin Configurations

Figure 5-1 32 TQFP Pinout ATmega328PB

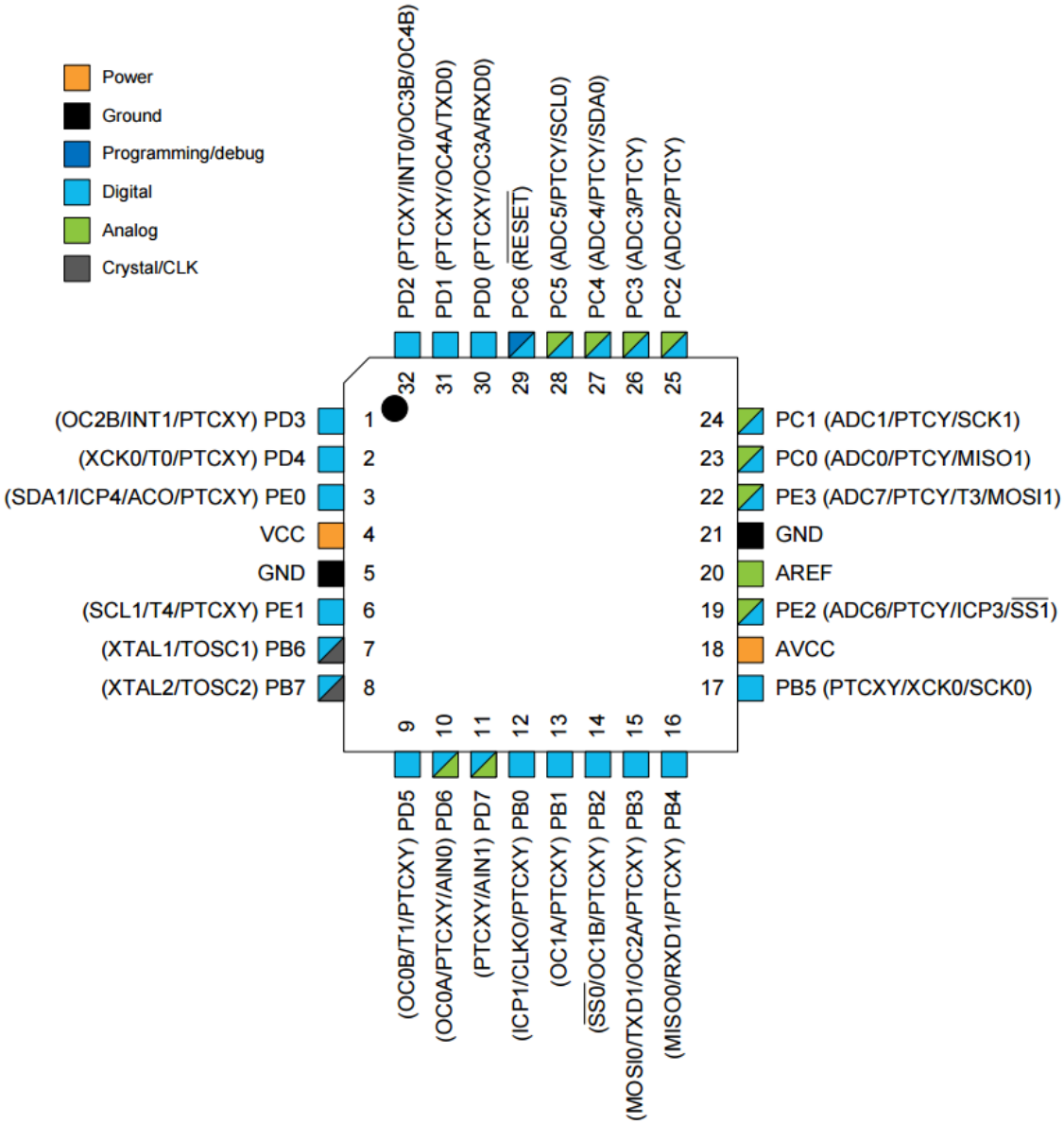

6. I/O Multiplexing

Each pin is by default controlled by the PORT as a general purpose I/O and alternatively it can be assigned to one of the peripheral functions.

The following table describes the peripheral signals multiplexed to the PORT I/O pins.

Table 6-1 PORT Function Multiplexing

No	PAD	EXTINT	PCINT	ADC/AC	PTC X	PTC Y	OSC	T/C # 0	T/C # 1	USART	I2C	SPI
1	PD[3]	INT1	PCINT19		X3	Y11		OC2A				
2	PD[4]		PCINT20		X4	Y12		T0		XCK0		
3	PE[0]		PCINT24	ACO	X8	Y16			ICP4		SDA1	
4	VCC											
5	GND											
6	PE[1]		PCINT25		X9	Y17			TC4		SCL1	
7	PB[6]		PCINT6				XTAL1/TOSC1					
8	PB[7]		PCINT7				XTAL2/TOSC2					
9	PD[5]		PCINT21		X5	Y13		OC0B	T1			
10	PD[6]		PCINT22	AIN0	X6	Y14		OC0A				
11	PD[7]		PCINT23	AIN1	X7	Y15						
12	PB[0]		PCINT0		X10	Y18	CLKO	ICP1				
13	PB[1]		PCINT1		X11	Y19		OC1A				
14	PB[2]		PCINT2		X12	Y20		OC1B				$\overline{SS0}$
15	PB[3]		PCINT3		X13	Y21		OC2A		TXD1		MOSI0
16	PB[4]		PCINT4		X14	Y22				RXD1		MISO0
17	PB[5]		PCINT5		X15	Y23				XCK0		SCK0
18	AVCC											
19	PE[2]		PCINT26	ADC6		Y6		ICP3				$\overline{SS1}$
20	AREF											
21	GND											
22	PE[3]		PCINT27	ADC7		Y7		T3				MOSI1
23	PC[0]		PCINT8	ADC0		Y0						MISO1
24	PC[1]		PCINT9	ADC1		Y1						SCK1
25	PC[2]		PCINT10	ADC2		Y2						
26	PC[3]		PCINT11	ADC3		Y3						
27	PC[4]		PCINT12	ADC4		Y4					SDA0	
28	PC[5]		PCINT13	ADC5		Y5					SCL0	
29	PC[6]/$\overline{RESET}$		PCINT14									
30	PD[0]		PCINT16		X0	Y8		OC3A		RXD0		
31	PD[1]		PCINT17		X1	Y9			OC4A	TXD0		
32	PD[2]	INT0	PCINT18		X2	Y10		OC3B	OC4B			

TEXAS INSTRUMENTS

DRV8872-Q1

SLIS175 – NOVEMBER 2016

DRV8872-Q1 Automotive 3.6-A Brushed DC Motor Driver With Fault Reporting

1 Features

- AEC-Q100 Qualified for Automotive Applications:
  - Device Temperature Grade 1: –40°C to +125°C Ambient Operating Temperature Range
  - Device HBM ESD Classification Level 2
  - Device CDM ESD Classification Level C4B
- H-Bridge Motor Driver
  - Drives One DC Motor, One Winding of a Stepper Motor, or Other Loads
- Wide 6.8-V to 45-V Operating Voltage
- 565-mΩ Typical $R_{DS(on)}$ (HS + LS)
- 3.6-A Peak Current Drive
- PWM Control Interface
- Integrated Current Regulation
- Low-Power Sleep Mode
- Fault Status Output Pin
- Small Package and Footprint
  - 8-Pin HSOP With PowerPAD™
  - 4.9 × 6 mm
- **Integrated Protection Features**
  - VM Undervoltage Lockout (UVLO)
  - Overcurrent Protection (OCP)
  - Thermal Shutdown (TSD)
  - Fault Reporting (nFAULT)
  - Automatic Fault Recovery

2 Applications

- Automotive Infotainment
- HUD Projector Adjustment
- Motorized Shifter Knobs
- Piezo Horn Driver

3 Description

The DRV8872-Q1 device is a brushed DC (BDC) motor driver for infotainment, HUD projector adjustment, motorized shifter knobs, and piezo horn drivers. Two logic inputs control the H-bridge driver, which consists of four N-channel MOSFETs that provide bidirectional control of motors up to 3.6-A peak current. The inputs can be pulse-width modulated (PWM) to control motor speed, using a choice of current-decay modes. Setting both inputs low enters a low-power sleep mode.

The DRV8872-Q1 device features integrated current regulation, based on an internal reference voltage and the voltage on the ISEN pin, which is proportional to motor current through an external sense resistor. The ability to limit current to a known level can significantly reduce the system power requirements and bulk capacitance needed to maintain stable voltage, especially for motor startup and stall conditions.

The device is fully protected from faults and short circuits, including undervoltage lockout (UVLO), overcurrent protection (OCP), and thermal shutdown (TSD). Faults are communicated by pulling the nFAULT output low. When the fault condition is removed, the device automatically resumes normal operation.

Device Information[1]

PART NUMBER	PACKAGE	BODY SIZE (NOM)
DRV8872-Q1	HSOP (8)	4.90 mm × 6.00 mm

(1) For all available packages, see the orderable addendum at the end of the data sheet.

Simplified Schematic

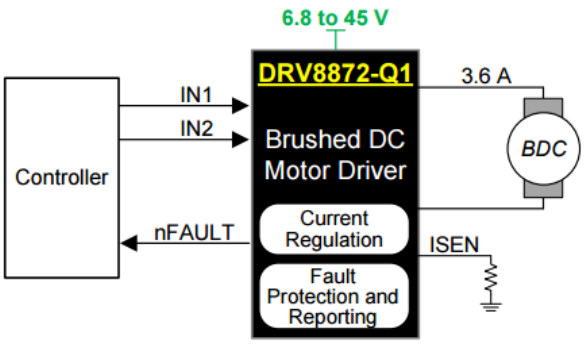

H-Bridge States

5 Pin Configuration and Functions

DDA Package
8-Pin HSOP With Exposed Thermal Pad
Top View

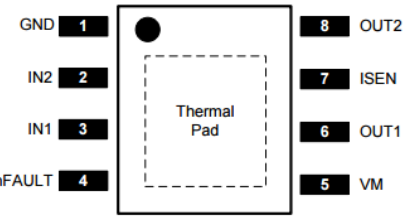

Pin Functions

PIN		TYPE	DESCRIPTION	
NAME	NO.			
GND	1	PWR	Logic ground	Connect to board ground.
IN1	3	I	Logic inputs	Controls the H-bridge output. Has internal pulldowns. (See Table 1.)
IN2	2			
ISEN	7	PWR	High-current ground path	If using current regulation, connect ISEN to a resistor (low-value, high-power-rating) to ground. If not using current regulation, connect ISEN directly to ground.
nFAULT	4	OD	Fault status (open-drain)	Low-level indicates UVLO, TSD, or OCP fault. Connect to a pullup resistor.
OUT1	6	O	H-bridge outputs	Connect directly to the motor, or other inductive load.
OUT2	8			
VM	5	PWR	6.8-V to 45-V power supply	Connect a 0.1-µF bypass capacitor to ground, as well as sufficient bulk capacitance, rated for the VM voltage.
PAD	—	—	Thermal pad	Connect to board ground. For good thermal dissipation, use large ground planes on multiple layers, and multiple nearby vias connecting those planes.

6 Specifications

6.1 Absolute Maximum Ratings

over operating free-air temperature range (unless otherwise noted)(1)

	MIN	MAX	UNIT
Power supply voltage (VM)	–0.3	50	V
Logic input voltage (IN1, IN2)	–0.3	7	V
Fault pin (nFAULT)	–0.3	6	V
Continuous phase node pin voltage (OUT1, OUT2)	–0.7	VM + 0.7	V
Current sense input pin voltage (ISEN)(2)	–0.5	1	V
Output current (100% duty cycle)		3.5	A
Operating junction temperature, T_J	–40	150	°C
Storage temperature, T_{stg}	–65	150	°C

(1) Stresses beyond those listed under *Absolute Maximum Ratings* may cause permanent damage to the device. These are stress ratings only, which do not imply functional operation of the device at these or any other conditions beyond those indicated under *Recommended Operating Conditions*. Exposure to absolute-maximum-rated conditions for extended periods may affect device reliability.
(2) Transients of ±1 V for less than 25 ns are acceptable

Future Technology Devices International Ltd.

FT230X

(USB to BASIC UART IC)

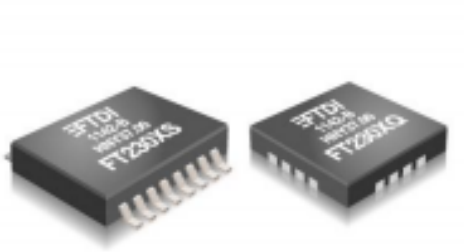

The FT230X is a USB to serial UART interface with optimised pin count for smaller PCB designs and the following advanced features:

- Single chip USB to asynchronous serial data transfer interface.
- Entire USB protocol handled on the chip. No USB specific firmware programming required.
- Fully integrated 2048 byte multi-time-programmable (MTP) memory, storing device descriptors and CBUS I/O configuration.
- Fully integrated clock generation with no external crystal required plus optional clock output selection enabling a glue-less interface to external MCU or FPGA.
- Data transfer rates from 300 baud to 3 Mbaud (RS422, RS485, and RS232) at TTL levels.
- 512 byte receive buffer and 512 byte transmit buffer utilising buffer smoothing technology to allow for high data throughput.
- FTDI's royalty-free Virtual Com Port (VCP) and Direct (D2XX) drivers eliminate the requirement for USB driver development in most cases.
- Configurable CBUS I/O pins.
- Transmit and receive LED drive signals.
- UART interface support for 7 or 8 data bits, 1 or 2 stop bits and odd / even / mark / space / no parity
- Synchronous and asynchronous bit bang interface options with RD# and WR# strobes.
- USB Battery Charger Detection. Allows for USB peripheral devices to detect the presence of a higher power source to enable improved charging.
- Device supplied pre-programmed with unique USB serial number.
- USB Power Configurations; supports bus- powered, self-powered and bus-powered with power switching
- Integrated +3.3V level converter for USB I/O.
- True 3.3V CMOS drive output and TTL input; operates down to 1V8 with external pull ups. Tolerant of 5V input
- Configurable I/O pin output drive strength; 4 mA (min) and 16 mA (max).
- Integrated power-on-reset circuit.
- Fully integrated AVCC supply filtering - no external filtering required.
- UART signal inversion option.
- + 5V Single Supply Operation.
- Internal 3V3/1V8 LDO regulators
- Low operating and USB suspend current; 8mA (active-typ) and 125uA (suspend-typ).
- UHCI/OHCI/EHCI host controller compatible.
- USB 2.0 Full Speed compatible.
- Extended operating temperature range; -40 to 85ºC.
- Available in compact Pb-free 16 pin SSOP and 16 pin QFN packages (both RoHS compliant).

1 Typical Applications

- USB to RS232/RS422/RS485 Converters
- Upgrading Legacy Peripherals to USB
- Utilising USB to add system modularity
- Incorporate USB interface to enable PC transfers for development system communication
- Cellular and Cordless Phone USB data transfer cables and interfaces
- Interfacing MCU/PLD/FPGA based designs to add USB connectivity
- USB Audio and Low Bandwidth Video data transfer
- USB Smart Card Readers
- USB Instrumentation
- USB Industrial Control
- USB MP3 Player Interface
- USB FLASH Card Reader and Writers
- Set Top Box PC - USB interface
- USB Digital Camera Interface
- USB Hardware Modems
- USB Wireless Modems
- USB Bar Code Readers
- USB dongle implementations for Software/ Hardware Encryption and Wireless Modules
- Detection of dedicated charging port for battery charging at higher supply currents.

1.1 Driver Support

Royalty free VIRTUAL COM PORT (VCP) DRIVERS for...

- Windows 10 32,64 bit
- Windows 8/8.1 32,64-bit
- Windows 7 32, 64-bit
- Windows Vista and Vista 64-bit
- Windows XP and XP 64-bit
- Server 2003, XP and Server 2008/2012
- Windows XP Embedded
- Windows CE 4.2-5.2, 6.0, 7.0, 2013
- Mac OS-X
- Linux 3.2 and greater
- Android

Royalty free D2XX *Direct* Drivers (USB Drivers + DLL S/W Interface)

- Windows 10 32,64 bit
- Windows 8/8.1 32,64-bit
- Windows 7 32,64-bit
- Windows Vista and Vista 64-bit
- Windows XP and XP 64-bit
- Server 2003, XP and Server 2008/2012
- Windows XP Embedded
- Windows CE 4.2-5.2, 6.0, 7.0, 2013
- Mac OS-X
- Linux 2.6 and greater
- Android

The drivers listed above are all available to download for free from FTDI website (www.ftdichip.com). Various 3rd party drivers are also available for other operating systems - see FTDI website (www.ftdichip.com) for details.

For driver installation, please refer to http://www.ftdichip.com/Documents/InstallGuides.htm

1.2 Part Numbers

Part Number	Package
FT230XQ-xxxx	16 Pin QFN
FT230XS-xxxx	16 Pin SSOP

Note: Packing codes for x is:

- R: Taped and Reel, (SSOP is 3,000pcs per reel, QFN is 5,000pcs per reel).
- U: Tube packing, 100pcs per tube (SSOP only)
- T: Tray packing, 490pcs per tray (QFN only)

For example: FT230XQ-R is 5,000pcs taped and reel packing

TEXAS INSTRUMENTS

LM22674, LM22674-Q1

SNVS590M – SEPTEMBER 2008 – REVISED NOVEMBER 2014

LM22674/-Q1 42 V, 500 mA SIMPLE SWITCHER® Step-Down Voltage Regulator with Features

1 Features

- Wide Input Voltage Range: 4.5 V to 42 V
- Internally Compensated Voltage Mode Control
- Stable with Low ESR Ceramic Capacitors
- 200 mΩ N-Channel MOSFET
- Output Voltage Options:
  -ADJ (Outputs as Low as 1.285 V)
  -5.0 (Output Fixed to 5 V)
- ±1.5% Feedback Reference Accuracy
- Switching Frequency of 500 kHz
- –40°C to 125°C Operating Junction Temperature Range
- Precision Enable Pin
- Integrated Boot-Strap Diode
- Integrated Soft-Start
- Fully WEBENCH® Enabled
- LM22674-Q1 is an Automotive Grade Product that is AEC-Q100 Grade 1 Qualified (–40°C to +125°C Operating Junction Temperature)
- SO PowerPAD (Exposed Pad)

2 Applications

- Industrial Control
- Telecom and Datacom Systems
- Embedded Systems
- Conversions from Standard 24 V, 12 V and 5 V Input Rails

3 Description

The LM22674 switching regulator provides all of the functions necessary to implement an efficient high voltage step-down (buck) regulator using a minimum of external components. This easy to use regulator incorporates a 42 V N-channel MOSFET switch capable of providing up to 500 mA of load current. Excellent line and load regulation along with high efficiency (> 90%) are featured. Voltage mode control offers short minimum on-time, allowing the widest ratio between input and output voltages. Internal loop compensation means that the user is free from the tedious task of calculating the loop compensation components. Fixed 5 V output and adjustable output voltage options are available. A switching frequency of 500 kHz allows for small external components and good transient response. A precision enable input allows simplification of regulator control and system power sequencing. In shutdown mode the regulator draws only 25 µA (typ). Built in soft-start (500 µs, typ) saves external components. The LM22674 also has built in thermal shutdown, and current limiting to protect against accidental overloads.

The LM22674 device is a member of Texas Instruments' SIMPLE SWITCHER® family. The SIMPLE SWITCHER® concept provides for an easy to use complete design using a minimum number of external components and the TI WEBENCH® design tool. TI's WEBENCH® tool includes features such as external component calculation, electrical simulation, thermal simulation, and Build-It boards for easy design-in.

Device Information(1)

PART NUMBER	PACKAGE	BODY SIZE (NOM)
LM22674	HSOP (8)	4.89 mm x 3.90 mm
LM22674-Q1		

(1) For all available packages, see the orderable addendum at the end of the data sheet.

Simplified Application Schematic

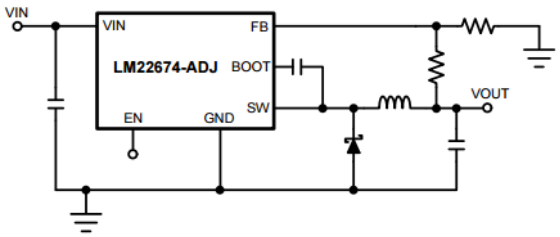

5 Pin Configuration and Functions

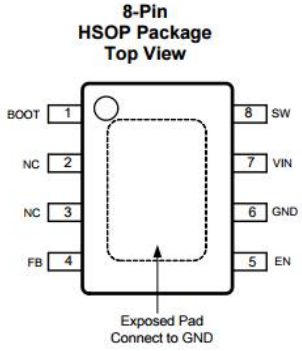

Pin Functions

PIN		TYPE	DESCRIPTION	APPLICATION INFORMATION
NAME	NO.			
BOOT	1	I	Bootstrap input	Provides the gate voltage for the high side NFET.
EN	5	I	Precision enable pin	Used to control regulator start-up and shutdown. See *Precision Enable and UVLO* section of data sheet.
EP	EP	—	Exposed Pad	Connect to ground. Provides thermal connection to PCB. See applications information.
FB	4	I	Feedback pin	Feedback input to regulator.
GND	6	—	System ground	System ground.
NC	2, 3	—	Not Connected	Pins are not electrically connected to die. Pins do function as thermal conductor.
VIN	7	I	Source input voltage	Input supply to regulator
SW	8	O	Switch pin	Switching output of regulator

SN54HC157, SN74HC157
QUADRUPLE 2-LINE TO 1-LINE DATA SELECTORS/MULTIPLEXERS

SCLS113D – DECEMBER 1982 – REVISED SEPTEMBER 2003

- Wide Operating Voltage Range of 2 V to 6 V
- Outputs Can Drive Up To 15 LSTTL Loads
- Low Power Consumption, 80-μA Max I_{CC}
- Typical t_{pd} = 11 ns
- ±6-mA Output Drive at 5 V
- Low Input Current of 1 μA Max

SN54HC157 . . . J OR W PACKAGE
SN74HC157 . . . D, DB, N, NS, OR PW PACKAGE
(TOP VIEW)

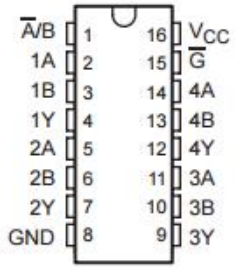

SN54HC157 . . . FK PACKAGE
(TOP VIEW)

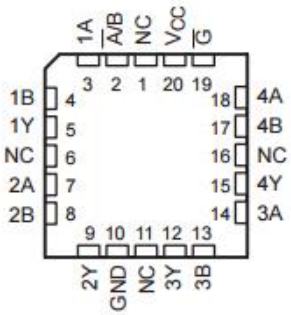

NC – No internal connection

description/ordering information

These data selectors/multiplexers contain inverters and drivers to supply full data selection to the four output gates. A separate strobe ($\overline{G}$) input is provided. A 4-bit word is selected from one of two sources and is routed to the four outputs. The 'HC157 devices present true data.

ORDERING INFORMATION

T_A	PACKAGE†	PACKAGE†	ORDERABLE PART NUMBER	TOP-SIDE MARKING
−40°C to 85°C	PDIP – N	Tube of 25	SN74HC157N	SN74HC157N
	SOIC – D	Tube of 40	SN74HC157D	HC157
		Reel of 2500	SN74HC157DR	
		Reel of 250	SN74HC157DT	
	SOP – NS	Reel of 2000	SN74HC157NSR	HC157
	SSOP – DB	Reel of 2000	SN74HC157DBR	HC157
	TSSOP – PW	Tube of 90	SN74HC157PW	HC157
		Reel of 2000	SN74HC157PWR	
		Reel of 250	SN74HC157PWT	
−55°C to 125°C	CDIP – J	Tube of 25	SNJ54HC157J	SNJ54HC157J
	CFP – W	Tube of 150	SNJ54HC157W	SNJ54HC157W
	LCCC – FK	Tube of 55	SNJ54HC157FK	SNJ54HC157FK

† Package drawings, standard packing quantities, thermal data, symbolization, and PCB design guidelines are available at www.ti.com/sc/package.

SN54HC157, SN74HC157
QUADRUPLE 2-LINE TO 1-LINE DATA SELECTORS/MULTIPLEXERS

SCLS113D – DECEMBER 1982 – REVISED SEPTEMBER 2003

FUNCTION TABLE

INPUTS				OUTPUT
$\overline{G}$	SELECT $\overline{A}$/B	DATA A	DATA B	Y
H	X	X	X	L
L	L	L	X	L
L	L	H	X	H
L	H	X	L	L
L	H	X	H	H

logic diagram (positive logic)

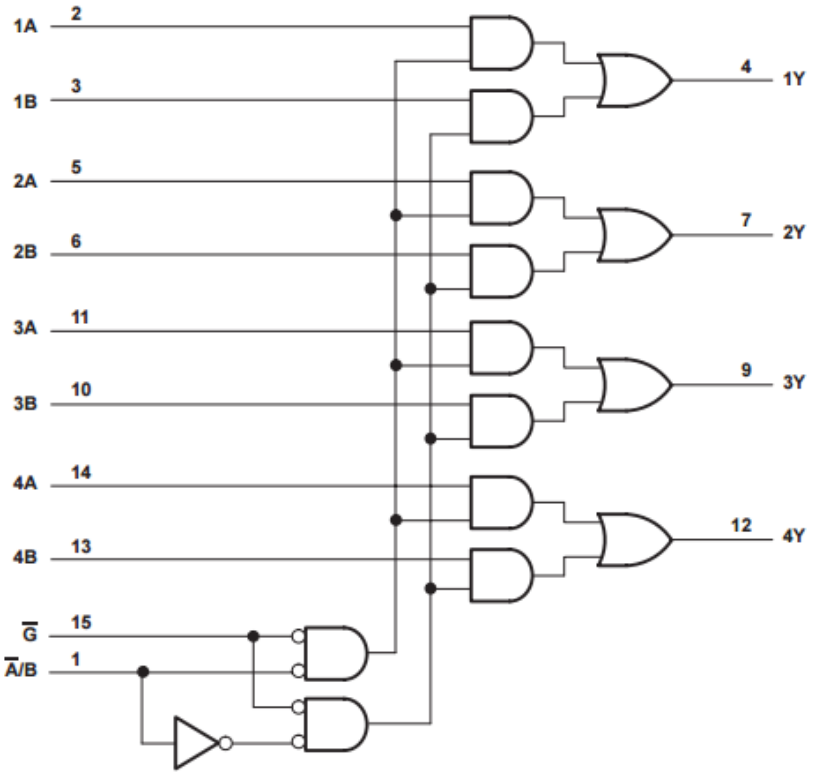

Pin numbers shown are for the D, DB, J, N, NS, PW, and W packages.

TEXAS INSTRUMENTS
POST OFFICE BOX 655303 • DALLAS, TEXAS 75265

ACS711

Hall Effect Linear Current Sensor with Overcurrent Fault Output for <100 V Isolation Applications

Features and Benefits

- No external sense resistor required; single package solution
- Reduced Power Loss:
  - 0.6 mΩ internal conductor resistance on EX package
  - 1.2 mΩ internal conductor resistance on LC package
- Economical low- and high-side current sensing
- Output voltage proportional to AC or DC currents
- ±12.5 A and ±25 A full scale sensing ranges on LC package
- ±15.5 A and ±31 A full scale sensing ranges on EX package
- Overcurrent $\overline{\text{FAULT}}$ trips and latches at 100% of full-scale current
- Low-noise analog signal path
- 100 kHz bandwidth
- Small footprint, low-profile SOIC8 and QFN packages
- 3.0 to 5.5 V, single supply operation
- Integrated electrostatic shield for output stability
- Factory-trimmed for accuracy
- Extremely stable output offset voltage
- Zero magnetic hysteresis
- Ratiometric output from supply voltage

Packages:

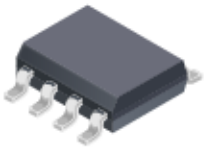

8-pin SOICN
with internally fused path
(LC package)

12-contact QFN
3 mm × 3 mm × 0.75 mm
(EX package)

Approximate Scale 1:1

Description

The Allegro™ ACS711 provides economical and precise solutions for AC or DC current sensing in <100 V audio, communications systems, and white goods. The device package allows for easy implementation by the customer. Typical applications include circuit protection, current monitoring, and motor and inverter control.

The device consists of a linear Hall sensor circuit with a copper conduction path located near the surface of the die. Applied current flowing through this copper conduction path generates a magnetic field which is sensed by the integrated Hall IC and converted into a proportional voltage. Device accuracy is optimized through the close proximity of the magnetic signal to the Hall transducer.

The output of the device has a positive slope proportional to the current flow from IP+ to IP– (pins 1 and 2, to pins 3 and 4). The internal resistance of this conductive path is 0.6 mΩ for the EX package, and 1.2 mΩ for the LC package, providing a non-intrusive measurement interface that saves power in applications that require energy efficiency.

The ACS711 is optimized for low-side current sensing applications, although the terminals of the conductive path are electrically isolated from the sensor IC leads, providing sufficient internal creepage and clearance dimensions for a low AC or DC working voltage applications. The thickness

Continued on the next page…

Typical Application

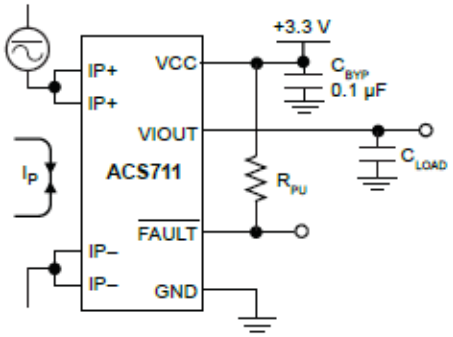

Application 1. The ACS711 outputs an analog signal, V_{IOUT}, that varies linearly with the bi-directional AC or DC primary current, I_P, within the range specified. The $\overline{\text{FAULT}}$ pin trips when I_P reaches ±100% of its full-scale current.

ACS711

Hall Effect Linear Current Sensor with Overcurrent Fault Output for < 100 V Isolation Applications

Description (continued)

of the copper conductor allows survival of the device at up to 5× overcurrent conditions.

The ACS711 is provided in small, surface mount packages: SOIC8 and QFN12. The leadframe is plated with 100% matte tin, which is compatible with standard lead (Pb) free printed circuit board assembly processes. Internally, the device is Pb-free, except for flip-chip high-temperature Pb-based solder balls, currently exempt from RoHS. The device is fully calibrated prior to shipment from the factory.

Selection Guide

Part Number	T_A (°C)	Optimized Accuracy Range, I_P (A)	Sensitivity[2], Sens (Typ) (mV/A)	Package	Packing[1]
ACS711ELCTR-12AB-T	–40 to 85	±12.5	110	8-pin SOICN	3000 pieces/reel
ACS711KLCTR-12AB-T	–40 to 125				
ACS711ELCTR-25AB-T	–40 to 85	±25	55		
ACS711KLCTR-25AB-T	–40 to 125				
ACS711EEXLT-15AB-T[3]	–40 to 85	±15.5	90	12-contact QFN with fused current loop	1500 pieces/reel
ACS711KEXLT-15AB-T[3]	–40 to 125				
ACS711EEXLT-31AB-T[3]	–40 to 85	±31	45		
ACS711KEXLT-31AB-T[3]	–40 to 125				

[1]Contact Allegro for additional packing options.
[2]Sensitivity measured with V_{CC} = 3.3 V.
[3]QFN package not qualified for automotive applications.

Absolute Maximum Ratings

Characteristic	Symbol	Notes	Rating	Units
Supply Voltage	V_{CC}		7	V
Reverse Supply Voltage	V_{RCC}		–0.1	V
Output Voltage	V_{IOUT}		7	V
Reverse Output Voltage	V_{RIOUT}		–0.1	V
Working Voltage for Basic Isolation	$V_{WORKING}$	Voltage applied between pins 1-4 and 5-8	100	VAC peak or VDC
$\overline{\text{FAULT}}$ Pin Voltage	V_{FAULT}		7	V
Overcurrent Transient Tolerance	I_{POC}	1 pulse, 100 ms	100	A
Nominal Operating Ambient Temperature	T_A	Range E	–40 to 85	°C
		Range K	–40 to 125	°C
Maximum Junction Temperature	T_J(max)		165	°C
Storage Temperature	T_{stg}		–65 to 170	°C

ACS711

Hall Effect Linear Current Sensor with Overcurrent Fault Output for < 100 V Isolation Applications

Functional Block Diagram

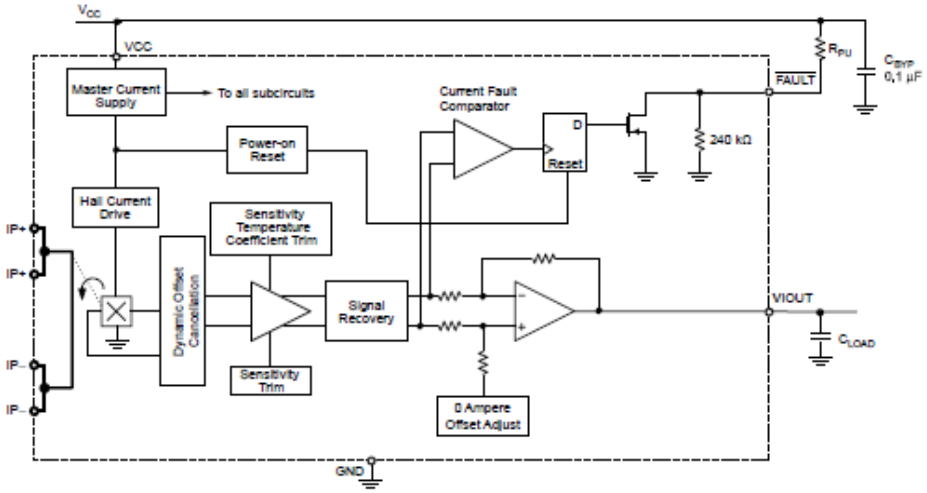

Pin-out Diagrams

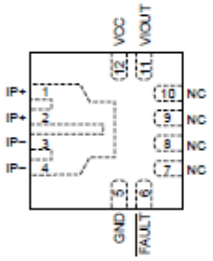

EX Package

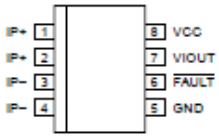

LC Package

Terminal List Table

Name	Number		Description
	EX	LC	
GND	5	5	Signal ground terminal
$\overline{\text{FAULT}}$	6	6	Overcurrent fault; active low
IP–	3 and 4	3 and 4	Terminals for current being sensed; fused internally
IP+	1 and 2	1 and 2	Terminals for current being sensed; fused internally
NC	7, 8, 9, 10	–	No connection; connect to GND for optimal ESD performance.
VCC	12	8	Device power supply terminal
VIOUT	11	7	Analog output signal

Details

The Tekpower TP1863 is a professional DC power supply for powering many devices such as Ham/CB radio and amplifiers. It is a highly stable, fused, high quality linear power supply with 13.8V fixed out DC power output, and 10-12A current. It comes with basic 1 Year USA warranty.

Specification:

Input Power: 110V AC 60Hz
Output: DC 13.8V, 10A-12A(Max)
Ripple voltage: <= 30mV
Dimensions: 5.5 X 4.3 X 10 inches
Weight: 9 lb

Package:

TP1863 Power Supply unit
User manual.
Warranty Registration Card

Additional Info

SKU	TP1863
Color	Black
Mode	Linear
Indication	Digital
Out Channels	Single
Free Shipping	No
Dimensions	14 x 13 x 11 inches
Weight (lb)	9.9000
Brand	Tekpower

ROBOT . HEAD to TOE
Product User's Manual – MD10C

---

1. INTRODUCTION/OVERVIEW

MD10C is another version of the MD10B which is designed to drive high current brushed DC motor up to 13A continuously. It offers several enhancements over the MD10B such as support for both locked-antiphase and sign-magnitude PWM signal as well as using full solid state components which result in faster response time and eliminate the wear and tear of the mechanical relay.

The MD10C has been designed with the capabilities and features of:

- Bi-directional control for 1 brushed DC motor.
- Support motor voltage ranges from 5V to ~~25V~~ 30V (for Rev3.0).
- Maximum current up to 13A continuous and 30A peak (10 second).
- 3.3V and 5V logic level input.
- Solid state components provide faster response time and eliminate the wear and tear of mechanical relay.
- Fully NMOS H-Bridge for better efficiency and no heat sink is required.
- Speed control PWM frequency up to 20KHz (Actual output frequency is same as input frequency).
- Support both locked-antiphase and sign-magnitude PWM operation.
- The new MD10C can be powered from a single power source and external Vin is not required.
- Support TTL PWM from microcontroller, **not PWM from RC receiver**.
- **Dimension:**75mm x 43mm

***MD10C is now Revision 3.0**.

3. BOARD LAYOUT AND SPECIFICATION

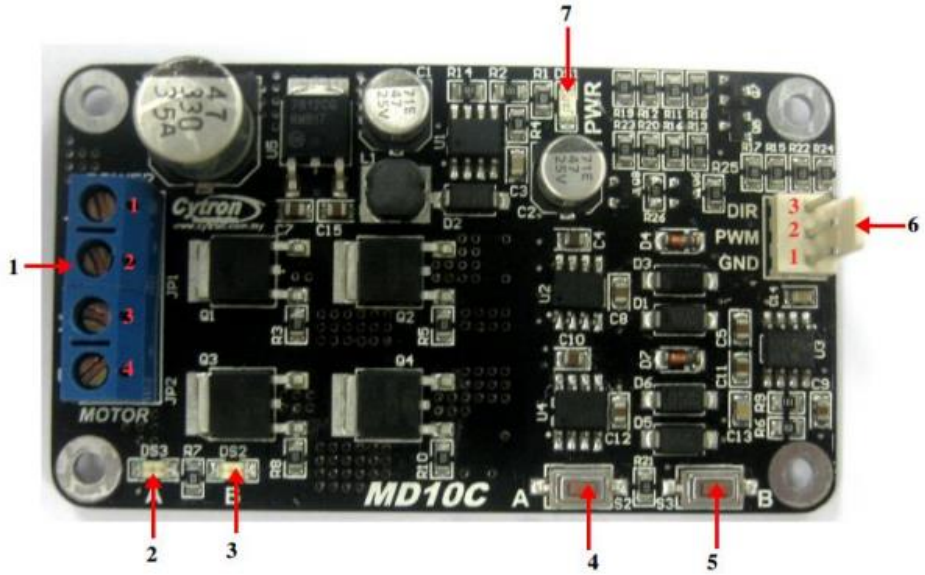

1. Terminal Block – Connect to motor and power source.

Pin No.	Pin Name	Description
1	POWER +	Positive Supply
2	POWER -	Negative Supply
3	Motor Output A	Connect to motor terminal A
4	Motor Output B	Connect to motor terminal B

2. Red LED A – Turns on when the output A is high and output B is low. Indicates the current flows from output A to B.

3. Red LED B – Turns on when the output A is low and output B is high. Indicates the current flows from output B to A.

4. Test Button A – When this button is pressed, current flows from output A to B and motor will turn CW (or CCW depending on the connection).

5. Test Button B – When this button is pressed, current flows from output B to A and motor will turn CCW (or CW depending on the connection).

6. Input

Pin No.	Pin Name	Description
1	GND	Logic ground.
2	**PWM	PWM input for speed control
3	DIR	Direction control.

**Note that it is not for RC PWM operation

The truth table for the control logic is as follow:

Pin 2 (PWM)	Pin 3 (DIR)	Output A	Output B
Low	X (Don't care)	Low	Low
High	Low	High	Low
High	High	Low	High

7. Green LED – Power LED. Should be on when the board is powered on.

Absolute Maximum Rating

No.	Parameters	Min	Typical	Max	Unit
1	Power Input Voltage	5	-	25	V
2	I_{MAX} (Maximum Continuous Motor Current)	-	-	13	A
3	I_{PEAK} – (Peak Motor Current) *	-	-	30	A
4	V_{IOH} (Logic Input – High Level)	3	-	5.5	V
5	V_{IOL} (Logic Input – Low Level)	0	0	0.5	V
6	Maximum PWM Frequency **	-	-	20	KHz

Must not exceed 10 seconds.
****Actual output frequency is same as input frequency.***

life.augmented

UM1974
User manual

STM32 Nucleo-144 boards

Introduction

The STM32 Nucleo-144 boards (NUCLEO-F207ZG, NUCLEO-F303ZE, NUCLEO-F412ZG, NUCLEO-F413ZH, NUCLEO-F429ZI, NUCLEO-F446ZE, NUCLEO-F722ZE, NUCLEO-F746ZG, NUCLEO-F767ZI and NUCLEO-H743ZI) provide an affordable and flexible way for users to try out new concepts and build prototypes, by choosing from the various combinations of performance and power consumption features provided by the STM32 microcontroller. The ST Zio connector, which extends the Arduino™ Uno V3 connectivity, and the ST morpho headers provide an easy means of expanding the functionality of the Nucleo open development platform with a wide choice of specialized shields. The STM32 Nucleo-144 boards do not require any separate probe as they integrate the ST-LINK/V2-1 debugger/programmer. The STM32 Nucleo-144 boards come with the comprehensive free software libraries and examples available with the STM32Cube package, as well as a direct access to the ARM® mbed Enabled™ on-line resources at http://mbed.org.

Figure 1. Nucleo-144 board (top view)

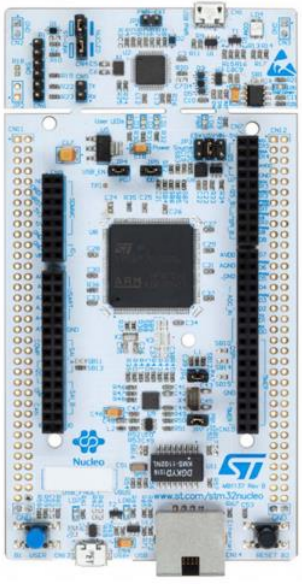

Figure 2. Nucleo-144 board (bottom view)

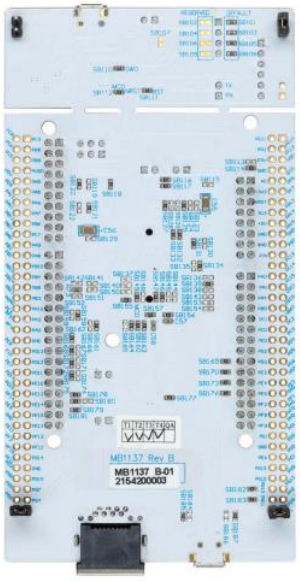

1 Features

The STM32 Nucleo-144 boards offer the following features:

- STM32 microcontroller in LQFP144 package
- USB OTG or full-speed device (depending on STM32 support)
- Ethernet compliant with IEEE-802.3-2002 (depending on STM32 support)
- 3 user LEDs
- 2 push-buttons: USER and RESET
- LSE crystal:
  - 32.768KHz crystal oscillator
- Board connectors:
  - USB with Micro-AB
  - Ethernet RJ45
- Expansion connectors:
  - ST Zio including Arduino™ Uno V3
  - ST morpho
- Flexible power-supply options: ST-LINK USB V_{BUS} or external sources
- On-board ST-LINK/V2-1 debugger/programmer with SWD connector:
  - ST-LINK/V2-1 standalone kit capability
  - USB re-enumeration capability: virtual COM port, mass storage, debug port
- Comprehensive free software libraries and examples available with the STM32Cube package
- Supported by wide choice of Integrated Development Environments (IDEs) including IAR™, Keil®, GCC-based IDEs, ARM® mbed Enabled™
- ARM® mbed Enabled™ (see http://mbed.org)

Appendix F – Detailed Analysis

ENGINEERING DATA SHEET	Sheet No.	1/3	Date
Helmholtz Cage Thermal Analysis	Prepared	ARN	2/11/17
	Checked	JMS	2/11/17
	Approved	MAT	2/12/17

Schematic

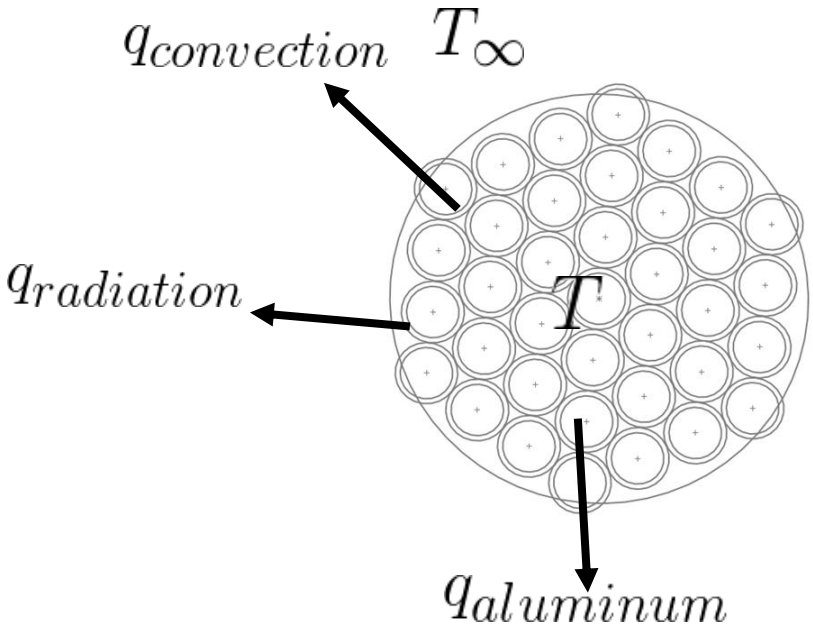

Assumptions

- Entire magnetic field created by one coil (max current)
- Bundle is a cylinder
- Neglect convection/conduction through aluminum frame
- 1D Problem (Temperature only varies with time)
- No forced air movement
- Constant Temperature through bundle
- Properties evaluated as cross section area weighted average of enamel and copper
- Room Temperature = 25 °C

ENGINEERING DATA SHEET	Sheet No.	2/3	Date
Helmholtz Cage Thermal Analysis	Prepared	ARN	2/11/17
	Checked	JMS	2/11/17
	Approved	MAT	2/12/17

Analysis

Properties- Cross-Section based weighted average for wire specific heat, conductivity, and density.

$$\rho_{cu} = 8833 \quad [kg/m^3]$$

$$k_{cu} = 401 \quad [W/(m*K)]$$

$$c_{cu} = 0.385 \quad [J/(kg*K)]$$

$$\rho_{enam} = 1700 \quad [kg/m^3]$$

$$k_{enam} = 0.4 \quad [W/(m*K)]$$

$$c_{enam} = 1000 \quad [J/(kg*K)]$$

$$A_{cu} = \pi \cdot \frac{D_{cu}^{\ 2}}{4}$$

$$A_{tot} = \pi \cdot \frac{D_{tot}^{\ 2}}{4}$$

$$P_{cu} = \frac{A_{cu}}{A_{tot}}$$

$$P_{enam} = 1 - P_{cu}$$

$$\rho_{avg} = P_{cu} \cdot \rho_{cu} + P_{enam} \cdot \rho_{enam}$$

$$k_{avg} = P_{cu} \cdot k_{cu} + P_{enam} \cdot k_{enam}$$

$$c_{avg} = P_{cu} \cdot c_{cu} + P_{enam} \cdot c_{enam}$$

Biot Number- To check the validity of our time dependent, 1D model, check the Biot Number. 'h' was calculated using the EES free conduction function for a cylinder suspended in air

$$B_i = \frac{h * L_c}{k} = \frac{13.4[\frac{W}{m^2*K}] * .0015[m]}{372[\frac{W}{m*K}]} = .000005 << 1$$

This allows us to use the general lump capacitance method (LCM),

Energy Balance

$$\rho_{avg} \cdot V \cdot c_{avg} \cdot \frac{dT}{dt} = \dot{E}_{gen} - h \cdot A \cdot (T - T_{\infty})$$

With

$$V = A_{tot} \cdot L \cdot N$$

$$\dot{E}_{gen} = N \cdot I^2 \cdot R$$

$$T = T_{init} + \int_0^{200} \left(\frac{dT}{dt}\right) d\,Time$$

And

$T_{init} = 25$

ENGINEERING DATA SHEET	Sheet No.	3/3	Date
Helmholtz Cage Thermal Analysis	Prepared	ARN	2/11/17
	Checked	JMS	2/11/17
	Approved	MAT	2/12/17

Results

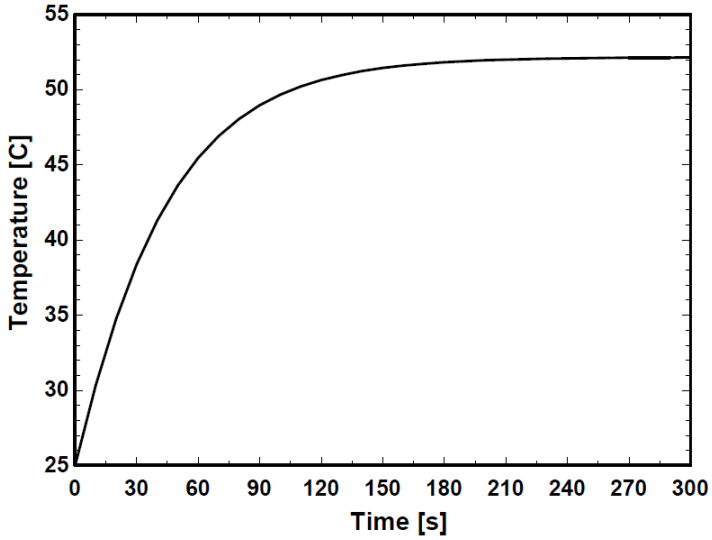

Letting EES solve the differential equation, we find a steady state temperature of 52.2°C after ~200 seconds. This is a very conservative estimate being as it neglects the aluminum U channel that surround the bundle, basically acting as a heat sink.

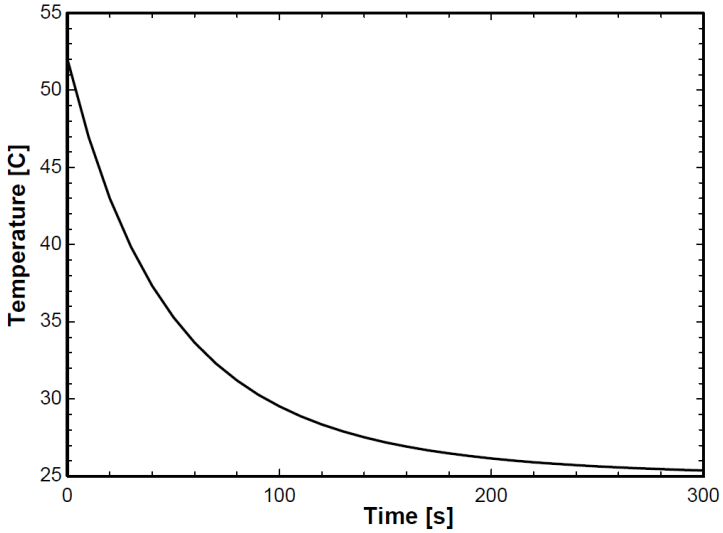

Similarly we ran the code without the heat generation term and an initial temperature of 52.2°C to find a cooling curve. While 52.2°C will not instantly burn human flesh, placing a 1 minute wait period after tests will assure that the coils are fully capable of being handled (34°C).

ENGINEERING DATA SHEET	Sheet No.	1/3	Date
Magnetics Attachment	Prepared	ARN	2/11/27
	Checked	JMS	2/11/17
	Approved	MAT	2/12/17

This attachment will outline how we optimized the wire gauge used in our Helmholtz cage. All properties of each wire came from our wire supplier: https://powerwerx.com/magnet-wire

Schematic

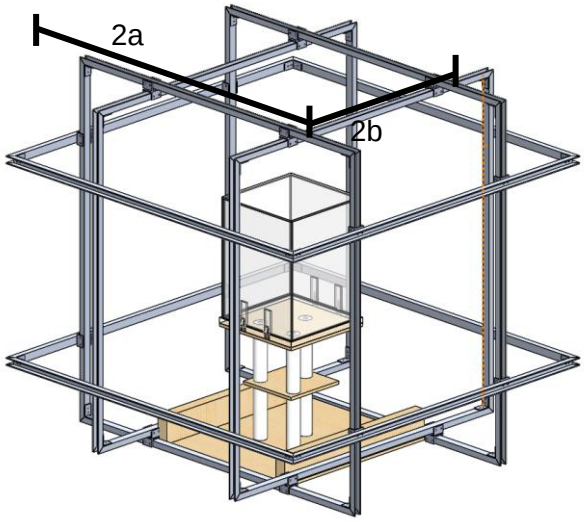

Assumptions

- The coil sizes (2a) were assumed to be 48", 44", and 40"
- Assumed ideal spacing between coils to be $\gamma = \frac{2b}{2a} = .5445$
- Desired field is 150 μT, 50% higher than minimum required
- The max current run is 50% of the current limit of the wire
- The coils in each axis are wired in series

Main Equations

- Generic square Helmholtz cage equation, where μ_o = permeability of air:

$$N = \frac{B\pi a(1+\gamma^2)\sqrt{2+\gamma^2}}{4\mu_o I}$$

- Power Dissipated

$$P = I^2R$$

- Coil properties (weight, resistance, cost, etc.) calculated using length

$$l = 4 * 2a$$

ENGINEERING DATA SHEET	Sheet No.	2/3	Date
Magnetics Attachment	Prepared	ARN	2/11/27
	Checked	JMS	2/11/17
	Approved	MAT	2/12/17

Results

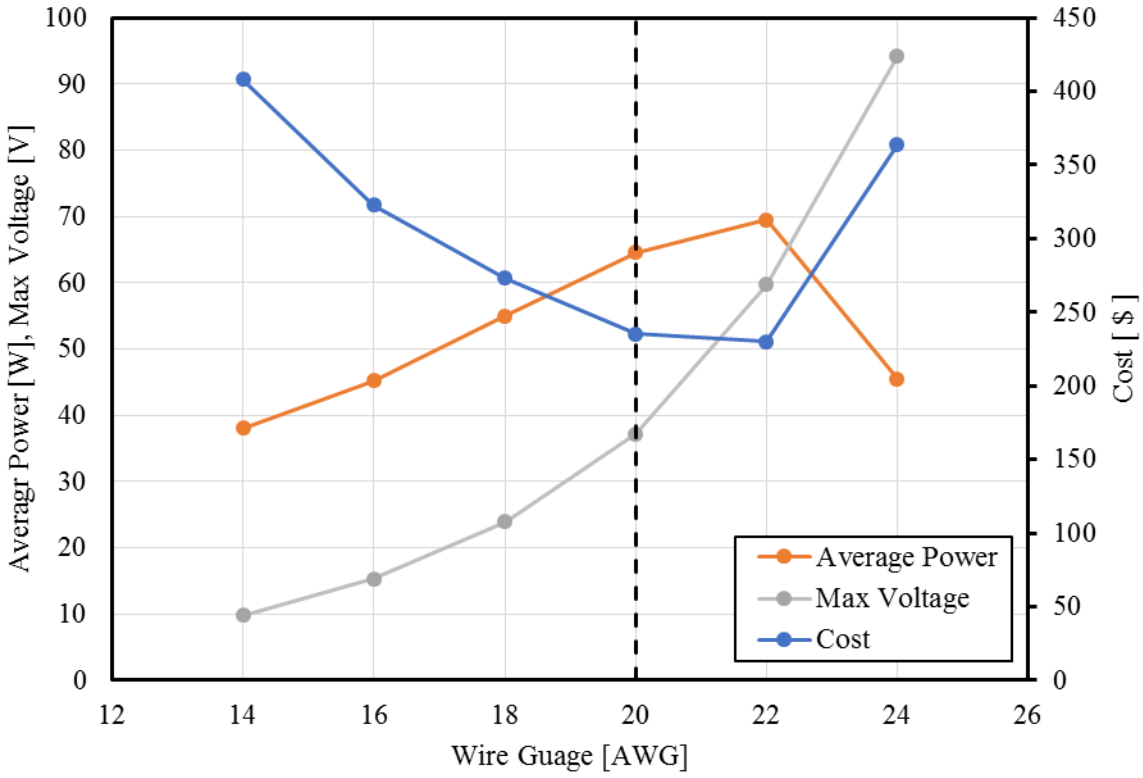

We selected a wire gauge of AWG 20 for the following reasons

- Minimize cost, < 3% between 20 and 22 gauge wires
- Voltage remains under 40 V for each axis for safety purposed
- The current in the wire (not show on the plot above) is below 3.5 V, the current limit on readily available H-Bridges for controller design

Full data sets are shown on the next page.

ENGINEERING DATA SHEET	Sheet No.	3/3	Date
Magnetics Attachment	Prepared	ARN	2/11/27
	Checked	JMS	2/11/17
	Approved	MAT	2/12/17

Gauge [AWG]	I Limit [A]	Mod I limit [A]	Wire Cost [$/ft]	Unit Weight [lb/1000ft]	Diameter [in]	Unit Resistance	N turns	Length [1000 ft]	Cost [$]	Weight [lb]	Resistance [ohms]	Voltage [v]	Power [W]
40” Coil													
14	17	8.5	0.332	12.6	0.066	2.57	13	0.190	126	4.8	0.49	4.1	35
16	13	6.5	0.206	7.9	0.052	4.09	16	0.234	96	3.7	0.96	6.2	40
18	10	5	0.134	5.0	0.042	6.51	21	0.308	83	3.0	2.00	10	50
20	7.5	3.75	0.088	3.1	0.033	10.3	28	0.410	72	2.5	4.23	15	59
22	5	2.5	0.057	1.9	0.026	16.5	42	0.616	70	2.4	10.2	25	63
24	2.1	1.05	0.038	1.2	0.021	26.1	98	1.437	110	3.5	37.6	39	41.
44” Coil													
14	17	8.5	0.332	12.6	0.066	2.57	13	0.199	132	5.0	0.51	4	37
16	13	6.5	0.206	7.9	0.052	4.09	17	0.260	107	4.1	1.06	6	45
18	10	5	0.134	5.0	0.042	6.51	22	0.337	90	3.3	2.19	10	54
20	7.5	3.75	0.088	3.1	0.033	10.3	29	0.444	78	2.8	4.58	17	64
22	5	2.5	0.057	1.9	0.026	16.5	44	0.674	77	2.6	11.1	27	69
24	2.1	1.05	0.038	1.2	0.021	26.1	103	1.579	121	3.9	41.3	43	45
48” Coil													
14	17	8.5	0.332	12.6	0.066	2.57	14	0.224	148	5.6	0.57	4	41
16	13	6.5	0.206	7.9	0.052	4.09	18	0.288	118	4.5	1.18	7	49
18	10	5	0.134	5.0	0.042	6.51	23	0.368	99	3.6	2.39	11	59
20	7.5	3.75	0.088	3.1	0.033	10.3	30	0.48	84	3.0	4.95	18	69
22	5	2.5	0.057	1.9	0.026	16.5	45	0.72	82	2.8	11.9	29	74
24	2.1	1.05	0.038	1.2	0.021	26.1	107	1.712	131	4.2	44.8	47	49

ENGINEERING DATA SHEET	Sheet No.	1/3	Date
Satellite and Cleanroom Box Pedestal Structural Analysis	Prepared	JMS	2/11/17
	Checked	ARN	2/12/17
	Approved	MAT	2/12/17

Schematic

1st model: 3 1.625” OD .5625” ID PVC Pipes 15.93” Tall

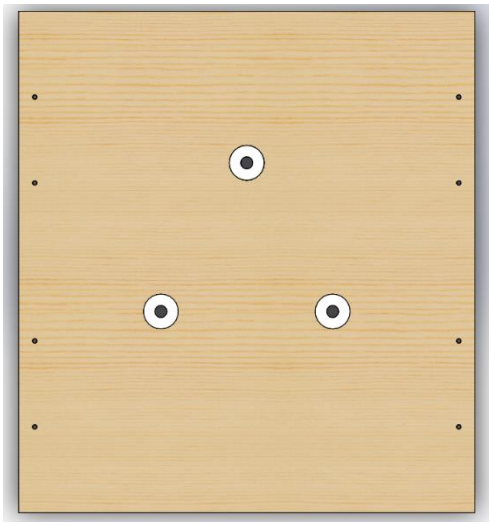

2nd model: 1 6.25” OD 5.9” ID PVC Pipe 15.93” Tall

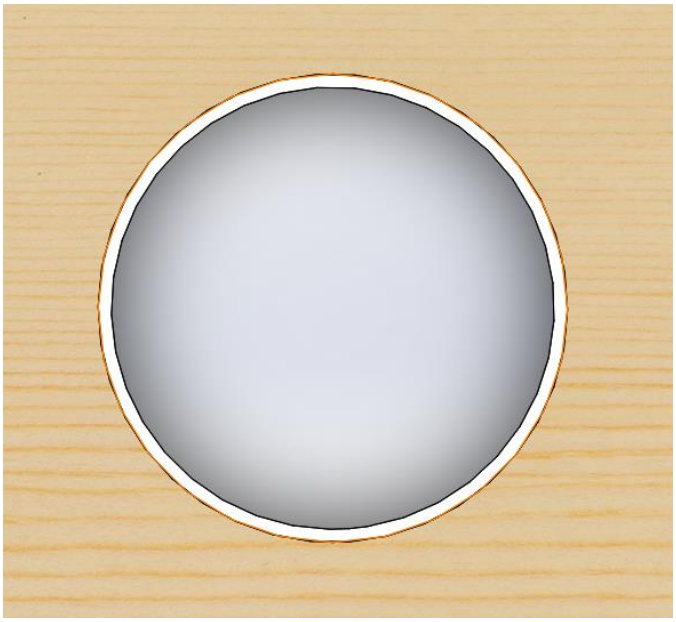

Assumptions

- None

ENGINEERING DATA SHEET	Sheet No.	2/3	Date
Satellite and Cleanroom Box Pedestal Structural Analysis	Prepared	JMS	2/11/17
	Checked	ARN	2/12/17
	Approved	MAT	2/12/17

Analysis

1st Model:

Slenderness Ratio

$$\frac{l}{r} = \frac{l}{\sqrt{\frac{I}{A}}} = \frac{15.9\ [in]}{\sqrt{\frac{0.33\ [in^4]}{1.83\ [in^2]}}} = 37.2$$

Critical Buckling Load

$$F = \frac{\pi^2 nEI}{l^2} = \frac{\pi^2 * .25 * .348E6\ [psi] * .337\ [in^4]}{15.9\ [in]} = 1140\ lbf$$

Safety Factor

$$SF = \frac{3 * 1140\ [lbf]}{100\ [lbf]} = 34.2$$

2nd Model:

Slenderness Ratio

$$\frac{l}{r} = \frac{l}{\sqrt{\frac{I}{A}}} = \frac{15.9\ [in]}{\sqrt{\frac{15.42\ [in^4]}{3.34\ [in^2]}}} = 7.4$$

Critical Buckling Load

$$F = \frac{\pi^2 nEI}{l^2} = \frac{\pi^2 * .25 * .348E6\ [psi] * 15.42\ [in^4]}{15.9\ [in]} = 52{,}200\ lbf$$

Safety Factor

$$SF = \frac{52200\ [lbf]}{100\ [lbf]} = 522$$

Normal Stress

$$Compression = \frac{100\ [lbf]}{3.33\ [in^2]} = 30.0\ [psi]$$

Safety Factor Yielding

$$SF\ yield = \frac{7{,}500\ [psi]}{30.0\ [psi]} = 250$$

ENGINEERING DATA SHEET	Sheet No.	3/3	Date
Satellite and Cleanroom Box Pedestal Structural Analysis	Prepared	JMS	2/11/17
	Checked	ARN	2/12/17
	Approved	MAT	2/12/17

Results

The 1st model had a more complicated design, lower safety factor and was more expensive than the 2nd model thus the 2nd model is being chosen.

The slenderness ratio for the 2nd model design wasn't greater than 10 thus we couldn't completely rely on Euler Buckling Analysis for the structural analysis and yielding via crushing had to be considered. With a conservative yield strength of 7,500 psi found from online data sheets, a safety factor against yield was determined to be 250. With a safety factor of 250 against crushing, we do not have any reason to be concerned.

Appendix G – Gantt Chart

	Task Name	Duration	Finish
1	CDR	3 wks	Tue 2/28/17
2	Order/Obtain Components	3 wks	Tue 3/21/17
3	**Manufacture Structure**	**28 days**	**Fri 5/5/17**
4	Saw/Drill Parts	7 days	Thu 4/6/17
5	Laser Cut Acryllic Walls	2 days	Mon 4/10/17
6	Shorten Bushings	7 days	Wed 4/19/17
7	Translation Brackets	7 days	Mon 4/17/17
8	Corner Brackets	7 days	Wed 4/26/17
9	Acryllic Base	7 days	Fri 5/5/17
10	**Software Development**	**35 days**	**Tue 4/25/17**
11	Create Python Build	2 wks	Tue 3/14/17
12	Develop Python Modules	2 wks	Tue 4/4/17
13	Firmware - Coms Code	2 wks	Tue 3/14/17
14	Firmware - Control Code	2 wks	Tue 4/4/17
15	Hardware Setup	3 wks	Tue 4/25/17
16	**PCB Fabrication/Testing**	**40 days**	**Tue 5/2/17**
17	Submit Board Art to PCB Way	1 wk	Tue 3/7/17
18	Make Corrections to Art	1 wk	Tue 3/14/17
19	Fabricate/Populate Board	3 wks	Tue 4/11/17
20	Troubleshoot/Test Board	3 wks	Tue 5/2/17
21	**Full System Assembly/Testing**	**18 days**	**Wed 5/31/17**
22	Assemble Cage, Electronics	3 days	Wed 5/10/17
23	Center Cage B Sweep	1 wk	Wed 5/17/17
24	Spatial Sweep	1 wk	Wed 5/24/17
25	Time Rate characterization	1 wk	Wed 5/31/17
26	Expo	0 days	Fri 6/2/17

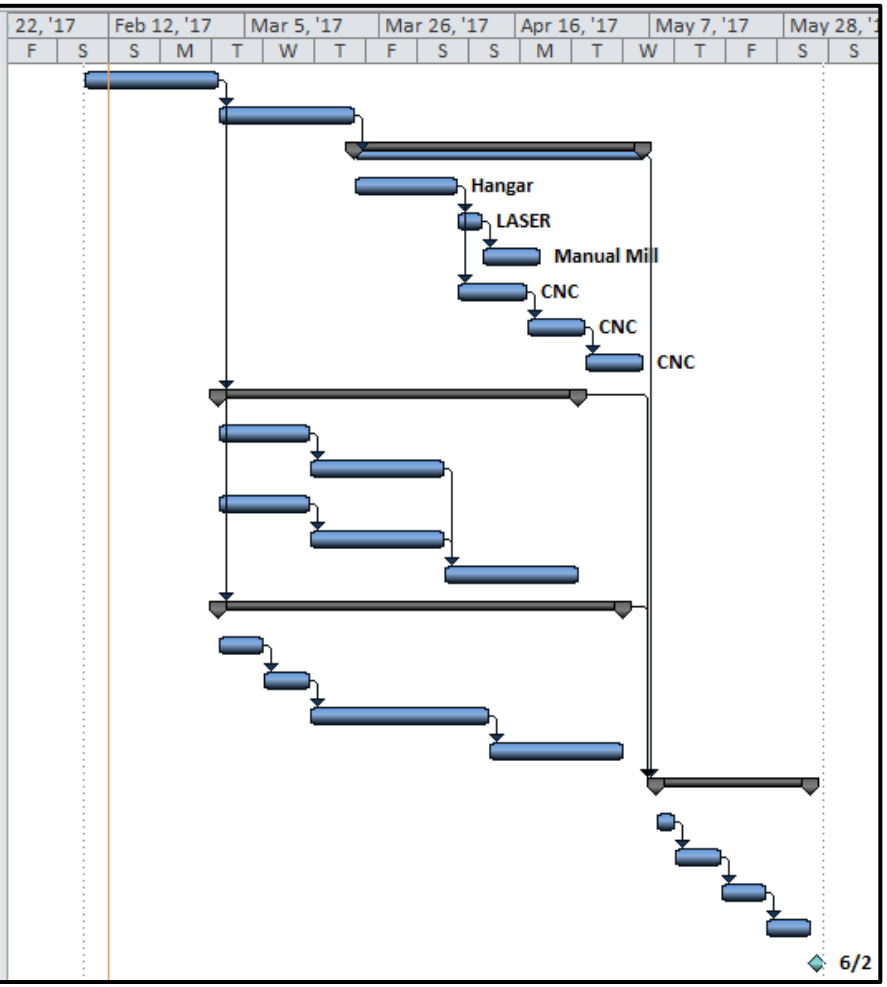

Appendix H – Safety Check List

SENIOR PROJECT CONCEPTUAL DESIGN REVIEW HAZARD IDENTIFICATION CHECKLIST

Y	N	
✔	☐	Will any part of the design create hazardous revolving, reciprocating, running, shearing, punching, pressing, squeezing, drawing, cutting, rolling, mixing or similar action, including pinch points and sheer points?
☐	✔	Can any part of the design undergo high accelerations/decelerations?
☐	✔	Will the system have any large moving masses or large forces?
☐	✔	Will the system produce a projectile?
✔	☐	Would it be possible for the system to fall under gravity creating injury?
☐	✔	Will a user be exposed to overhanging weights as part of the design?
☐	✔	Will the system have any sharp edges?
✔	☐	Will all the electrical systems properly grounded?
☐	✔	Will there be any large batteries or electrical voltage in the system above 40 V either AC or DC?
☐	✔	Will there be any stored energy in the system such as batteries, flywheels, hanging weights or pressurized fluids?
☐	✔	Will there be any explosive or flammable liquids, gases, dust fuel part of the system?
☐	✔	Will the user of the design be required to exert any abnormal effort or physical posture during the use of the design?
☐	✔	Will there be any materials known to be hazardous to humans involved in either the design or the manufacturing of the design?
☐	✔	Can the system generate high levels of noise?
☐	✔	Will the device/system be exposed to extreme environmental conditions such as fog, humidity, cold, high temperatures, etc.?
✔	☐	Will the system easier to use safely than unsafely?
☐	✔	Will there be any other potential hazards not listed above? If yes, please explain below?